AD

MEMORANDUM REPORT ARBRL-MR-02989

THE INFLUENCE OF PROPELLANT GRAIN GEOMETRY ON IGNITION-INDUCED, TWO-PHASE FLOW DYNAMICS IN GUNS

A. W. Horst
J. R. Kelso
J. J. Rocchio
A. A. Koszoru

February 1980

US ARMY ARMAMENT RESEARCH AND DEVELOPMENT COMMAND
BALLISTIC RESEARCH LABORATORY
ABERDEEN PROVING GROUND, MARYLAND

Destroy this report when it is no longer needed.
Do not return it to the originator.

Secondary distribution of this report by originating or sponsoring activity is prohibited.

Additional copies of this report may be obtained from the National Technical Information Service, U.S. Department of Commerce, Springfield, Virginia 22151.

The findings in this report are not to be construed as an official Department of the Army position, unless so designated by other authorized documents.

The use of trade names or manufacturers' names in this report does not constitute indorsement of any commercial product.

UNCLASSIFIED

SECURITY CLASSIFICATION OF THIS PAGE *(When Data Entered)*

REPORT DOCUMENTATION PAGE

READ INSTRUCTIONS BEFORE COMPLETING FORM

1. REPORT NUMBER: MEMORANDUM REPORT ARBRL-MR-02989
2. GOVT ACCESSION NO.:
3. RECIPIENT'S CATALOG NUMBER:

4. TITLE *(and Subtitle)*: THE INFLUENCE OF PROPELLANT GRAIN GEOMETRY ON IGNITION-INDUCED, TWO-PHASE FLOW DYNAMICS IN GUNS

5. TYPE OF REPORT & PERIOD COVERED: Memorandum Report

6. PERFORMING ORG. REPORT NUMBER:

7. AUTHOR(s):
A.W. HORST
J.R. KELSO
J.J. ROCCHIO A.A. KOSZORU

8. CONTRACT OR GRANT NUMBER(s):

9. PERFORMING ORGANIZATION NAME AND ADDRESS:
US Army Ballistic Research Laboratory
(ATTN: DRDAR-BLP)
Aberdeen Proving Ground, MD 21005

10. PROGRAM ELEMENT, PROJECT, TASK AREA & WORK UNIT NUMBERS:
62618A
1L162618AH80

11. CONTROLLING OFFICE NAME AND ADDRESS:
US Army Armament Research & Development Command
US Army Ballistic Research Laboratory
(ATTN: DRDAR-BL)
Aberdeen Proving Ground, MD 21005

12. REPORT DATE: February 1980

13. NUMBER OF PAGES: 74

14. MONITORING AGENCY NAME & ADDRESS *(if different from Controlling Office)*:

15. SECURITY CLASS. *(of this report)*: UNCLASSIFIED

15a. DECLASSIFICATION/DOWNGRADING SCHEDULE:

16. DISTRIBUTION STATEMENT *(of this Report)*

Approved for public release; distribution unlimited.

17. DISTRIBUTION STATEMENT *(of the abstract entered in Block 20, if different from Report)*

18. SUPPLEMENTARY NOTES

19. KEY WORDS *(Continue on reverse side if necessary and identify by block number)*
Interior Ballistics
Pressure Waves
Grain Geometry
Interphase Drag

20. ABSTRACT *(Continue on reverse side if necessary and identify by block number)*

dek Localized ignition of a bed of granular propellant can result in a substantial pressure gradient accompanying the convectively driven flame front. For the common example of base ignition of a moderately long, cylindrical, propellant charge, this wave front may, upon arrival at the projectile base, be reflected as a longitudinal pressure wave which can dissipate or grow to catastrophic levels. Previous studies investigated the use of 19-perforation grain designs as an alternate to the standard 7-perforation grain commonly employed. The larger

DD FORM 1 JAN 73 1473 EDITION OF 1 NOV 65 IS OBSOLETE

UNCLASSIFIED

SECURITY CLASSIFICATION OF THIS PAGE *(When Data Entered)*

size and reduced initial surface area of a ballistically equivalent 19-perforation charge were shown to reduce the level of pressure waves for a given igniter and charge configuration. This paper extends the scope of these studies to include the 37-perforation grain design. Both theoretical and experimental studies suggest a significant potential for further reduction in the level of pressure waves, though the feasibility of a base-ignited, high-performance, artillery charge employing granular propellant was not demonstrated.

TABLE OF CONTENTS

LIST OF ILLUSTRATIONS

LIST OF TABLES

I. INTRODUCTION

The presence of pressure waves in gun chambers is thought to have been first recognized by Vielle[1], in the late 19th century with his invention of the recording pressure gage. The significance of pressure waves as a leading cause of ballistic irregularities was not appreciated until some 50 years later, when R.H. Kent introduced the use of piezoelectric pressure gages[2,3]. During the course of his studies, Kent noted the importance of roles played by the ignition train, propellant bed permeability, and the distribution of ullage in the gun chamber. Today, after many lessons painfully learned as a result of serious gun ammunition malfunctions[4,5,6], we recognize these features of the charge to be key contributors to the overall ignition process, and efforts are now underway to exploit each of these design areas. A recent project to investigate three alternative propellant grain geometries to determine their relative influences on ignition-induced pressure waves is reported herein.

II. BACKGROUND

In order to better appreciate the nature of these efforts, let us first look briefly at the phenomenology of an idealized (though certainly not ideal) propelling charge, depicted schematically in Figure 1. Typically, the ignition system is initiated by

---

[1] *P. Vielle, Quoted by Cranz in "Lehrbuch der Ballistik" Volume II, Springer Verlag, Berlin, 1926, p. 151.*

[2] *R.H. Kent, "Study of Ignition of 155-mm Gun in Connection with Project KW 250 --- Study of the Factors Involved in the Design of Propelling Charges", USA Ballistic Research Laboratories, Aberdeen Proving Ground, Maryland, Memorandum Report 4, February 1935.* (AD493405)

[3] *R.H. Kent, "Study of Ignition of 155-mm Gun", USA Ballistic Research Laboratories, Aberdeen Proving Ground, Maryland, Report No. 22, October 1935.* (AD494763)

[4] *D.W. Culbertson, M.C. Shamblen, and J.S. O'Brasky, "Investigation of 5"/38 Gun In-Bore Ammunition Malfunctions", Naval Weapons Laboratory, Dahlgren, Virginia, TR-2624, December 1971.*

[5] *I.W. May, and E.V. Clarke Jr., "A Case History: Gun Ignition Related Problems and Solutions for the XM-198 Howitzer", USA Ballistic Research Laboratories, Aberdeen Proving Ground, Maryland, Interim Memorandum Report No. 150, October 1973 (no longer available).*

[6] *P.J. Olenick, "Investigation of the 76-mm/62 Caliber Mark 75 Gun Mount Malfunction", Naval Surface Weapons Center, Dahlgren, Virginia, TR-3411, October 1975.*

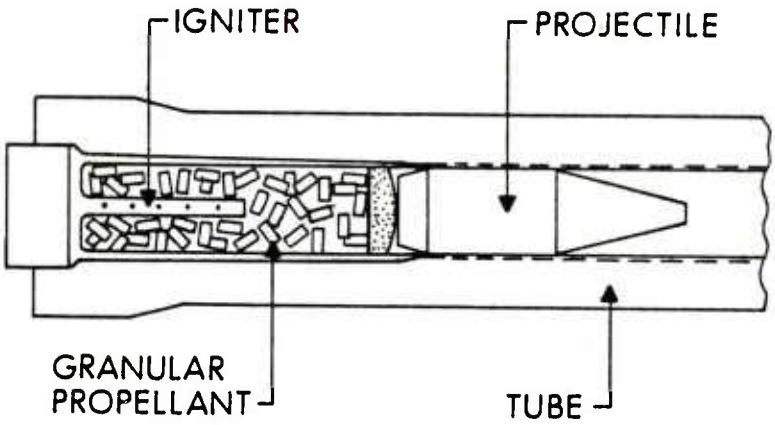

Figure 1. Idealized Propelling Charge

electrical or mechanical impulse, leading to the venting of hot combustion products into the propellant bed. The intensity and spatial/temporal distributions of this output are highly system-dependent. The surfaces of nearby propellant grains are heated sufficiently to initiate combustion. Hot propellant gases then join those from the igniter to penetrate the rest of the bed, convectively heating the propellant and resulting in flamespread. During this phase, resistance to gas flow offered by the packed bed may result in large pressure gradients capable of inducing substantial propellant motion. In particular, localized ignition at the breech end of a propellant charge with ullage present between the propellant and the projectile base can generate large forward velocities in both gas and solid phases. Stagnation at the projectile base is then accompanied by locally high pressures, bed compaction, and perhaps even grain fracture[7]. Severe pressure waves can result, as depicted in Figure 2. The presence of a longitudinal pressure wave is more readily apparent in the pressure-difference profile (spindle pressure minus forward pressure) shown at the bottom of the figure.

Based on this picture of the interior ballistic cycle, one can readily comprehend how each of the areas identified by Kent can be manipulated to minimize the formation of pressure waves. In all cases, the intent would be to reduce the ultimate effect of the igniter-induced convective deflagration wave on the formation of locally high pressures and a severe flow-stagnation event. Uniform ignition of the propellant

---

[7] *A.W. Horst, I.W. May, and E.V. Clarke, "The Missing Link Between Pressure Waves and Breechblows", USA ARRADCOM, Ballistic Research Laboratory, Aberdeen Proving Ground, Maryland, Memorandum Report No. 02849, July 1978.* (A058354)

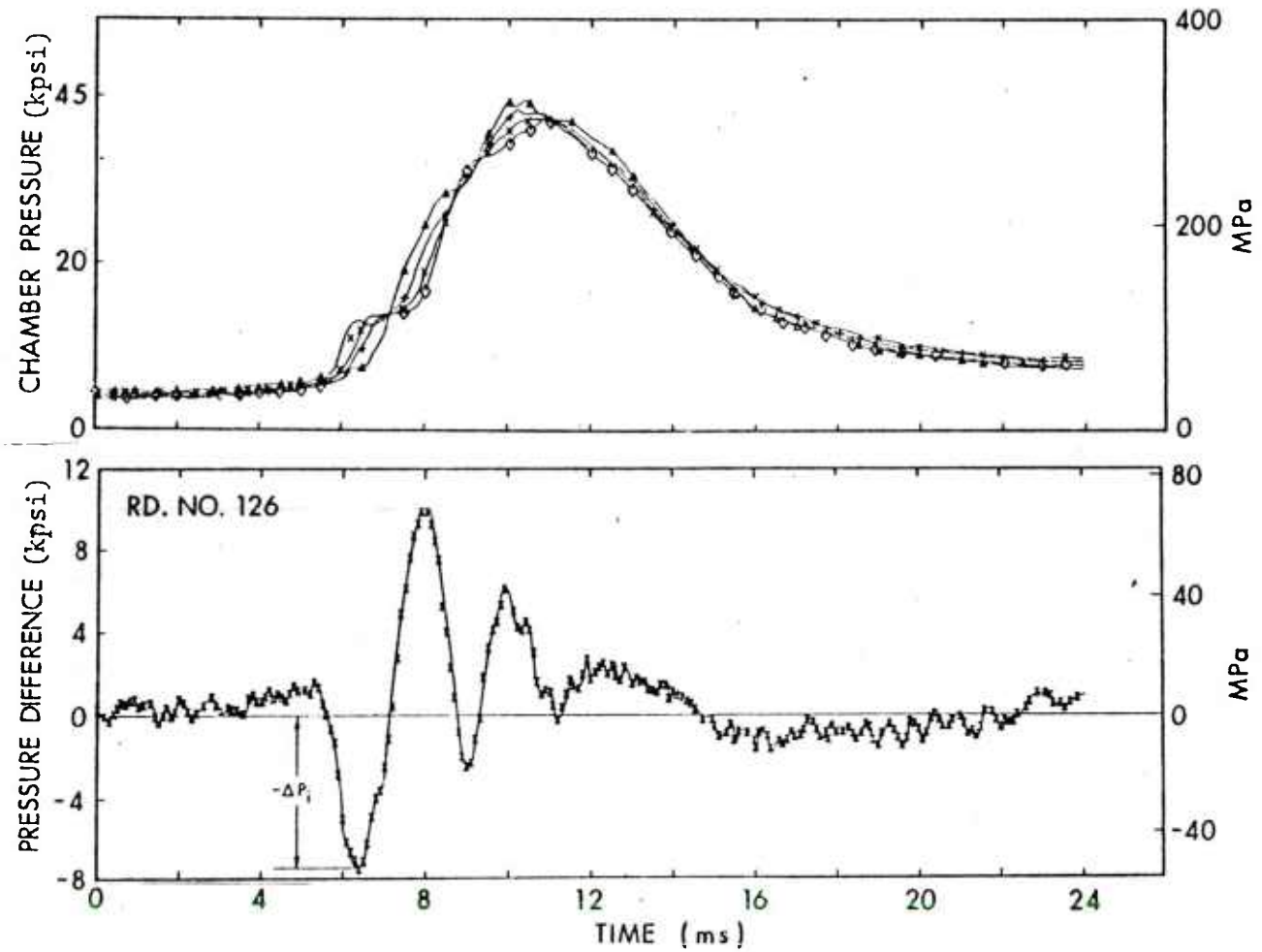

Figure 2. High-Amplitude Pressure Waves Resulting from Improper Ignition of a 155-mm Propelling Charge (Zone 8)

bed, were it possible, would eliminate the very ignition wave and associated pressure gradient which constitute the source of the problem. Increased bed permeability could be expected to reduce the pressure gradient associated with the ignition transient, likewise reducing mechanical forces tending to accelerate the propellant bed into the projectile base. Finally, elimination of forward ullage would minimize bed mobility during flamespread, reducing bed compaction as well as the possibility of grain fracture. It might also be expected that the presence of longitudinal ullage external to the charge (see Figure 3) could lead to pressure gradients and propellant mobility, despite a nearly ideal (instantaneous) ignition of all propellant surfaces. Radially-distributed ullage, usually present with bagged charges, and shown in Figure 4, may, on the other hand, allow equilibration of longitudinal pressure gradients.

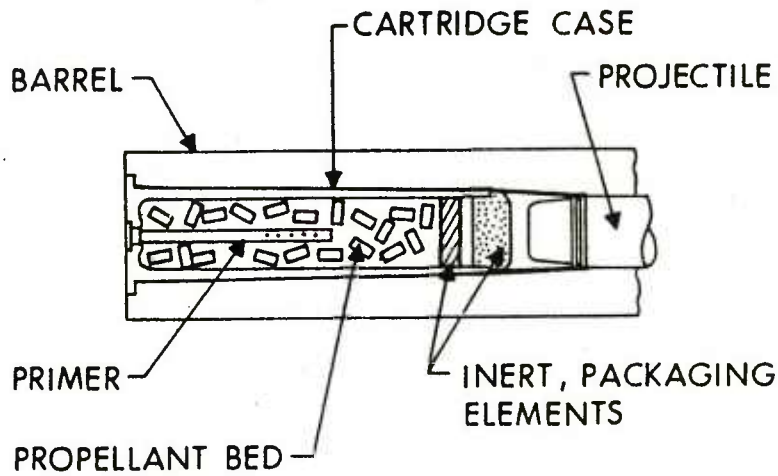

Figure 3. Cased Propelling Charge

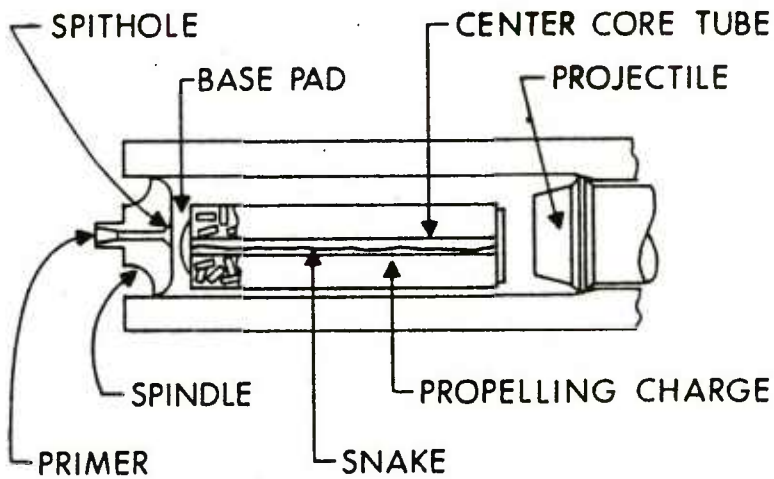

Figure 4. Bagged Propelling Charge

A recent study was performed in the Navy 5-Inch, 54-Caliber Gun[8] providing comparative information on each of these design techniques. Work has since continued on Rapid-Ignition-Propagation (RIP) primers[9-11], 19-perforation propellants[12-14], and the elimination of forward ullage[15]. The study reported herein addresses advantages offered through the use of non-standard grain geometries, both in terms of increasing bed permeability to gas flow and reducing initial gas generation rates during flamespread. While it is well known that the natural flow channels provided by bundles of sticks or tubular propellant present a favorable geometry with respect to the aforementioned points, several advantages associated with the production of granular propellant have led to its continued use in the United States. Therefore, this study was conducted to examine the comparative advantages of 19- and 37-perforation granular propellant as alternatives to the standard 7-perforation geometry.

This particular body of work was devised as a direct extention to previous BRL efforts in this area[12-14] which confirmed the predicted

---

[8] *A.W. Horst, T.C. Smith, and S.E. Mitchell, "Key Design Parameters in Controlling Gun-Environment Pressure Wave Phenomena - Theory vs. Experiment," 13th JANNAF Combustion Meeting, CPIA Publication 281, Vol. I, pp. 341-367, December 1976.*

[9] *J.L. East, Jr., "A Consumable, Tubeless Igniter for Gun Pressure Wave Reduction and Improved Ignition", 13th JANNAF Combustion Meeting, CPIA Publication 281, Vol. I, pp. 451-474, December 1976.*

[10] *J. Foster, "Detonation Rate Ignition Propagation Primer", 15th JANNAF Combustion Meeting, CPIA Publication 297, Vol. I, pp. 411-455, February 1979.*

[11] *S. Livanis, "Novel Ignition Systems for Improved Gun Interior Ballistic Performance", 15th JANNAF Combustion Meeting, CPIA Publication 297, Vol. I, pp. 367-381, February 1979.*

[12] *J.J. Rocchio, K.J. White, C.R. Ruth, and I.W. May, "Propellant Grain Tailoring to Reduce Pressure Wave Generation in Guns", 12th JANNAF Combustion Meeting, CPIA Publication 273, Vol. I, pp. 275-301, December 1975.*

[13] *J.J. Rocchio, C.R. Ruth, and I.W. May, "Grain Geometry Effects on Wave Dynamics in Large Caliber Guns", 13th JANNAF Combustion Meeting, CPIA Publication 281, Vol. I, pp. 369-382, December 1976.*

[14] *J.J. Rocchio and C.R. Ruth, "An Investigation of the Interior Ballistic Performance of a 19-Perforation, M30A1 Propellant Granulation in the Zone 8 Charge of the 155-mm, M198 Howitzer", USA ARRADCOM, Ballistic Research Laboratory, Aberdeen Proving Ground, Maryland, Memorandum Report, (report in preparation).*

[15] *C.T. Boyer, Jr., "Interim Charge Assemblies Developed for Use with the 8-Inch Paveway GP in the MK 71 Gun", Naval Surface Weapons Center, Dahlgren, Virginia, NSCW/DL TR-5707, December 1977.*

reduction in pressure waves with the substitution of larger 19-perforation grains for the standard 7-perforation geometry. Unexpected results were, however, obtained during one of these earlier tests[13], in which the lengths of the 19-perforation grains were increased (to 1.4 and 2 times the normal length) to further increase bed permeability and reduce the total initial surface areas of the charges. While both of these factors should have resulted in diminished pressure waves, little effect was observed. One possible explanation for this behavior emanates from a consideration of the comparative initial surface areas, based on external (i.e., excluding perforations) grain surfaces only. This parameter provided a better correlation with pressure-wave levels than did bed permeability or total initial charge surface area based on calculations including the perforations. Motivation for consideration of external surfaces only is not particularly obscure, as delayed flamespread into the perforations has long been a suspected problem[16].

A program was thus undertaken to clarify and extend these results by comparing the influence of an even larger, 37-perforation, grain design on pressure waves to data obtained using 7- and 19-perforation granulations. As part of this study, it was also planned to explore the effect of the surface area of the perforations on pressure waves. To this end, three 37-perforation grains were designed to provide the same nominal performance, but with different perforation diameters. The larger the diameter of the holes, the more readily flamespread therein should occur, and the earlier the internal (perforation) surfaces should contribute to gas generation. The effect of stacking the grains in an effort to increase bed permeability was to be investigated as well.

III. PRELIMINARY STUDIES

A. Propellant Grain Design

Three 37-perforation grains were designed to match the ballistics of the M203, Zone 8, Propelling Charge for the M198, 155-mm Howitzer. The perforation diameters were varied to be approximately 1, 2, or 3 times that of a "normal" grain design; the idea being that flamespread into the perforation should occur earlier in the interior ballistic cycle as the perforation diameter was increased. The design dimensions, geometric ratios and computer performance of these grains are given in Table I. Permeability of the propellant bed is expected to increase with grain size and thus with perforation diameter. This trend also holds for total surface area of the charge. In contrast, the total exterior surface area (i.e., excluding that of the perforations) decreases with increasing perforation diameter.

---

[16] *Personal communication, R.W. Deas, USA ARRADCOM, Ballistic Research Laboratory, Aberdeen Proving Ground, Maryland, June 1979.*

TABLE I. GRAIN DIMENSIONS, COMPUTED PERFORMANCE, AND SURFACE AREAS FOR 37-PERFORATION PROPELLANT CHARGES

Design Grain Geometries	A	B	C
Length (L, mm)	34.6	41.7	50.2
Diameter (D, mm)	23.1	27.8	33.5
Perforation Diameter (DP, mm)	1.0	1.7	2.5
Web (mm)	2.0	2.0	2.0
L/D	1.5	1.5	1.5
L/DP	35.0	25.0	20.0
Computed Performance			
Charge Mass (kg)	11.79	11.79	11.79
Maximum Pressure (MPa)	321	321	325
Muzzle Velocity (m/s)	834	832	831
Surface Area of Charge			
Perforations (m^2)	2.15	2.73	3.11
External (m^2)	1.81	1.59	1.42
Total (m^2)	3.96	4.32	4.53

A hexagonal grain geometry was chosen for the 37-perforation grain, a general form function[17] being available to design a hexagonal grain with numbers of perforations equal to $3N^2 + 3N + 1$, where N is the number of concentric pin circles (N = 3 for 37-perforation). The hexagonal grain was being investigated in other studies because the outer slivers which result at web burn-through are reduced in size relative to those from a cylindrical grain, thus leading to improved progressivity and ballistic performance. A length-to-diameter ratio of 1.5 was selected to achieve better packing densities with the large grains.

The three lots of 37-perforation M30A1 propellant were produced at the Radford Army Ammunition Plant. Due to the novel nature of the geometry, technical problems were encountered and only two of the three lots ("A" and "B") could be produced in time for the test program; even these had unequal webs (see description sheets in Appendix A). A photograph of the grains along with the standard 7-perforation grain and a 19-perforation grain is included as Figure 5.

[17] *This form-function was developed by Mr. F.R. Lynn based on the ideas of Mr. R.W. Deas, both of this Laboratory.*

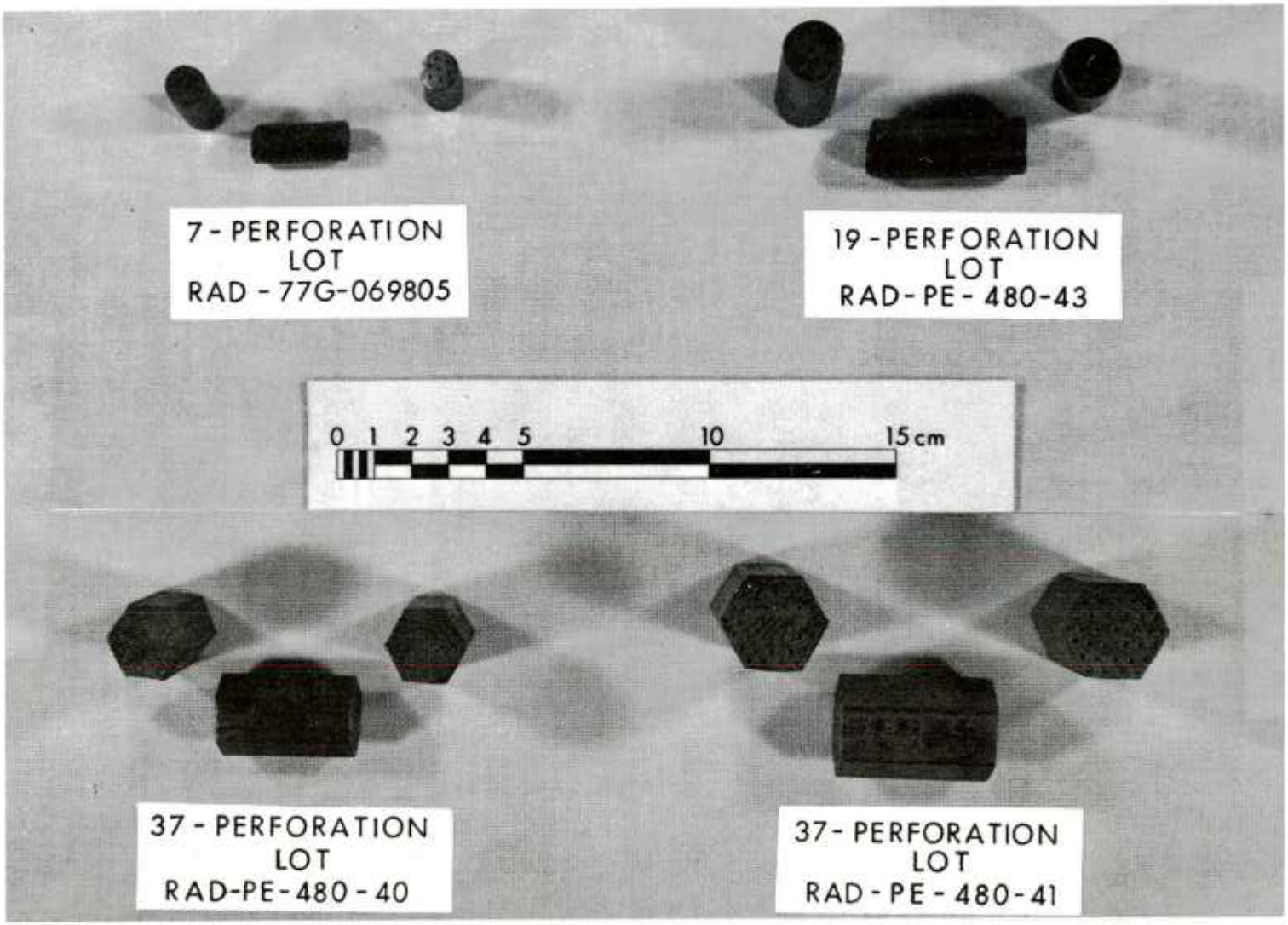

Figure 5. Sample Propellant Grains

B. NOVA Simulations

The NOVA two-phase flow interior ballistic code[18] was employed in an attempt to predict flamespread and pressure-wave characteristics of 155-mm propelling charges loaded with the various available propellant geometries. Charges employing 7-, 19-, and 37-perforation propellant were to be tested in a base-ignited, full-bore configuration, specifically selected to promote the formation of pressure waves (see Figure 6). The charges were thus of an appropriate geometry for treatment by the one-dimensional representation of NOVA. Input data for the simulations were independently determined (including propellant burning rate and projectile engraving/bore resistance) as discussed recently in a related report[19].

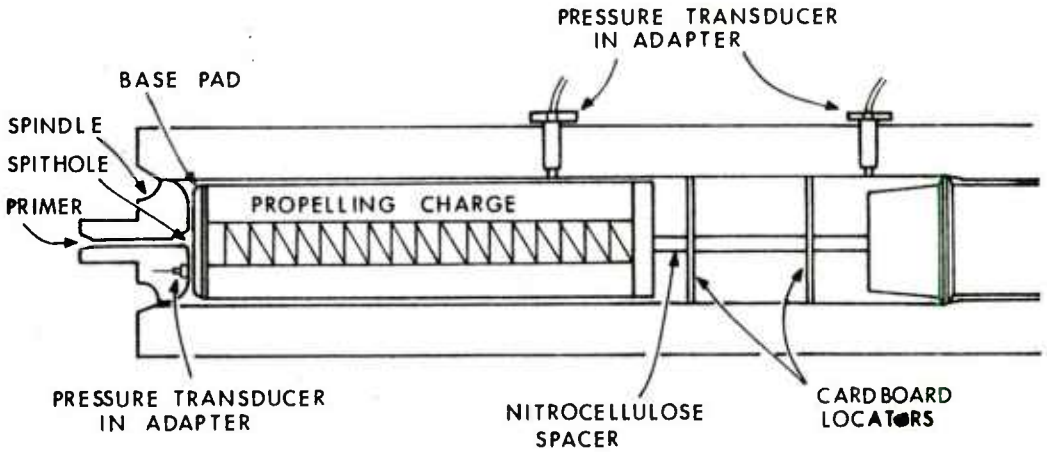

Figure 6. Full-Bore Test Configuration

A comparison of predicted pressure-difference profiles is presented in Figure 7. As expected, pressure-wave levels are predicted to decrease with increasing grain size. It must be remembered, however, that while NOVA models the macroscopic process of convectively-driven flamespread through the propellant bed, it assumes instantaneous flamespread over individual grain surfaces, including the perforations, so any effects related to delayed ignition of internal surfaces will not be captured in the simulation. Moreover, interphase drag is calculated from

---

[18] *P.S. Gough and F.J. Zwarts, "Modeling Heterogeneous Two-Phase Reacting Flow", AIAA Journal, Volume 17, No. 1, January 1979, pp. 17-25.*

[19] *A.W. Horst and T.R. Trafton, "NOVA Code Simulation of a 155-mm Howitzer: An Update", USA ARRADCOM, Ballistic Research Laboratory, Aberdeen Proving Ground, Maryland,* ARBRL-MR-02967.

empirical correlations, using an effective diameter

$$\left(D_p = \frac{6 \times \text{Volume of particle}}{\text{Surface of particle}}\right)$$

evaluated with full consideration of the presence of perforations. As flow may be blind to the perforations, this form may be inappropriate, at least during the early portion of the ballistic cycle.

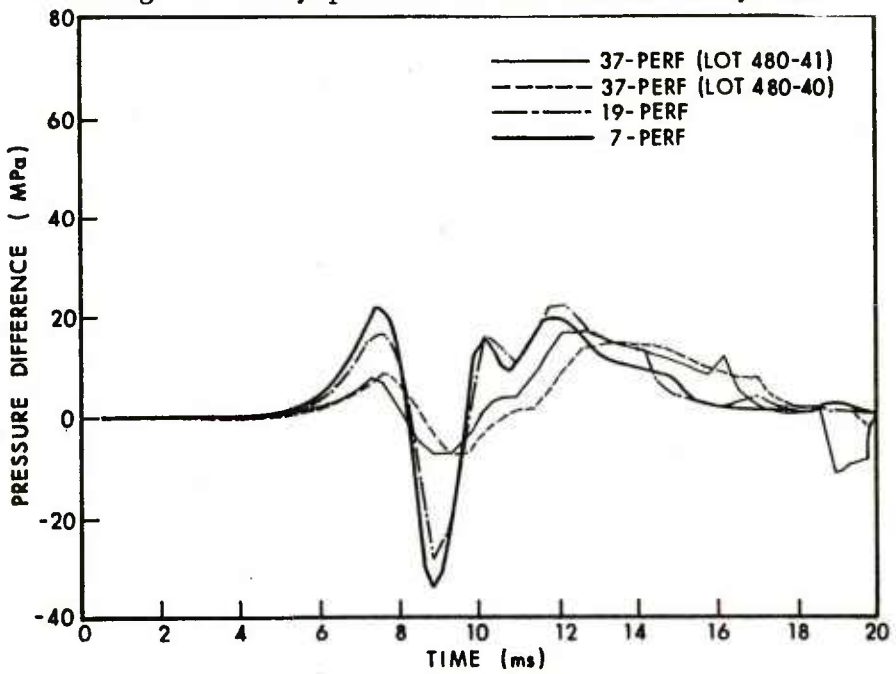

Figure 7. Comparison of NOVA Predictions for Pressure-Difference Profiles

In an earlier report, Rocchio et al[13], suggested that the effective particle diameter should be calculated neglecting perforations. Gough[20] subsequently commented that this correction is well-motivated but that the expression would still be an "inappropriate interpretation of grain parameters pertaining to the drag" in that the relatively low drag coefficient of a sphere is embedded in the correlations, and the perforation surfaces serve to partially (though fortuitously) compensate for this error. A more correct approach might then be to utilize a projected area and drag coefficient appropriate for a cylinder. Indeed, Gough provided sample calculations showing the resulting friction factor to be more than 100 percent higher for such a prescription than for that suggested by Rocchio with the present NOVA formulism leading to inter-

[20] *P.S. Gough, "Design and Analysis of Propellant Bed Permeability Test Fixture", Task III Report for Contract N00174-77-C-0103, Paul Gough Associates, Inc., Portsmouth, New Hampshire, December 1977.*

mediate values. Thus, unacceptable uncertainties in interphase drag are to be expected, even after one assumes the applicability of such correlations to unsteady flow at high Reynolds numbers.

C. Experimental Drag Studies

Because of the uncertainty associated with the estimation of potentially significant interphase drag forces, independent measurements were made to characterize this interaction for each of the propellants to be fired. In the NOVA code, interphase drag is calculated using Ergun's correlation[21] for steady flow through packed beds, modified to include a tortuosity factor suggested by Andersson[22] for fluidization:

$$\hat{f}_s = \frac{f_s}{\frac{1-\varepsilon}{D_p}\rho u^2} = \begin{cases} 1.75 & \varepsilon \le \varepsilon_o \\ 1.75\left[\frac{\varepsilon_o}{\varepsilon}\left(\frac{1-\varepsilon}{1-\varepsilon_o}\right)\right]^{0.45} & \varepsilon_o < \varepsilon \le \varepsilon_1 \\ 0.3 & \varepsilon_1 < \varepsilon \le 1 \end{cases}$$

where f_s = steady state component of the interphase drag force

ε = bed porosity

ε_o = settling porosity

$\varepsilon_1 = \left[1 + .02\left(\frac{1-\varepsilon}{\varepsilon_o}\right)\right]^{-1}$

ρ = gas density

u = relative velocity of phases

D_p = effective particle diameter = $\frac{6V_p}{S_p}$

Here $\hat{f}_s$ can be interpreted as a friction factor, which according to Ergun's data, is 1.75 for high Reynolds numbers. It must be remembered, however, that Ergun's results were for spherical shapes and for flows

[21] *S. Ergun, "Fluid Flow Through Packed Columns", Chemical Engineer Progr., Vol. 48, 1952, pp. 89-95.*

[22] *K.E.B. Andersson, "Pressure Drop in Ideal Fluidization", Chemical Engineer Science, Vol. 15, 1961, pp. 176-297.*

characterized by values of $\left(\frac{\varepsilon\ Re_p}{1-\varepsilon}\right)$ up to about 4000. An extension of data up to the flow regime of interest $\left(\frac{\varepsilon\ Re_p}{1-\varepsilon} \sim 10^5\right)$ and for actual grain shapes was clearly desirable.

Such an effort has been under way during the past year at the Naval Ordnance Station, Indian Head[23]. A schematic of their test fixture is shown in Figure 8. In general, a known quantity of propellant is loaded into the third section of the fixture, and N_2 gas is allowed to flow through the system at regulated levels. Pressure is measured at the sonic nozzle, the first orifice plate, and at various stations along the propellant bed. The temperature is also monitored as shown. The friction factor, $\hat{f}_s$, is then computed, according to:

$$\hat{f}_s = \frac{(P_j^2 - P_i^2)\ \varepsilon^3 A^2 D_p g_o}{2(1-\varepsilon)\dot{m}^2 RTL}$$

where: $\hat{f}_s$ = friction factor

P_i, P_j = pressure at stations i,j,i>j

ε = porosity

A = area

D_p = effective diameter of particle $(6V_p/S_p)$

$\dot{m}$ = mass flow rate

R = gas constant

T = temperature

L = length between gages i and j

g_o = constant to reconcile units.

Data from such testing employing samples of the 7-, 19-, and 37-perforation propellant fired in this study are summarized in Table II. Were the variations in dimensions between the different granulations properly accounted for in terms of the effective particle diameter, D_p, one would expect similar values of $\hat{f}_s$ for testing with all three propellant lots. Differences in bed porosity should have been compensated for similarly. One unavoidable problem was the relative influence of flow along the outside of the bed, where the porosity approaches unity at the wall. As the grains increase in size, the diameter of the

[23] *F.W. Robbins and P.S. Gough, "An Experimental Determination of Flow Resistance in Packed Beds of Gun Propellant", 15th JANNAF Combustion Meeting, CPIA Publication 297, Vol. I, p. 35-59, February 1979.*

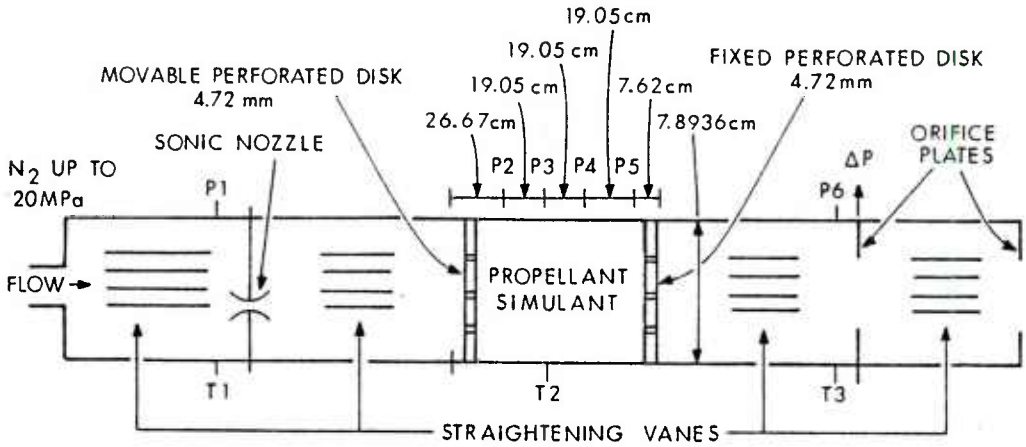

Figure 8. Test Fixture for Measuring Interphase Drag
(Naval Ordnance Station, Indian Head, MD)

test section becomes more important. Resistance to flow through the bed may become masked by the component of flow near the wall, as the one-dimensional analysis breaks down. The observed reduction in the apparent values of $\hat{f}_s$ as we replace the 7-perforation propellant with 19-perforation grains is consistent with this explanation. However, the increase in $\hat{f}_s$ for the 37-perforation, hexagonal granulation is not similarly explicable. Perhaps the large flat surfaces on these grains allow for tighter packing against the wall of the test section, significantly lowering the local porosity. These results suggest a need for continued studies in this area.

TABLE II. COMPARISON OF FRICTION FACTORS+

$\frac{\varepsilon Re_p}{1-\varepsilon}$	Ergun*	7-Perf (RAD-77-G-069805)	19-Perf (RAD-PE-480-43)	37-Perf (RAD-PE-480-40)
1000	1.90			
5000	1.78			
10000	1.77	1.45 (.99)	1.11 (.53)	
20000	1.76	1.35 (.92)	1.07 (.51)	1.5 (.85)
50000	1.75	1.25 (.85)	1.04 (.50)	1.6 (.91)
100000	1.75	1.20 (.82)	1.02 (.49)	1.6 (.90)
500000	1.75	1.20 (.82)	0.95 (.45)	
1000000	1.75			

* These values extrapolated beyond Ergun's data

\+ Values in parentheses include presence of perforations in calculation of D_p

D. Closed Bomb Studies

Closed bomb firings were conducted for each of the experimental propellants, and results were compared to data generated using a conventional 7-perforation, M30A1 granulation. All propellants exhibited similar burning rates (see Figure 9), though the RAD-PE-480-41 exhibited an unexplained slope break at ∿ 100 MPa. This anomaly may have resulted from the inability of the data reduction program to accurately represent the unfortunate inequality of webs exhibited by this lot. These results had little bearing on the selection of charges since much of the burning rate data were unavailable until after the howitzer firings were completed.

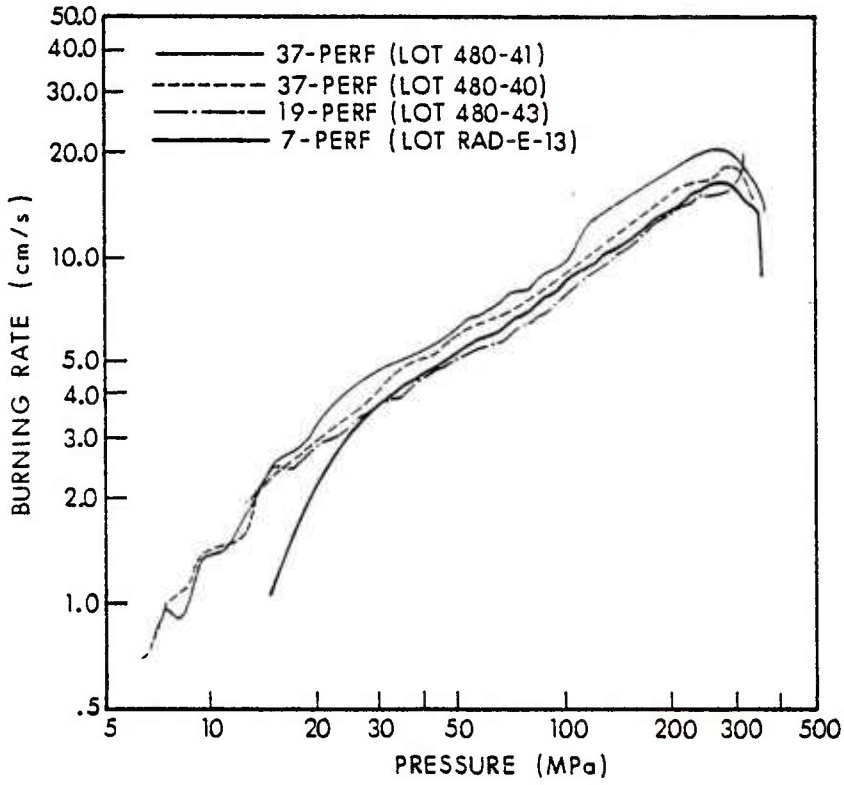

Figure 9. Closed Bomb Burning Rates for 7-, 19-, and 37-Perforation, M30A1, Propellants

IV. 155-mm HOWITZER FIRINGS

A. Fabrication of Charges

Fabrication of the full-bore diameter, random and stacked/random charges was accomplished using components from M203E1 Propelling Charges. The bag was modified by inserting a tapered wedge of cloth to form a sleeve with a base of 170-mm (6.7 in.) diameter at the spindle end and a 160-mm (6.3 in.) diameter opening at the other end. The random-loaded charges were filled through the 160-mm diameter opening. The stacked charges were assembled by attaching the base covers and stitching one-third the length of the bags. These partially sewn bags were then placed in an open-ended steel canister, 170-mm I.D. x 200-mm high, and a plastic insert was placed inside the bags to press them against the wall of the canister. When the propellant had been stacked to one-third the length of the finished charge, the plastic insert was removed, the seam sewn shut and the remaining propellant added. Due to the stacking of the propellant, the length of the charges was shortened, creating an excess of cloth, which was removed and the end cover added.

Base pads were prepared by altering the standard 8-inch M2 base pads. A circular pouch, 38-mm (1.5 in.) diameter, was sewn in the center into which 14 g (1/2 oz) of Class 5 black powder was inserted and the balance of the base pad filled with 56 g (2 oz) of CBI. The finished base pads were tied to the larger end of the loaded charges and the whole assembly tightly laced with a jacket. Figure 10 schematically depicts these charges.

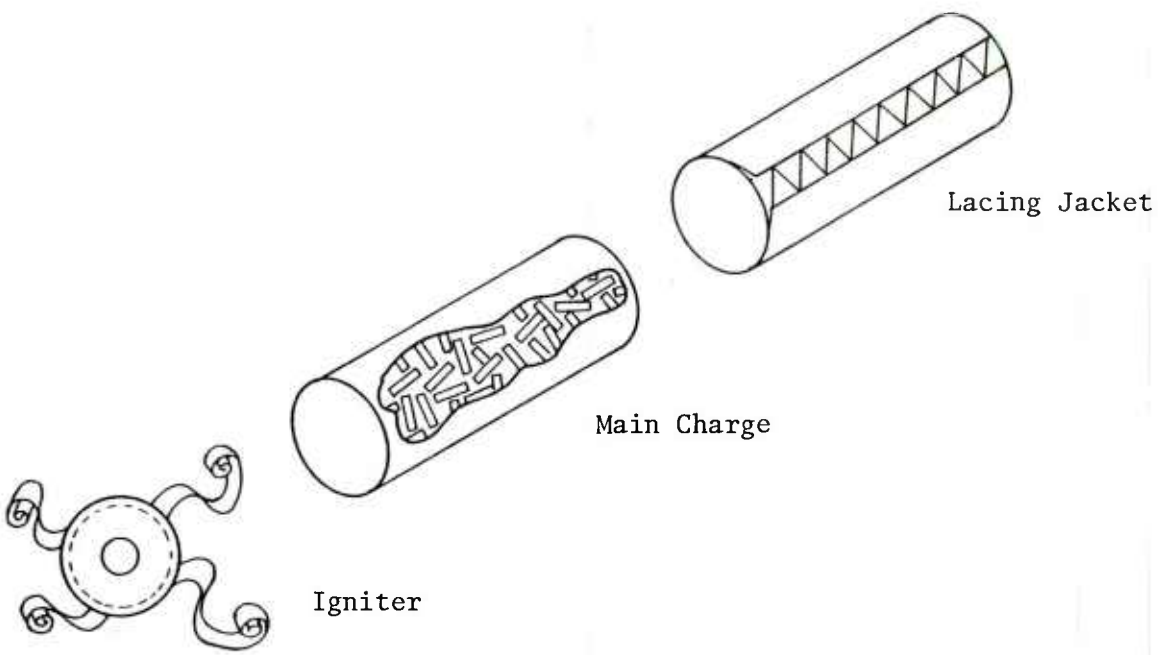

Figure 10. Exploded View of Test Charges

B. Test Procedures

All firings were conducted at the Ballistic Research Laboratory Sandy Point Firing Facility (R-18) in an M185 Cannon, modified to provide a chamber configuration similar to that of the M199 Cannon (see Figure 11). Multiple-station pressure-time data, differential pressures, and projectile velocities were recorded by the Ballistic Data Acquisition System (BALDAS), under the control of a PDP11/45 minicomputer. Pressures were measured using Kistler 607C3 piezoelectric transducers, and solenoid coils approximately 20 and 35 meters from the muzzle registered projectile velocities. Ignition delays were recorded by measuring the interval between the time the firing pulse was sent to the gun to the time a pressure of ∿10 MPa was first detected on the spindle gage. A backup analog magnetic tape system also recorded all data.

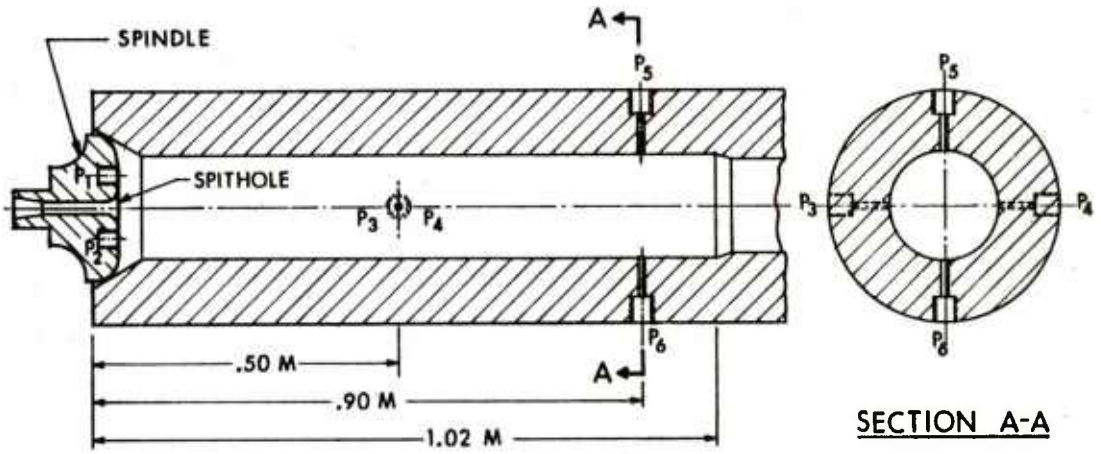

Figure 11. Locations of Pressure Taps in the Modified, M185 Cannon (Range 18)

All charges were conditioned in cardboard shipping containers at a temperature of 295-300 K for at least 24 hours prior to firing. The charges were loaded into the cannon chamber with zero standoff distance between the spindle face and the base of the charge to increase the likelihood of strong base ignition and large pressure waves. A spacer, made of nitrocellulose tubing and centered with cardboard locators, was placed between the base of the projectile and the forward end of the charge. Charge weights were assessed for each of the granulations such that expected maximum pressures would not exceed 350 MPa. These assessed weights were employed throughout the balance of the program. All firings were conducted using inert, M101 projectiles.

C. Firing Results

Firing data are tabulated in Appendix B, with computer-generated plots of selected data channels (spindle and forward pressures vs. time, pressure-difference vs. time) included as Appendix C.

Random-Loaded, Full-Bore Charges. Base-ignited, full-bore charges manufactured using the various propellant granulations, random-loaded, were first tested to provide a direct comparison of pressure-wave characteristics in this "worst-case" configuration. Table III summarizes firing results from this series. As expected, the magnitude of longitudinal pressures waves, as measured by the initial reverse pressure difference ($-\Delta P_i$) tends to decrease with increasing grain size.

TABLE III. SUMMARY OF FIRING DATA* FOR RANDOM-LOADED, FULL-BORE CHARGES

Propellant Lot	Charge Wt (kg)	Muzzle Velocity (m/s)	$P_{max}(P_2)$ (MPa)	$-\Delta P_i$ (P_2-P_6) (MPa)	Ignition Delay (ms)
7-Perf (77G-069805)	10.89	796 (18.5)	340 (31.9)	87 (17.4)	37 (20.8)
19-Perf (PE-480-43)	11.34	802 (7.5)	320 (28.7)	66 (14.1)	26 (3.8)
37-Perf (PE-480-40)	10.89	789 (3.7)	302 (4.8)	34 (12.6)	32 (9.0)
37-Perf (PE-480-41)	11.34	770 (16.9)	299 (33.2)	40 (18.6)	35 (16.4)

*Values shown are averages for 3-5 firings; sample standard deviations are shown in parentheses.

Interpretation of these data is, however, somewhat confounded by several factors. Production difficulties with the 37-perforation grains led to unequal webs and some shift in performance levels. In addition, excessive pressure waves and peak pressures with the 7-perforation charges precluded use of the full Zone 8 charge. Hence, differences in initial loading density (and porosity) for the various granulations accompanied the difference in charge weights, potentially masking some of the effects of granulation on bed permeability and initial mass generation rates. Nevertheless, the uncorrected relationship between the effective particle diameter ($D_p = 6V_p/S_p$) and the average differential pressure level ($-\Delta P_i$) for each of the granulations, shown in Figure 12, reveals the expected trend. The expected inverse relationship is seen to hold for total initial burning surface (excluding perforations) and $-\Delta P_i$ (see Figure 13).

Just as important as the level of pressure waves associated with each granulation is the sensitivity of maximum chamber pressures to such waves. A charge configuration tolerant of fluctuations in the level of pressure waves present without an accompanying shift in peak pressures or muzzle velocities is second best only to a system producing no waves at all! Such mechanisms as grain fracture and transient burning effects have already been listed as possible links between pressure waves and increases

in peak chamber pressure[7]. It is of more than just academic interest to us whether or not the different granulations may be susceptible to these mechanisms in varying degrees.

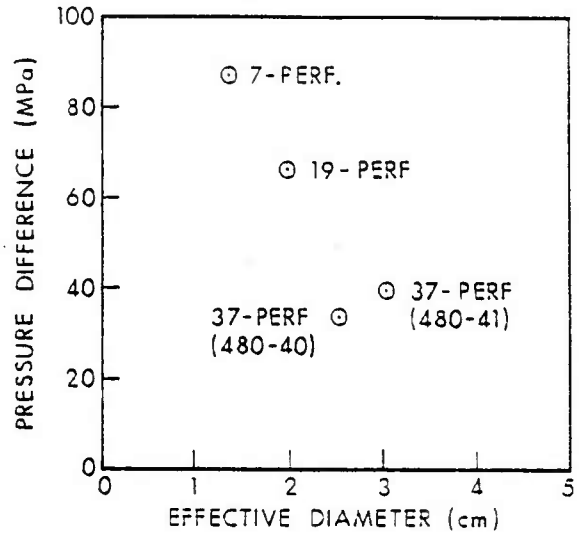

Figure 12. Initial Reverse Pressure Difference ($-\Delta P_i$) versus Effective Particle Diameter (D_p, perfs excluded)

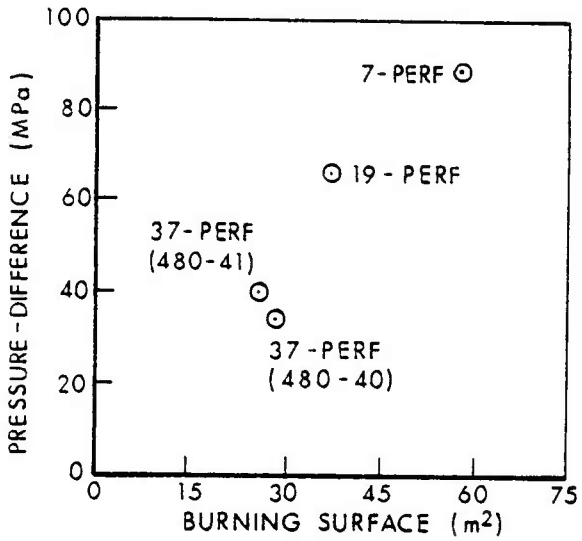

Figure 13. Initial Reverse Pressure Difference ($-\Delta P_i$) versus Total, Initial Burning Surface (perfs excluded)

The data, as depicted in Figure 14, do not, however, suggest that a lower sensitivity of peak pressure to pressure waves accompanies the use of the larger granulations. Again, the true relationship between these quantities may be obscured by differences in loading densities.

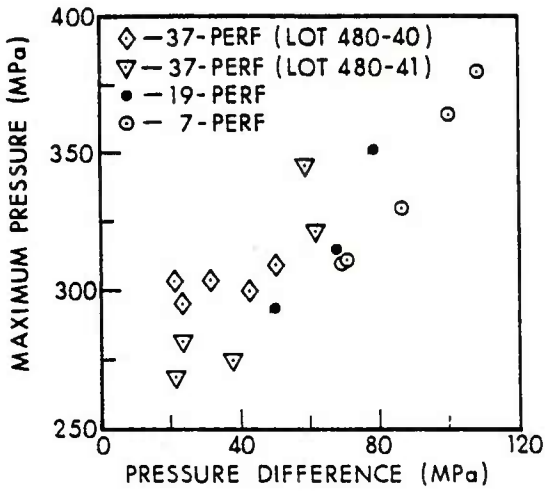

Figure 14. Maximum Chamber Pressure versus Initial Reverse Pressure Difference for Random-Loaded Propellant

Partially-Stacked, Full-Bore Charges. In an effort to approach the greater permeability to gas flow afforded by stick propellant, charges were loaded as shown in Figure 15, with one-third of the total bed length composed of stacked rather than random-loaded grains. Table IV summarizes firing results for this series of tests. Stacked, 37-perforation propellant charges were not fired because of the extremely tight packing of the hexagonally-shaped grains, leading to reduced rather than increased permeability.

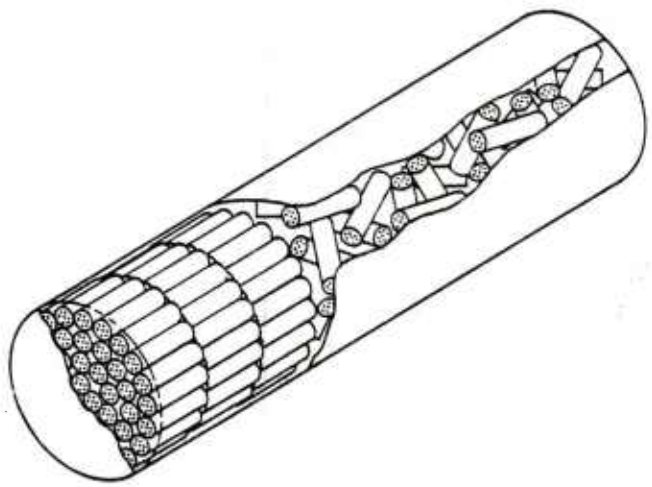

Figure 15. Partially-Stacked Test Charge

TABLE IV. SUMMARY OF FIRING DATA* FOR 1/3-STACKED, FULL-BORE CHARGES

Propellant Lot	Charge Wt(kg)	Muzzle Velocity (m/s)	P_{max} (P_2) (MPa)	$-\Delta P_i$ (P_2-P_6) (MPa)	Ignition Delay (ms)
7-Perf (77G-069805)	10.89	802 (18.5)	328 (42.9)	79 (30.3)	21 (10.8)
19-Perf (PE-480-43)	11.34	804 (3.8)	296 (11.7)	48 (15.4)	32 (21.7)

*Values shown are averages for 3-round groups; sample standard deviations are shown in parentheses.

Muzzle velocities are seen to be virtually unchanged from those of the random-loaded charges. However, average values for the differential pressures and, interestingly enough, maximum chamber pressures are reduced. Individual data points are plotted in Figure 16; general trends for P_{max} versus $-\Delta P_i$ remain largely unaffected.

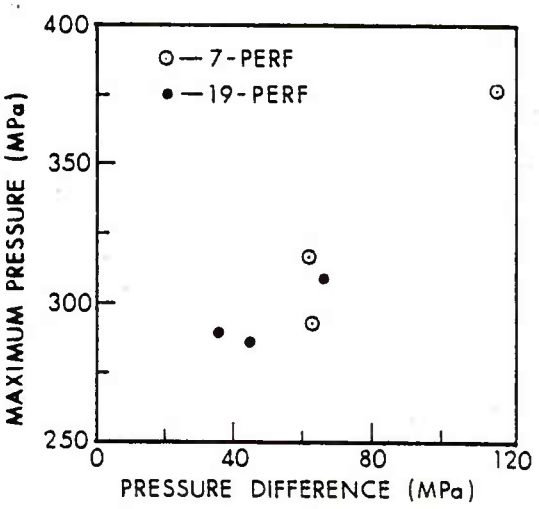

Figure 16. Maximum Chamber Pressure versus Initial Reverse-Pressure Difference for 1/3 Stacked Propellant

37-Perforation Propellant, Subcaliber Charge. A final configuration tested was a base-ignited, 37-perforation propellant charge with a reduced diameter. This variation was included to determine whether the added longitudinal permeability associated with the annular ullage in the chamber might result in acceptable Zone 8 ballistics from a base-ignited charge. The larger of the two 37-perforation propellant granulations (RAD PE-480-41) was employed, this time constrained to a charge diameter of about 150 mm. Table V summarizes the firing data for this configuration. Mean peak pressures and differential pressures were again reduced when compared to their full-bore counterparts. The average value for the initial reverse differential pressure was halved. More important, however, might be the reduction in the associated standard deviation: from 18.6 to 1.2 MPa!

TABLE V. COMPARISON OF FIRING DATA* FOR FULL-BORE AND SUBCALIBER CHARGES

Charge Configuration+	Charge Wt(kg)	Muzzle Velocity (m/s)	P_{max} (P_2) (MPa)	$-\Delta P_i$ (P_2-P_6) (MPa)	Ignition Delay(ms)
Full-Bore	11.34	770 (16.9)	299 (33.2)	40 (18.6)	35 (16.4)
Sub-Caliber	11.34	774 (10.0)	283 (14.6)	20 (1.2)	51 (21.1)

*Values shown are 3-5 round averages; sample standard deviations are shown in parentheses.
+Both configurations employed the same base pad igniter and 37-perforation propellant (RAD PE-480-41).

V. CONCLUSIONS & RECOMMENDATIONS

Initial goals for this study were somewhat compromised by the elimination of one of the lots of 37-perforation propellant because of production difficulties. Nevertheless, several conclusions can be drawn, based on the results of this study.

1. Results from the full-bore, random-loaded firings corroborate earlier data suggesting the importance of grain size to bed permeability and hence to the evolution of pressure waves. A similar statement might also be made concerning the relationship between initial (external) burning surface and pressure waves. The relative importance of the two factors cannot be discerned from limited data obtained during this program. In any case, one can expect that, for the full-bore configuration, the magnitude of longitudinal pressure waves will decrease with increases in grain size or with reductions in the initial (external) burning surface. Both these conditions are readily achievable by using 19- or 37-perforation granular propellant instead of the standard 7-perforation geometry. The same effect may be possible by choosing a larger 7-perforation grain with appropriately increased perforation diameters to achieve ballistic equivalence. The accompanying reduction in loading density may not, however, always be tolerable. Moreover, the larger perforation diameter may lead to earlier ignition of these internal burning surfaces and thereby mitigate the desired reduction in pressure waves.

2. Stacking or even partially stacking cylindrical propellant grains apparently increases propellant bed permeability, effecting a slight reduction in pressure waves. Since it is unlikely that this re-ordering of the individual grains in the bed will reduce the effective burning surface, the observed reduction in pressure waves verifies that bed permeability alone can be of significant importance. Stick and

tubular propellant configurations should offer even much greater increases in permeability to gas flow.

3. The data obtained using reduced-diameter charges reveal the importance of annular ullage to achieving pressure equilibration early in the ballistic cycle. This configural characteristic of many standard artillery bagged charges may be responsible for the forgivability of some charge/cannon combinations to such conditions as centercore misalignment or blockage. At the same time, one cannot help but wonder how much of the lack of reproducibility in pressure-wave levels exhibited by some charges may be attributable to variability in the persistence of annular ullage as influenced by differences in bag component materials or workmanship.

4. Despite some previous indicators that a reduced sensitivity of peak pressures to pressure waves might accompany use of 19- or 37-perforation propellant, no such trends can be observed from the results of this study. It might well be, however, that we have insufficient data to reveal any differences.

The above conclusions should be of some direct utility to the charge designer. There have been numerous studies throughout the gun community which provide convincing evidence supporting the desirability of 19- and 37-perforation propellant granulations for reduced pressure waves. Even in bag charges, where the flow area associated with annular ullage may dominate normal performance, this external path for pressure equilibration may be lost prematurely and the larger grains may offer life-saving benefits. The real challenge now is to develop a comprehensive understanding of the interaction between the various charge design parameters (e.g., propellant granulation, charge geometry, ignition performance, packaging) to exploit any possible synergistic effects.

REFERENCES

1. P. Vielle, Quoted by Cranz in "Lehrbuch der Ballistik" Volume II, Springer Verlag, Berlin, 1926, p. 151.

2. R.H. Kent, "Study of Ignition of 155-mm Gun in Connection with Project KW 250 --- Study of the Factors Involved in the Design of Propelling Charges", USA Ballistic Research Laboratories, Aberdeen Proving Ground, Maryland, Memorandum Report 4, February 1935. AD493405

3. R.H. Kent, "Study of Ignition of 155-mm Gun", USA Ballistic Research Laboratories, Aberdeen Proving Ground, Maryland, Report No. 22, October 1935. AD494763

4. D.W. Culbertson, M.C. Shamblen, and J.S. O'Brasky, "Investigation of 5"/38 Gun In-Bore Ammunition Malfunctions", Naval Weapons Laboratory, Dahlgren, Virginia, TR-2624, December 1971.

5. I.W. May, and E.V. Clarke Jr., "A Case History: Gun Ignition Related Problems and Solutions for the XM-198 Howitzer", USA Ballistic Research Laboratories, Aberdeen Proving Ground, Maryland, Interim Memorandum Report No. 150, October 1973 (no longer available).

6. P.J. Olenick, "Investigation of the 76-mm/62 Caliber Mark 75 Gun Mount Malfunction", Naval Surface Weapons Center, Dahlgren, Virginia, TR-3411, October 1975.

7. A.W. Horst, I.W. May, and E.V. Clarke, "The Missing Link Between Pressure Waves and Breechblows", USA ARRADCOM, Ballistic Research Laboratory, Aberdeen Proving Ground, Maryland, Memorandum Report No. 02849, July 1978. AO58354

8. A.W. Horst, T.C. Smith, and S.E. Mitchell, "Key Design Parameters in Controlling Gun-Environment Pressure Wave Phenomena - Theory vs. Experiment", 13th JANNAF Combustion Meeting, CPIA Publication 281, Vol. I, pp. 341-367, December 1976.

9. J.L. East, Jr., "A Consumable, Tubeless Igniter for Gun Pressure Wave Reduction and Improved Ignition", 13th JANNAF Combustion Meeting, CPIA Publication 281, Vol. I, pp. 451-474, December 1976.

10. J. Foster, "Detonation Rate Ignition Propagation Primer", 15th JANNAF Combustion Meeting, CPIA Publication 297, Vol. I, pp. 411-455, February 1979.

11. S. Livanis, "Novel Ignition Systems for Improved Gun Interior Ballistic Performance", 15th JANNAF Combustion Meeting, CPIA Publication 297, Vol. I, pp. 367-381, February 1979.

12. J.J. Rocchio, K.J. White, C.R. Ruth, and I.W. May, "Propellant Grain Tailoring to Reduce Pressure Wave Generation in Guns", 12th JANNAF Combustion Meeting, CPIA Publication 273, Vol. I, pp. 275-301, December 1975.

13. J.J. Rocchio, C.R. Ruth, and I.W. May, "Grain Geometry Effects on Wave Dynamics in Large Caliber Guns", 13th JANNAF Combustion Meeting, CPIA Publication 281, Vol. I, pp. 369-382, December 1976.

14. J.J. Rocchio and C.R. Ruth, "An Investigation of the Interior Ballistic Performance of a 19-Perforation, M30A1 Propellant Granulation in the Zone 8 Charge of the 155-mm, M198 Howitzer", USA ARRADCOM, Ballistic Research Laboratory, Aberdeen Proving Ground, Maryland, Memorandum Report, (report in preparation).

15. C.T. Boyer, Jr., "Interim Charge Assemblies Developed for Use with the 8-Inch Paveway GP in the MK 71 Gun", Naval Surface Weapons Center, Dahlgren, Virginia, NSCW/DL TR-5707, December 1977.

16. Personal communication, R.W. Deas, USA ARRADCOM, Ballistic Research Laboratory, Aberdeen Proving Ground, Maryland, June 1979.

17. This form-function was developed by Mr. F.R. Lynn based on the ideas of Mr. R.W. Deas, both of this Laboratory.

18. P.S. Gough and F.J. Zwarts, "Modeling Heterogeneous Two-Phase Reacting Flow", AIAA Journal, Volume 17, No. 1, January 1979, pp. 17-25.

19. A.W. Horst and T.R. Trafton, "NOVA Code Simulation of a 155-mm Howitzer: An Update", USA ARRADCOM, Ballistic Research Laboratory, Aberdeen Proving Ground, Maryland, ARBRL-MR-02967.

20. P.S. Gough, "Design and Analysis of Propellant Bed Permeability Test Fixture", Task III Report for Contract N00174-77-C-0103, Paul Gough Associates, Inc., Portsmouth, New Hampshire, December 1977.

21. S. Ergun, "Fluid Flow Through Packed Columns", Chemical Engineer Progr., Vol. 48, 1952, pp. 89-95.

22. K.E.B. Andersson, "Pressure Drop in Ideal Fluidization", Chemical Engineer Science, Vol. 15, 1961, pp. 176-297.

23. F.W. Robbins and P.S. Gough, "An Experimental Determination of Flow Resistance in Packed Beds of Gun Propellant", 15th JANNAF Combustion Meeting, CPIA Publication 297, Vol. I, p. 35-59, February 1979.

APPENDIX A

PROPELLANT DESCRIPTION SHEETS

PROPELLANT DESCRIPTION SHEET

CORRECTED COPY*

U.S. Army Lot No. RAD77G-069805 Contract No. M30A1 for Use in Propelling Charge M203, f/155mm How., M198

Name and Address of Contractor RADFORD ARMY AMMUNITION PLANT, RADFORD, VA. Packed Amount 320,975 lbs

Contract No. DAAA09-77-C-4007 Date 4-1-77 Specification No. MIL-P-48367A

NITROCELLULOSE

Accepted Blend Numbers	Nitrogen Content	Ether Solubility (25°C)	Stability (134.5°C)
C-35,556; 557; 558; 565; 566; 570; 573; 576; 577; 579	Maximum 12.60 %	Min.	Min.
	Minimum 12.50 %	Min.	Min.
	Average 12.56 %	45+ Min.	30+ Min.
			Explosion Min.

MANUFACTURE OF PROPELLANT

0.22 Parts Solvent per Parts Dry Weight Nitrocellulose Consisting of 60 Percent Ether and 40 Percent ALCOHOL Percent Solvent Recovered

Percentage Ether to Alcohol 12

Temperature °F From	Temperature °F To	PROCESS-SOLVENT RECOVERY AND DRYING	Time Hours	Time Minutes
		Load Forced Air Dry at Ambient Temperature		
Ambient	140	Increase Temperature 5°F per Hour		
140	140	Hold at Temperature		72

TESTS OF FINISHED PROPELLANT

PROPELLANT COMPOSITION

Constituent	Percent Formula	Percent Tolerance	Percent Recovered
Nitrocellulose	28.00	±1.30	27.18
Nitroglycerin	22.50	±1.00	22.80
Nitroguanidine	47.00	±1.00	47.54
Ethyl Centralite	1.50	±0.10	1.55
Potassium Sulfate	1.00	±0.30	0.93
TOTAL	100.00		100.00
Graphite Glaze (added)	0.13	Max.	0.08
Total Volatiles	0.50	Max.	0.33

STABILITY AND PHYSICAL TESTS

	Formula	Actual
Heat Test 5.P. 120°F	NO CC 40'	60'
No Fumes	- - -	60'
Form of Propellant, Type I		Cylinder
No. of Perforations		7

CLOSED BOMB

	Lot Number	Temp °F	Relative Quickness	Relative Force
Test	RAD77G-069805	+90	96.51 %	99.74 %
	RAD77G-069805	-40	92.58 %	98.16 %
Standard	RAD-E-14		100.00%	100.00%
Remarks				
FIRED IN ACCORDANCE WITH MIL-STD-286B, METHOD 801.1,				
IN A NOMINAL SIZE 700 CC CLOSED BOMB. TEST				
FOR INFORMATIONAL PURPOSES ONLY.				

PROPELLANT DIMENSIONS (inches)

	Specification	Die	Finished	Mean Variation in % of Mean Dimension: Spec.	Actual
Length (L)		0.949	0.9481	±.25 Max.	1.08
Diameter (D)		0.470	0.4173	±.125 Max.	1.28
Perforation (d)		0.039	0.0338		
WEB					
Inner		0.0930	0.0793		
Outer		0.0845	0.0806		
Average		0.0888	0.0800		
Web Difference/ Std. Dev. in % of Web Average	15 Max.		2		
L/D	2.10 to 2.50		2.27		
D/d	5.0 to 15		12.4		

DATES

Packed	7-20-77
Sampled	7-20-77
Test Finished	7-27-77
Offered	8-18-77
Description Sheets Forwarded	8-23-77

Type of Packing Container FIBER DRUMS PER MIL-STD-662C WITH NOTICE 1

Remarks This is the first propellant lot using toluene as an alcohol denaturant.

*Issued to replace description sheet dated 8-10-77 to add statement concerning type of alcohol denaturant used.

THIS LOT MEETS ALL THE CHEMICAL AND PHYSICAL REQUIREMENTS OF THE APPLICABLE SPECIFICATION.

Contractor's Representative H. C. Dickinson H.C. Dickinson

Government Quality Assurance Representative JAMES E. BLAND James E Bland

PREVIOUS EDITION MARCH 1975

(Orig. 7/76)

PROPELLANT DESCRIPTION SHEET

U S Army Lot No. RAD PE 480-43 Composition No. M30A1 19MP

Manufactured at RADFORD ARMY AMMUNITION PLANT, RADFORD, VA. Process Amount 978 lbs.

Contract No DAAA09-77-C-4007 Date 4-1-77 Specification No COR letter SARRA-IE, dated 5/18/78

NITROCELLULOSE

ACCEPTED BLEND NUMBERS: C-35,996

Nitrogen Content	Ac Starch (65.5°C)	Stability (134.5°C)
Maximum ____ %	____ Mins	____ Mins
Minimum ____ %	____ Mins	____ Mins
Average 12.60 %	- ____ Mins	30 Mins
		Explosion ____ Mins

MANUFACTURE OF PROPELLANT

0.22 Pounds Solvent per Pound NC/Dry Weight Ingredients Consisting of 60 Pounds Alcohol and 40 Pounds acetone per 100 Pounds Solvent

Percentage Ratio to Whole 50

TEMPERATURES °C From	To	PROCESS-SOLVENT RECOVERY AND DRYING	TIME Days	Hours
		Load forced air dry at ambient temperature		
Ambient	140	Increase temperature 5°F per hour		12
140	140	Hold at temperature		100

TESTS OF FINISHED PROPELLANT

PROPELLANT COMPOSITION

Constituent	Percent Formula	Percent Tolerance	Percent Measured
Nitrocellulose	28.00	± 1.30	28.44
Nitroglycerin	22.50	± 1.00	21.21
Nitroguanidine	47.00	± 1.00	47.72
Ethyl Centralite	1.50	± 0.10	1.53
Potassium Sulfate	1.00	± 0.10	1.10
TOTAL	100.00		100.00
Total Volatiles	0.50	Max	0.12
Graphite Glaze	0.2	Max	0.09

STABILITY AND PHYSICAL TESTS

	Formula	Actual
Heat Test SP, 120°C	No CC 40'	60"+
No fumes		1 hr
Form of Propellant		Cyld
No. Perforations		19
Density, gm/cc	N/A	1.674
Heat of Explosion, cal/gm	N/A	966.2

CLOSED BOMB

	Lot Number	Temp °F	Relative Quickness	Relative Force
Test	RAD -PE-480-43	+90	98.79	98.48
	RAD -PE-480-43	-40	94.74	96.65
Standard	RAD-E-1	+90	100.00%	100.00%

Remarks: Fired in accordance with MIL-STD-286B, Method 801.1, in a nominal size 700cc closed bomb. Test for informational purposes only. Loading Density was 0.2 gm/cc

PROPELLANT DIMENSIONS (inches)

	Specification	Die	Finished	Mean Variation in % of Mean Dimensions: Spec.	Actual
Length(L)	1.59 nom	1.595	1.632	N/A	1.45
Diameter(D)		0.703	0.615	N/A	--
Perf. Dia.(d)		0.044	0.0384		
Web, Avg	0.071, Nom	0.0822	0.0706		
Inner		0.0930	0.0726		
Outer(1)		0.0880	0.0719		
Outer(2)		0.0655	0.0672		
Web Difference/ Std. Dev. in % of Web Average	10% Max	0	4.16		
L/D	2.5 Nom	2.27	2.64		
D/d	15.5 Nom	15.98	16.06		

DATES

Packed 6/12/78

Sampled 6/12/78

Test Finished 7/10/78

Offered 7/10/78

Description Sheets Forwarded 7/12/78

Type of Packing Container Fiber Drums: 6 @ 150 lbs. net; 1 @ 70 lbs. net.

Remarks

This lot meets all the chemical and physical requirements of the applicable specification, except for nitroglycerin content.

Contractor's Representative: R. A. Williams — R. A. Williams

Government Quality Assurance Representative: James E. Bland — James E. Bland

DRU FORM 1647B MARCH 1979

PROPELLANT DESCRIPTION SHEET

U.S. Army Lot No. RAD-PE-480-40 Composition No. M30A1 37MP

Manufactured at RADFORD ARMY AMMUNITION PLANT, RADFORD, VA. Packed Amount 356 lbs.

Contract No. DAAA09-77-C-4007 Date 4-1-77 Specification No.

NITROCELLULOSE

ACCEPTED BLEND NUMBERS	Nitrogen Content	KI Starch (65.5°C)	Stability (134.5°C)
C-35,945	Maximum %	Mins.	Mins
	Minimum %	Mins.	Mins.
	Average 12.63 %	Mins.	30+ Mins
			Explosion Mins.

MANUFACTURE OF PROPELLANT

Pounds Solvent per Pound NC/Dry Weight Ingredients Consisting of Pounds Alcanol and Pounds per 100 Pounds Solvent.

Percentages Remix to Whole

TEMPERATURES °C From	To	PROCESS-SOLVENT RECOVERY AND DRYING	TIME Days	Hours
80	140	Temperature increased at rate of 5°F/hour		12
140	140	Dried 40 hours prior to sawing		40
140	140	Dried 40 hours after sawing		40

TESTS OF FINISHED PROPELLANT

PROPELLANT COMPOSITION

Constituent	Percent Formula	Percent Tolerance	Percent Measured
Nitrocellulose	28.00	± 1.30	28.30
Nitroglycerin	22.50	± 1.00	22.03
Ethyl Centralite	1.50	± 0.10	1.55
Nitroguanidine	47.00	± 1.00	47.08
Potassium Sulfate	1.00	± 0.30	1.04
Total	100.00		100.00
Graphite Glaze	0.15	Max	0.12
Total Volatiles	0.50	Max	0.19

STABILITY AND PHYSICAL TESTS

	Formula	Actual
S.P. 120°C		
Heat Test S.P., 120°C	No CC 40'	60' +
No. Fumes		60'
Form of Propellant	Hexagon	Hexagon
No. of Perfs	37	37
Avg Grain Wt, gms	N/A	16.926
Std Dev	N/A	0.7638
Heat of Explo. cal/gm	N/A	975.8

CLOSED BOMB

	Lot Number	Temp °F	Relative Quickness	Relative Force
Test	RAD-PE-472-40	+90	103.46	97.67
	RAD-PE-472-40	-40	101.04	97.18
Standard	RAD-E-14-73	+90	100.00%	100.00%
Remarks	Fired in 700 cc closed bomb using 0.2 g/cc loading density using method 801.1 of MIL-STD-286B			

PROPELLANT DIMENSIONS (inches)

	Specification	Dia	Finished	Mean Variation in % of Mean Dimensions Spec.	Actual
Length (L)	1.4 nom	1.4	1.385	N/A	0.97
Diameter (D)	0.909, nom	1.027	0.873	N/A	1.50
Perf. Dia. (d)	0.039, nom	0.043	0.0343		
Web, Inner	0.080, nom	0.132	0.0936		
Web, Mid-I	0.080, nom	0.105	0.0792		
Web, Mid-O	0.080, nom	0.0715	0.0692		
Web, Outer	0.080, nom	0.0545	0.0783		
Web Difference/ Std. Dev. in % of Web Average	N/A		12.6		
L/D	N/A		1.58		
D/d	N/A		25.45		

DATES

Packed 6/28/78

Sampled 6/28/78

Test Finished 7-13-78

Offered 7-13-78

Description Sheets Forwarded 7-24-78

Type of Packing Container FIBER DRUMS: 2 @ 150 lbs. net; 1 @ 48 lbs. net.

Remarks Average web = 0.0800 inch.

Lot produced on best efforts basis. Dimensional data were acceptable to BRL.

Contractor's Representative R. J. Reese 37

Government Quality Assurance Representative James E Bland

SMU FORM 1047R MARCH 1971

PROPELLANT DESCRIPTION SHEET

U.S. Army Lot No. RAD-PE-480-41 Composition No. M30A1 37MP

Manufactured at RADFORD ARMY AMMUNITION PLANT, RADFORD, VA. Packed Amount 428 lbs.

Contract No. DAAA09-77-C-4007 Date 4-1-77 Specification No.

NITROCELLULOSE

ACCEPTED BLEND NUMBERS	Nitrogen Content	KI Starch (65.5°C)	Stability (134.5°C)
C-15,135	Maximum %	Mins.	Mins.
C35945	Minimum %	Mins.	Mins.
	Average 12.63 %	Mins.	30+ Mins.
			Explosion Mins.

MANUFACTURE OF PROPELLANT

Pounds Solvent per Pound NC/Dry Weight Ingredients Consisting of Pounds Alcohol and Pounds per 100 Pounds Solvent.

Percentage Ratio to Whole

TEMPERATURES °F From	To	PROCESS-SOLVENT RECOVERY AND DRYING	TIME Days	Hours
80	140	Temperature increased at rate of 5°F/hr		12
140	140	Dried 40 hours prior to sawing		40
140	140	Dried 40 hours after sawing		40

TESTS OF FINISHED PROPELLANT

PROPELLANT COMPOSITION Constituent	Percent Formula	Percent Tolerance	Percent Measured	STABILITY AND PHYSICAL TESTS	Formula	Actual
Nitrocellulose	28.00	± 1.30	27.95	Heat Test S.P., 120°C	No CC 40'	60'+
Nitroglycerin	22.50	± 1.00	22.21	No fumes		60'
Ethyl Centralite	1.50	± 0.10	1.54	Form of Propellant	Hexagon	Hexagon
Nitroguanidine	47.00	± 1.00	47.26	No. Perfs	37	37
Potassium Sulfate	1.00	± 0.30	1.04	Avg Grain Wt, g	N/A	27.474
Total	100.00		100.00	Std Dev	N/A	0.9544
Graphite Glaze	0.15	max	0.13	Heat of Explo	N/A	971.7
Total Volatiles	0.50	max	0.21	cal/gm		

CLOSED BOMB

	Lot Number	Temp °F	Relative Quickness	Relative Force
Test	RAD-PE-472-41	+90	89.64	99.16
	RAD-PE-472-41	-40	83.66	97.00
Standard	RAD-E-14-73	+90	100.00%	100.00%
Remarks	Fired in 700 cc closed bomb using 0.2 g/cc loading density using method 801.1 of MIL-STD-286B			

PROPELLANT DIMENSIONS (inches)

	Specification	Dia	Finished	Mean Variation In % of Mean Dimensions Spec.	Actual
Length (L)	1.6 nom	1.6	1.595	N/A	0.84
Diameter (D)	1.09 nom	1.231	1.059	N/A	2.15
Perf. Dia. (d)	0.066 nom	0.073	0.0618		
Web, inner	0.079 nom	0.1405	0.1249		
Web, Mid-I	0.079 nom	0.1070	0.0926		
Web, Mid-O	0.079 nom	0.0655	0.0553		
Web, Outer	0.079 nom	0.04700	0.0417		
Web Difference/ Std. Dev. in % of Web Average	N/A		47.85		
L/D	N/A		1.51		
D/d	N/A		17.14		

DATES

Packed 6/28/78

Sampled 6/28/78

Test Finished 7-13-78

Offered 7-13-78

Description Sheets Forwarded 7/24/78

Type of Packing Container FIBER DRUMS: 2 @ 150 lbs. net; 1 @ 120 lbs. net.

Remarks Avg Web = 0.0786 inch

Lot produced on best effort basis. Dimensional data were acceptable to BRL.

Contractor's Representative R. J. Reese 38

Government Quality Assurance Representative James E Blanc

SMU FORM 10-47R (MARCH 1971)

APPENDIX B

TABULATION OF FIRING DATA

TABULATION OF FIRING DATA

IDENT. NO.	PROP. & LOT	CHG. WT. (kg)	PROJ. WT. (kg)	CHARGE CONFIG.	CHARGE LENGTH (cm)	SEATING (cm)	VELOCITY (m/s)	MAX. CHAMBER PRESSURE (MPa) Spindle P_1	Spindle P_2	Forward P_5	Forward P_6	IGN. DELAY (ms)	$-\Delta P_j$ (MPa)
68		10.89	43.4		64.0	89.9	790	+	+	+	+	+	+
69		"	43.2		66.3	90.0	788	302	300	289	290	25	43
70	37-Perf.	"	43.4	Full-	67.3	89.8	796	311	309	305	304	24	50
71	RAD-PE-	"	43.0	Bore	67.3	89.9	786	+	+	+	+	+	+
72	480-40	"	43.2	Random	67.3	90.0	792	306	304	290	289	31	31
73		"	43.3		66.8	89.9	787	305	303	288	284	36	21
74		"	43.1		66.8	90.0	787	298	296	282	280	46	23
						(Avg.)	789	304	302	291	289	32	34
						(Std. Dev.)	(3.7)	(4.8)	(4.8)	(8.5)	(9.1)	(9.0)	(12.6)
75		10.89	43.4		70.6	89.9	733	254	252	*	241	*	14
78		11.34	43.0		71.4	89.9	759	276	275	261	257	57	37
79	37-Perf.	"	43.1	Full-	71.6	89.9	776	*	322	*	278	13	60
80	RAD-PE-	"	43.0	Bore	71.4	89.8	763	281	282	270	266	31	23
81	480-41	"	42.9	Random	71.9	89.9	796	349	345	307	310	30	58
82		"	43.1		71.7	89.9	754	269	269	255	254	43	21
						(Avg.)	770	294	299	273	273	35	40
						(Std. Dev.)	(16.9)	(37.2)	(33.2)	(23.3)	(22.7)	(16.4)	(18.6)
103	37-Perf.	11.34	42.8	Sub-	73.7	90.1	763	*	266	*	244	40	19
104	RAD-PE-	"	42.8	Caliber	74.9	90.0	778	289	293	274	272	37	21
105	480-41	"	42.7		74.3	90.1	782	288	289	274	272	75	19
						(Avg.)	774	289	283	274	263	51	20
						(Std. Dev.)	(10.0)	(0.7)	(14.6)	(0.0)	(16.2)	(21.1)	(1.2)

\+ Unexpected ignition delay; missed data acquisition window
* Data not reduced
All Charges fired at +21°C and zero standoff

TABULATION OF FIRING DATA

IDENT. NO.	PROP. & LOT	CHG. WT. (kg)	PROJ. WT. (kg)	CHARGE CONFIG.	CHARGE LENGTH (cm)	SEATING (cm)	VELOCITY (m/s)	MAX. CHAMBER PRESSURE (MPa) Spindle P_1	Spindle P_2	Forward P_5	Forward P_6	IGN. DELAY (ms)	$-\Delta P_j$ (MPa)
88	7-Perf.	10.89	43.2	Full-	60.9	89.9	812	373	368	320	318	23	100
89	IND	"	43.3	Bore	61.5	90.0	779	333	331	291	291	29	86
90	78-G-	"	43.1	Random	60.9	89.9	817	387	379	352	333	24	108
91	069805	"	43.1		60.5	89.8	795	301	310	278	279	35	69
92		"	43.2		60.9	89.9	777	*	312	*	272	73	70
						(Avg.)	796	348	340	310	299	37	87
						(Std.Dev.)	(18.5)	(39.1)	(31.9)	(32.9)	(26.1)	(20.8)	(17.4)
98	7-Perf.	10.89	42.7	Full Bore	56.9	89.9	788	290	293	268	272	33	62
99	IND 78-G-	"	42.8	Lower 1/3	56.4	90.0	795	*	316	*	273	18	61
100	069805	"	42.7	Stacked	55.9	90.0	823	403	376	371	358	12	114
						(Avg.)	802	347	328	320	301	21	79
						(Std.Dev.)	(18.5)	(79.9)	(42.9)	(72.8)	(49.4)	(10.8)	(30.3)
83	19-Perf.	10.89	43.2	Full-Bore	61.0	89.8	765	+	+	+	+	+	+
84	RAD-PE	11.34	43.0	Random	62.2	89.9	794	*	294	*	280	29	51
85	480-43	"	43.2		62.5	"	809	*	351	*	313	28	79
86		"	43.1		62.7	"	802	*	315	*	296	22	67
						(Avg.)	802		320		296	26	66
						(Std.Dev.)	(7.5)		(28.7)		(16.5)	(3.8)	(14.1)
95	19-Perf.	11.34	42.8	Full-Bore	59.7	89.9	808	307	309	290	290	20	65
96	RAD-PE-	"	42.8	Lower 1/3	59.9	90.0	802	293	291	275	276	57	35
97	480-43	"	42.8	Stacked	59.9	89.9	801	287	287	272	271	19	44
						(Avg.)	804	296	296	279	279	32	48
						(Std.Dev.)	(3.8)	(10.3)	(11.7)	(9.6)	(9.9)	(21.7)	(15.4)

\+ Unexpected ignition delay; missed data acquisition window
* Data not reduced
All Charges fired at +21°C and zero standoff

APPENDIX C

PLOTS OF PRESSURES (SPINDLE AND FORWARD)

AND PRESSURE-DIFFERENCES VERSUS TIME

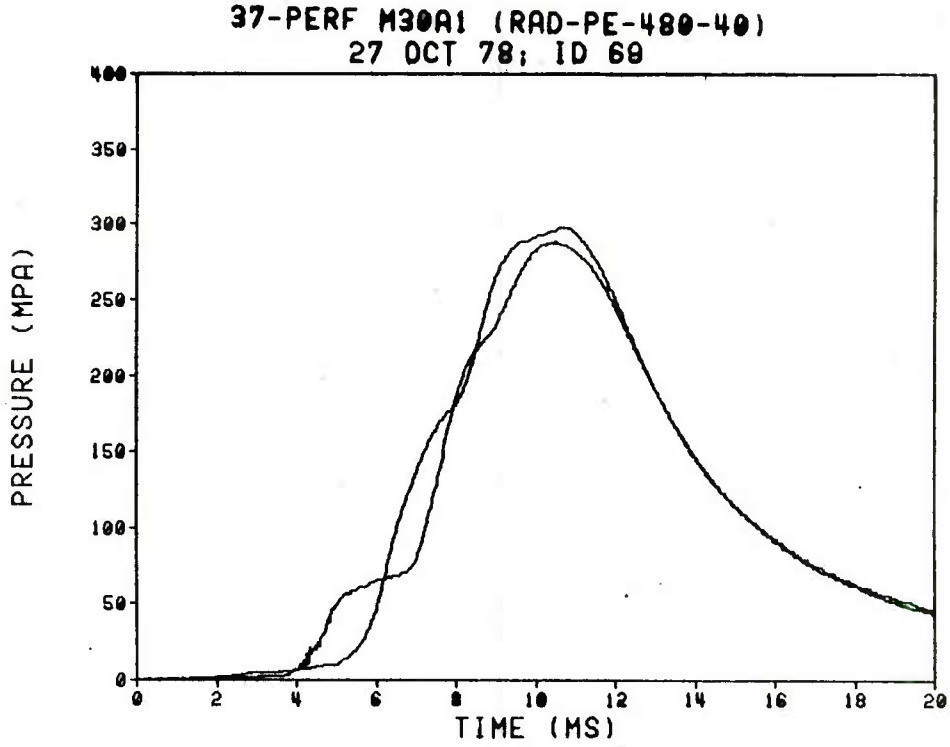
37-PERF M30A1 (RAD-PE-480-40)
27 OCT 78; ID 69
PRESSURE (MPA)
400
350
300
250
200
150
100
50
0
0
2
4
6
8
10
12
14
16
18
20
TIME (MS)

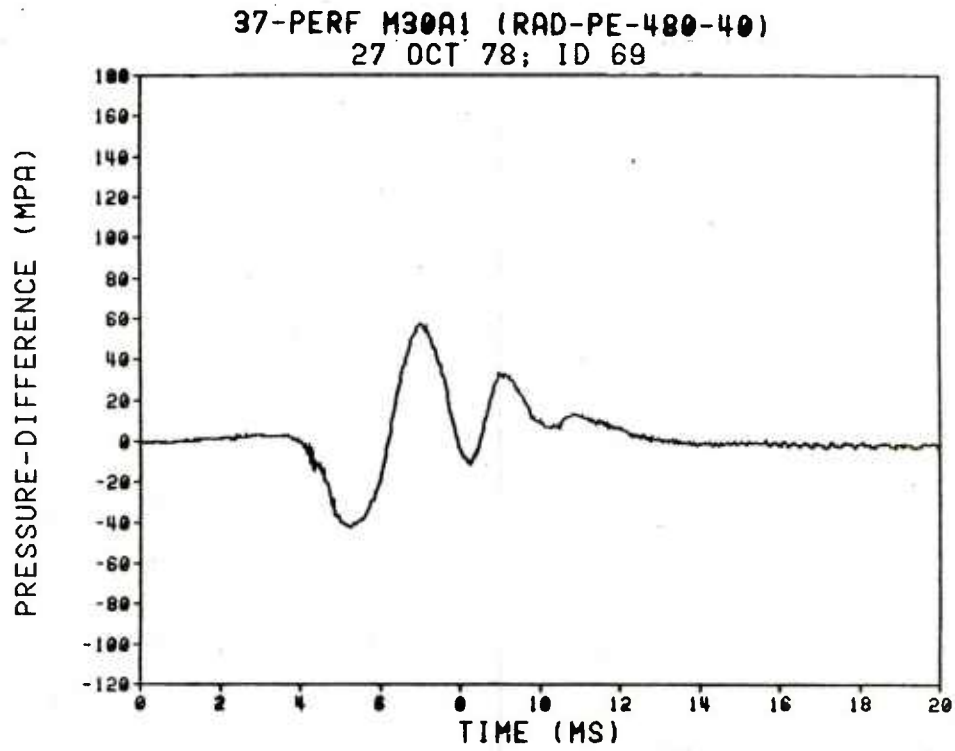
37-PERF M30A1 (RAD-PE-480-40)
27 OCT 78; ID 69
PRESSURE-DIFFERENCE (MPA)
180
160
140
120
100
80
60
40
20
0
-20
-40
-60
-80
-100
-120
0
2
4
6
8
10
12
14
16
18
20
TIME (MS)

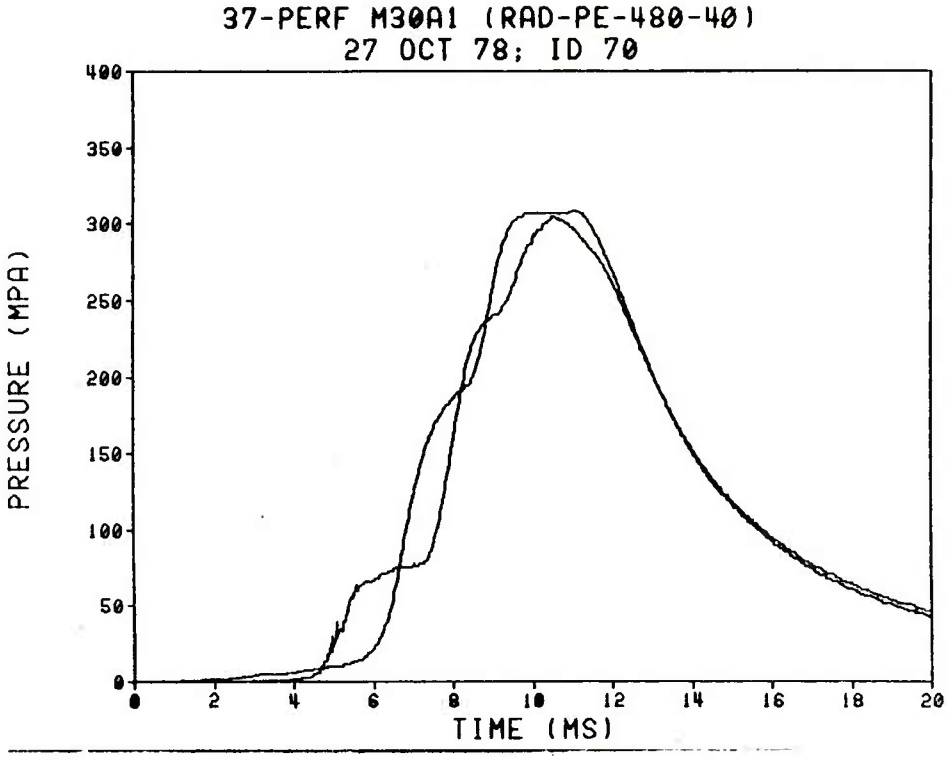
37-PERF M30A1 (RAD-PE-480-40)
27 OCT 78; ID 70
PRESSURE (MPA)
400
350
300
250
200
150
100
50
0
0
2
4
6
8
10
12
14
16
18
20
TIME (MS)

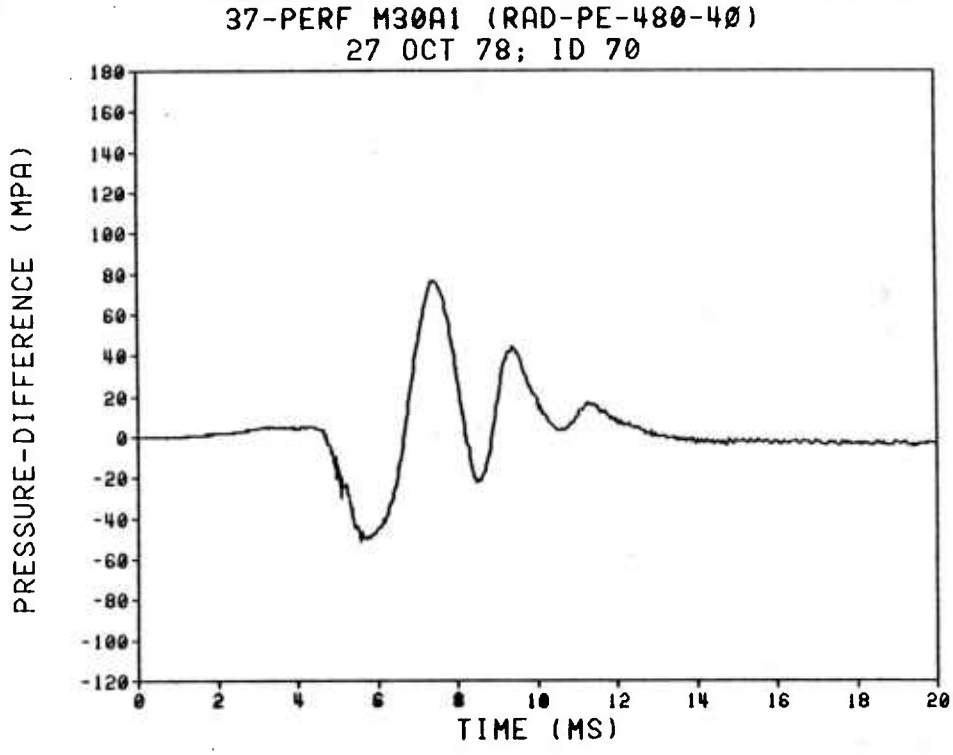
37-PERF M30A1 (RAD-PE-480-40)
27 OCT 78; ID 70
PRESSURE-DIFFERENCE (MPA)
180
160
140
120
100
80
60
40
20
0
-20
-40
-60
-80
-100
-120
0
2
4
6
8
10
12
14
16
18
20
TIME (MS)

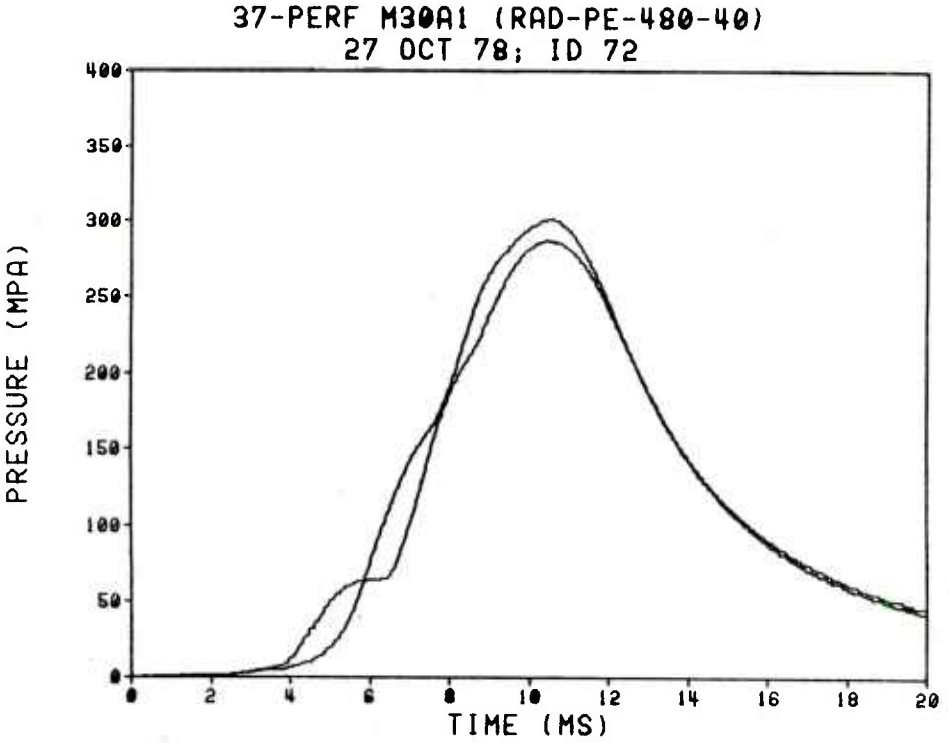
37-PERF M30A1 (RAD-PE-480-40)
27 OCT 78; ID 72
PRESSURE (MPA)
400
350
300
250
200
150
100
50
0
0
2
4
6
8
10
12
14
16
18
20
TIME (MS)

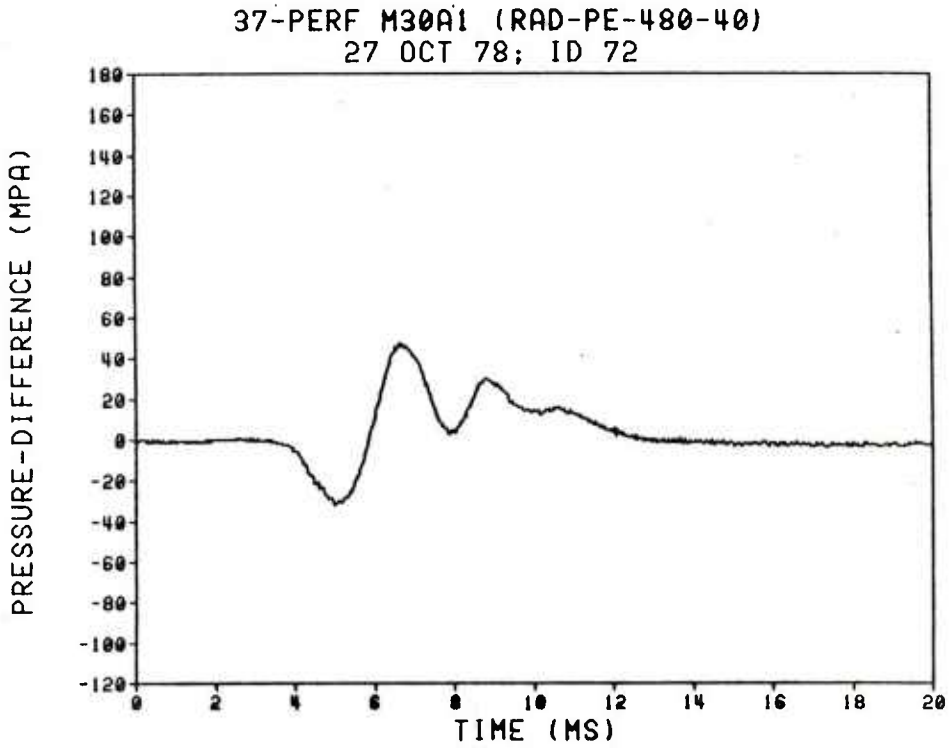
37-PERF M30A1 (RAD-PE-480-40)
27 OCT 78; ID 72
PRESSURE-DIFFERENCE (MPA)
180
160
140
120
100
80
60
40
20
0
-20
-40
-60
-80
-100
-120
0
2
4
6
8
10
12
14
16
18
20
TIME (MS)

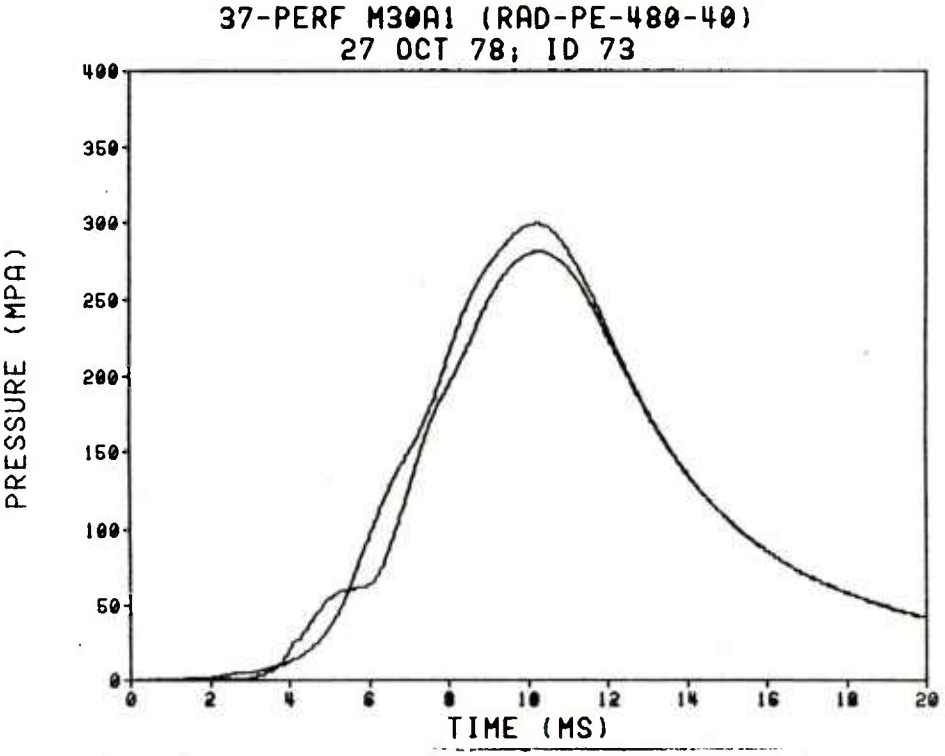
37-PERF M30A1 (RAD-PE-480-40)
27 OCT 78; ID 73
PRESSURE (MPA)
400
350
300
250
200
150
100
50
0
0
2
4
6
8
10
12
14
16
18
20
TIME (MS)

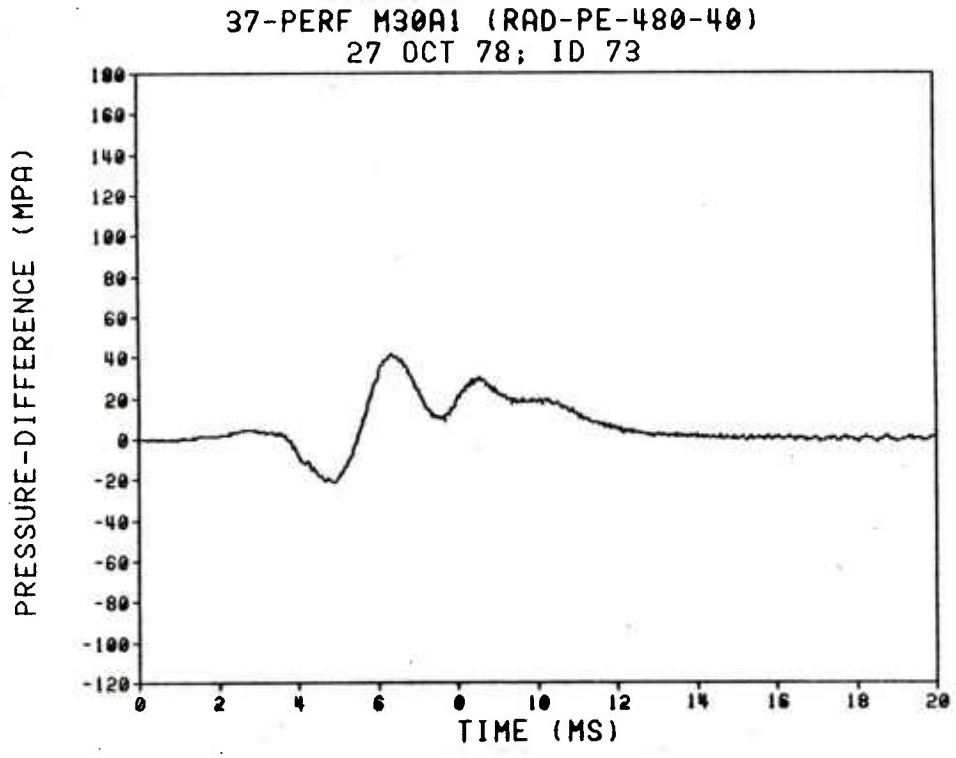
37-PERF M30A1 (RAD-PE-480-40)
27 OCT 78; ID 73
PRESSURE-DIFFERENCE (MPA)
180
160
140
120
100
80
60
40
20
0
-20
-40
-60
-80
-100
-120
0
2
4
6
8
10
12
14
16
18
20
TIME (MS)

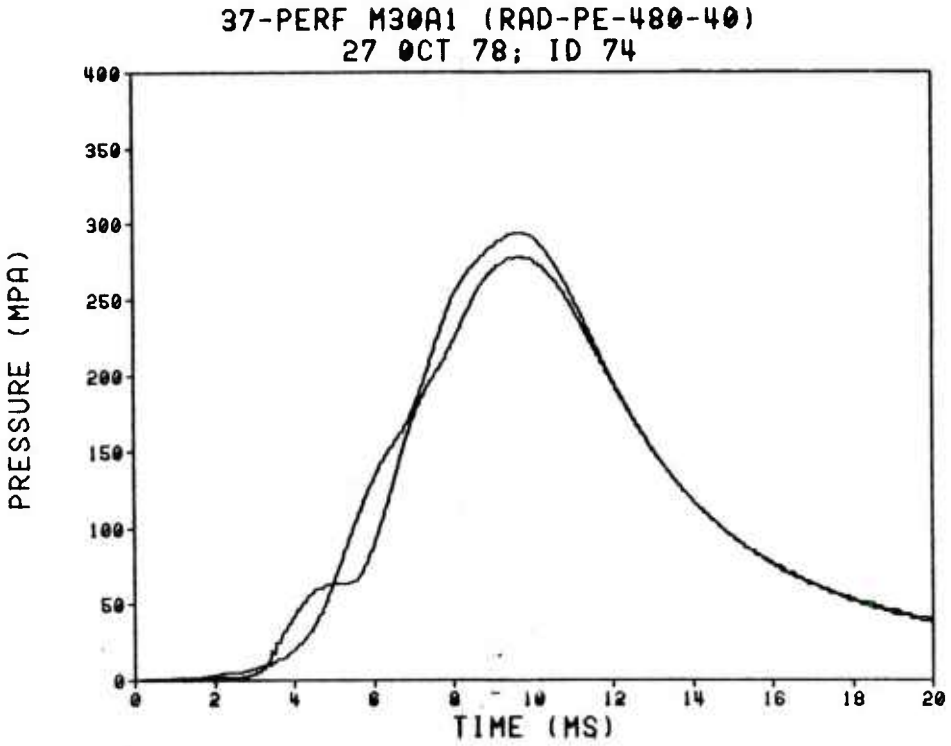
37-PERF M30A1 (RAD-PE-480-40)
27 OCT 78; ID 74
PRESSURE (MPA)
400
350
300
250
200
150
100
50
0
0
2
4
6
8
10
12
14
16
18
20
TIME (MS)

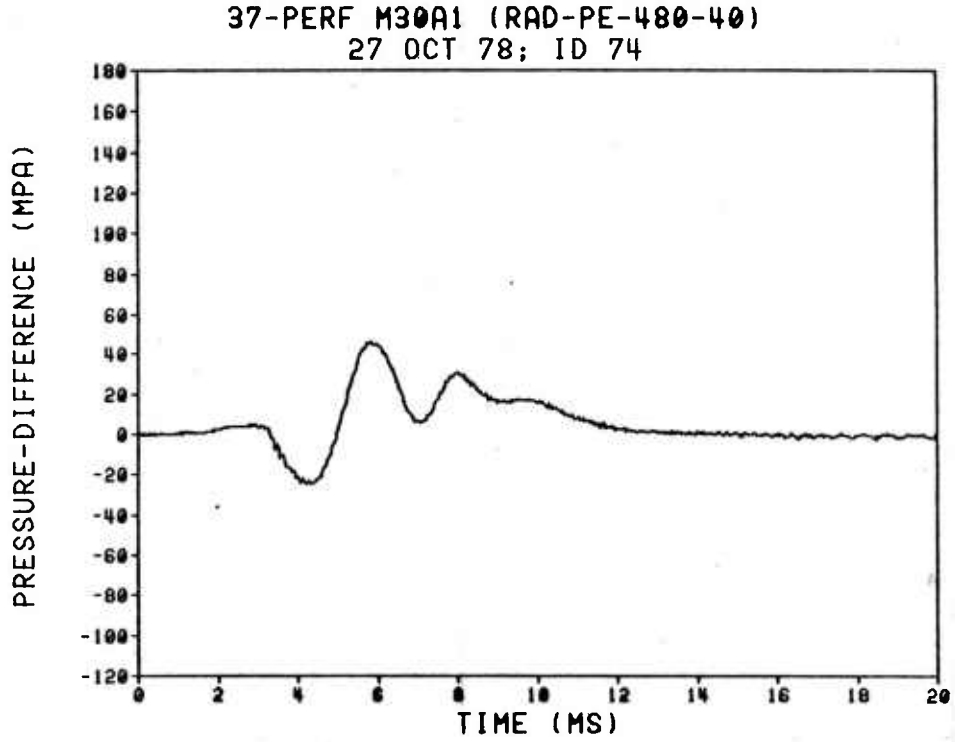
37-PERF M30A1 (RAD-PE-480-40)
27 OCT 78; ID 74
PRESSURE-DIFFERENCE (MPA)
180
160
140
120
100
80
60
40
20
0
-20
-40
-60
-80
-100
-120
0
2
4
6
8
10
12
14
16
18
20
TIME (MS)

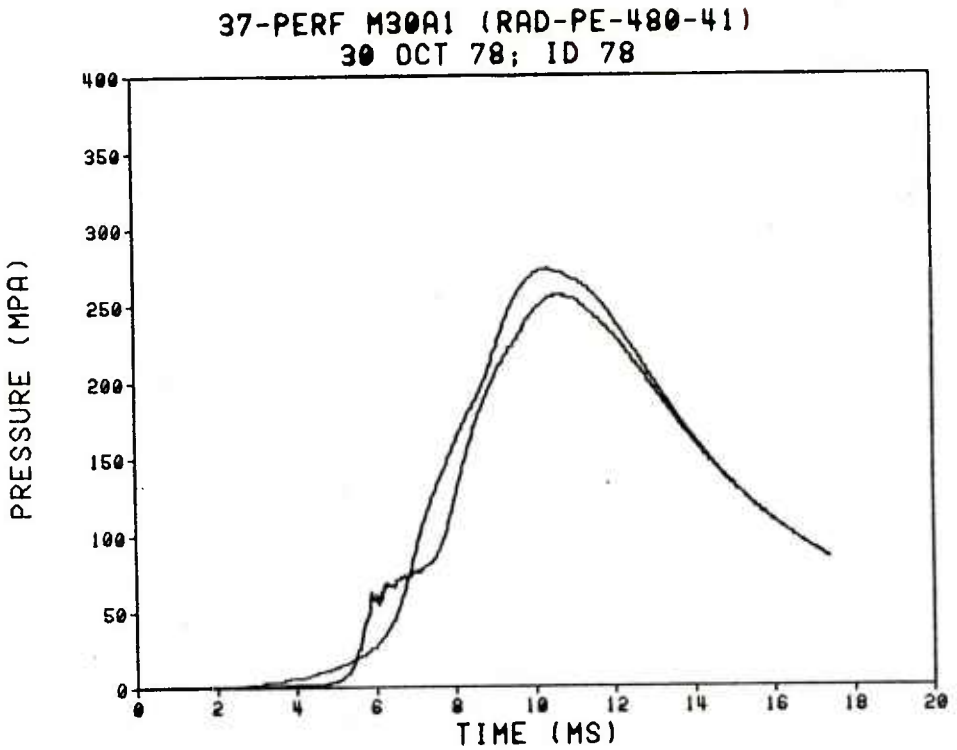
37-PERF M30A1 (RAD-PE-480-41)
30 OCT 78; ID 78
PRESSURE (MPA)
400
350
300
250
200
150
100
50
0
0
2
4
6
8
10
12
14
16
18
20
TIME (MS)

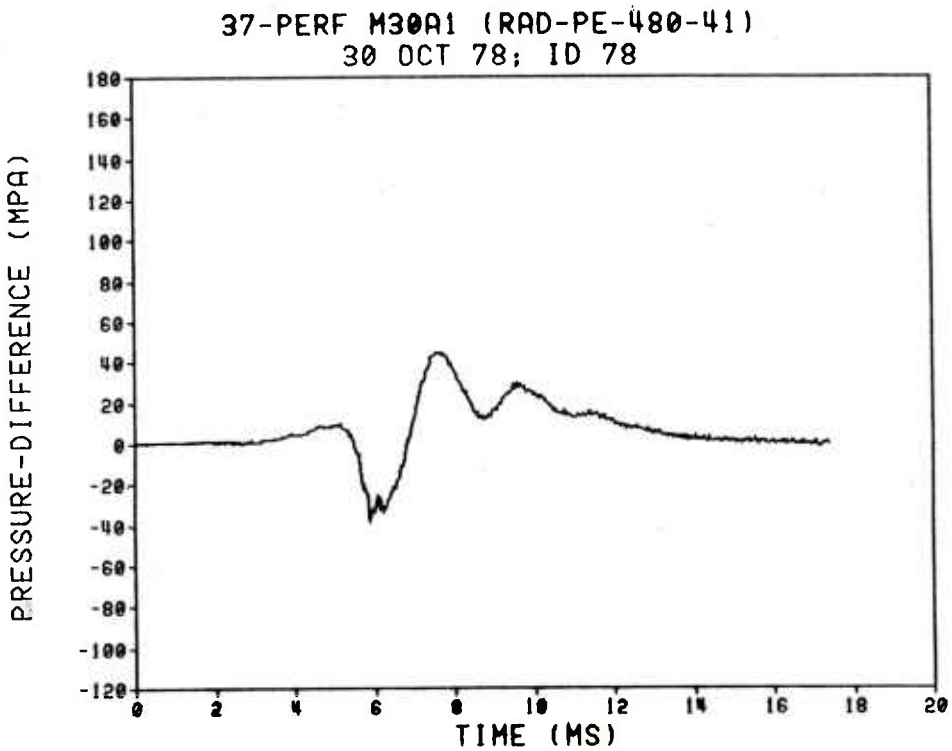
37-PERF M30A1 (RAD-PE-480-41)
30 OCT 78; ID 78
PRESSURE-DIFFERENCE (MPA)
180
160
140
120
100
80
60
40
20
0
-20
-40
-60
-80
-100
-120
0
2
4
6
8
10
12
14
16
18
20
TIME (MS)

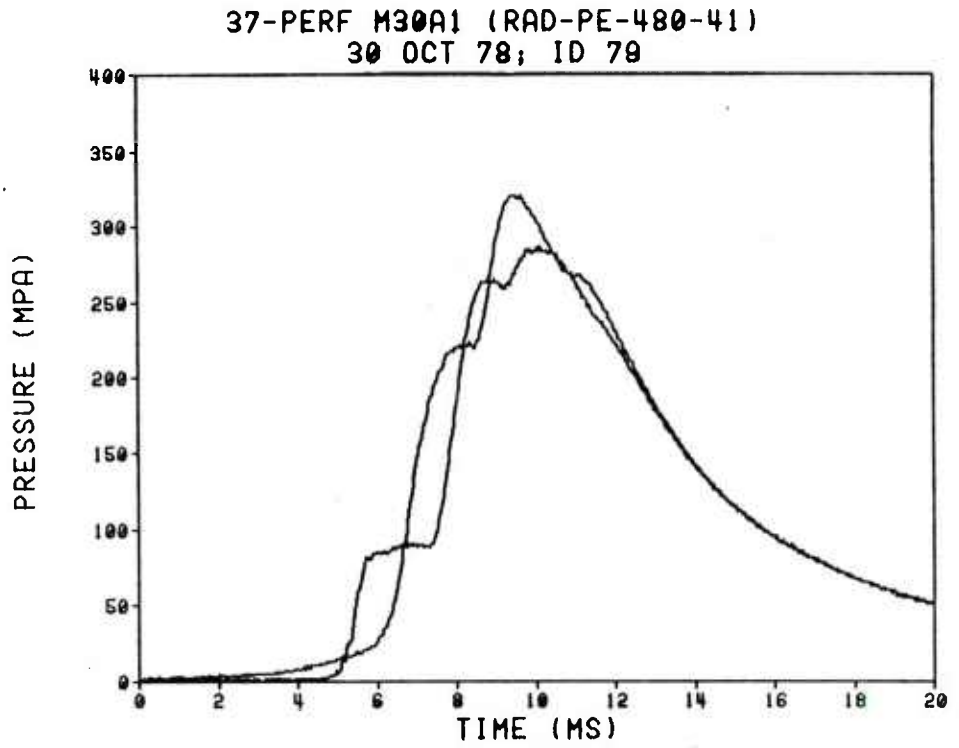
37-PERF M30A1 (RAD-PE-480-41)
30 OCT 78; ID 79
PRESSURE (MPA)
400
350
300
250
200
150
100
50
0
0
2
4
6
8
10
12
14
16
18
20
TIME (MS)

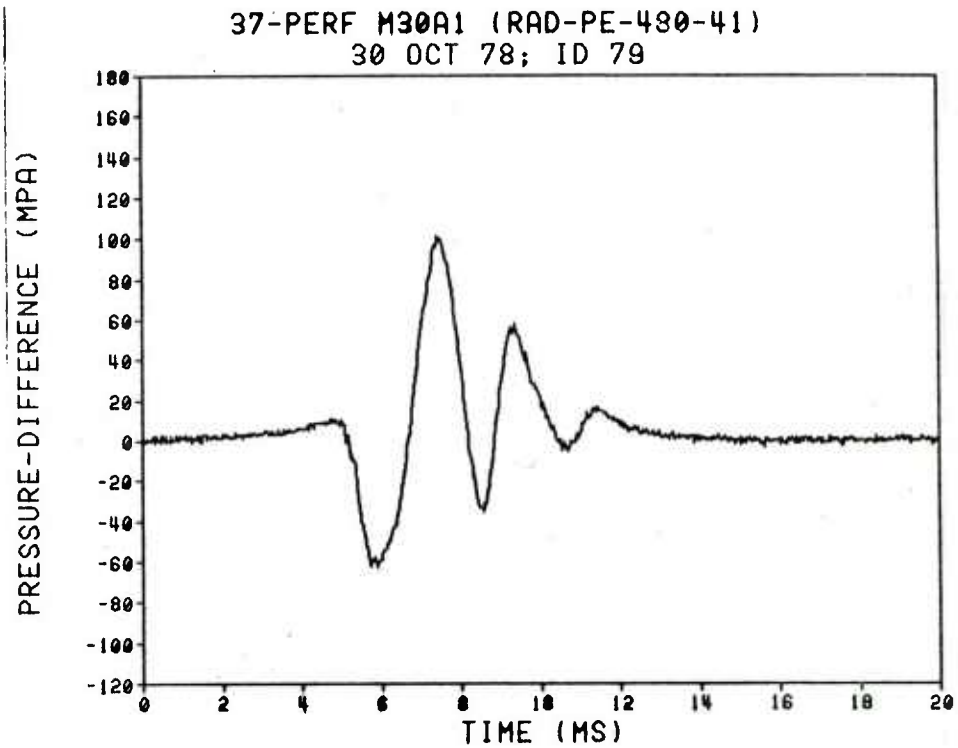
37-PERF M30A1 (RAD-PE-480-41)
30 OCT 78; ID 79
PRESSURE-DIFFERENCE (MPA)
180
160
140
120
100
80
60
40
20
0
-20
-40
-60
-80
-100
-120
0
2
4
6
8
10
12
14
16
18
20
TIME (MS)

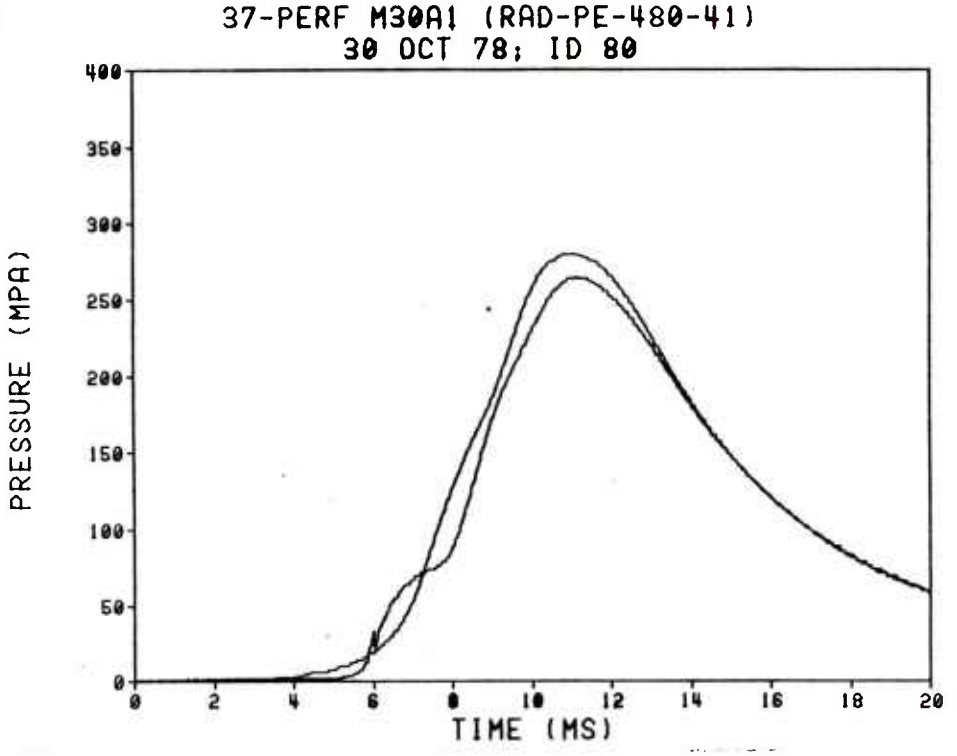
37-PERF M30A1 (RAD-PE-480-41)
30 OCT 78; ID 80
PRESSURE (MPA)
400
350
300
250
200
150
100
50
0
0
2
4
6
8
10
12
14
16
18
20
TIME (MS)

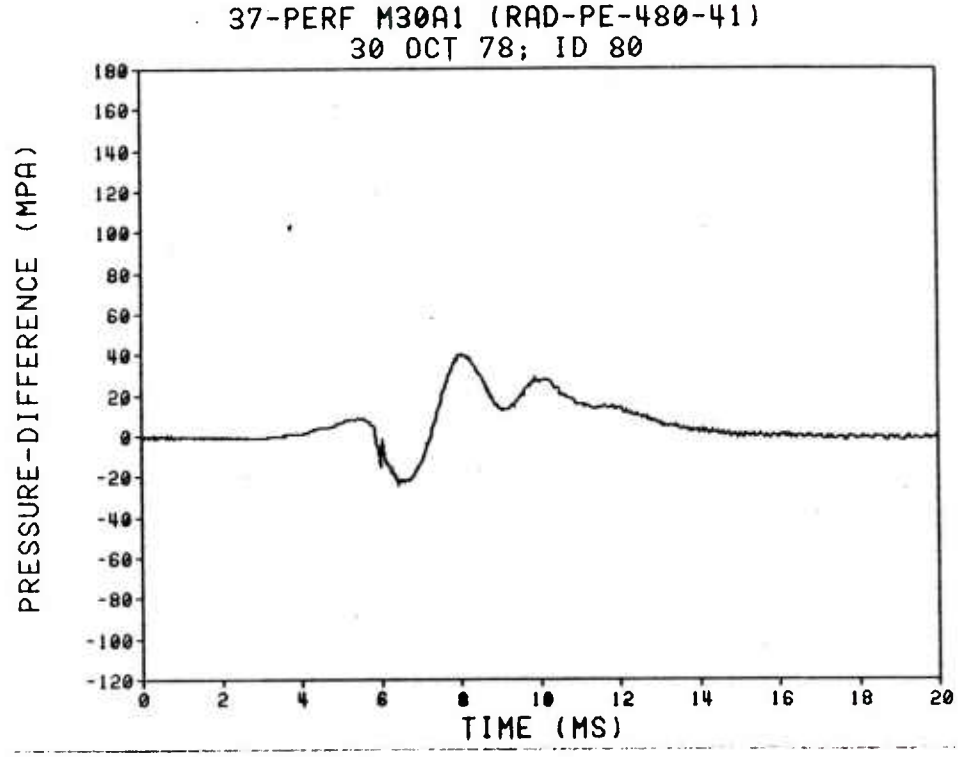
37-PERF M30A1 (RAD-PE-480-41)
30 OCT 78; ID 80
PRESSURE-DIFFERENCE (MPA)
180
160
140
120
100
80
60
40
20
0
-20
-40
-60
-80
-100
-120
0
2
4
6
8
10
12
14
16
18
20
TIME (MS)

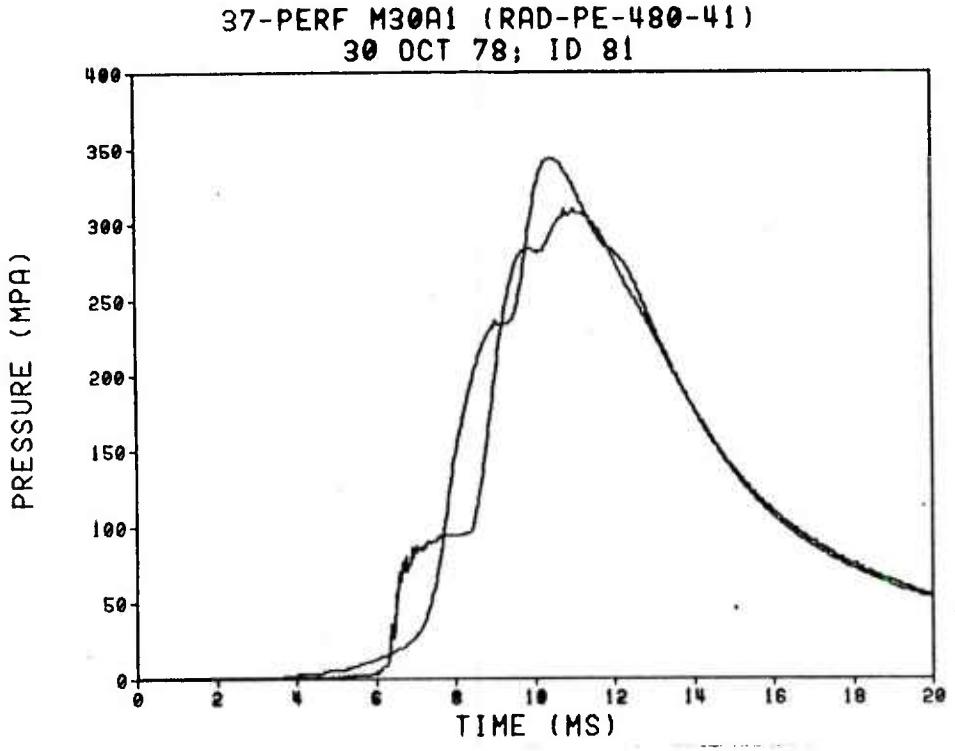
37-PERF M30A1 (RAD-PE-480-41)
30 OCT 78; ID 81
PRESSURE (MPA)
400
350
300
250
200
150
100
50
0
0
2
4
6
8
10
12
14
16
18
20
TIME (MS)

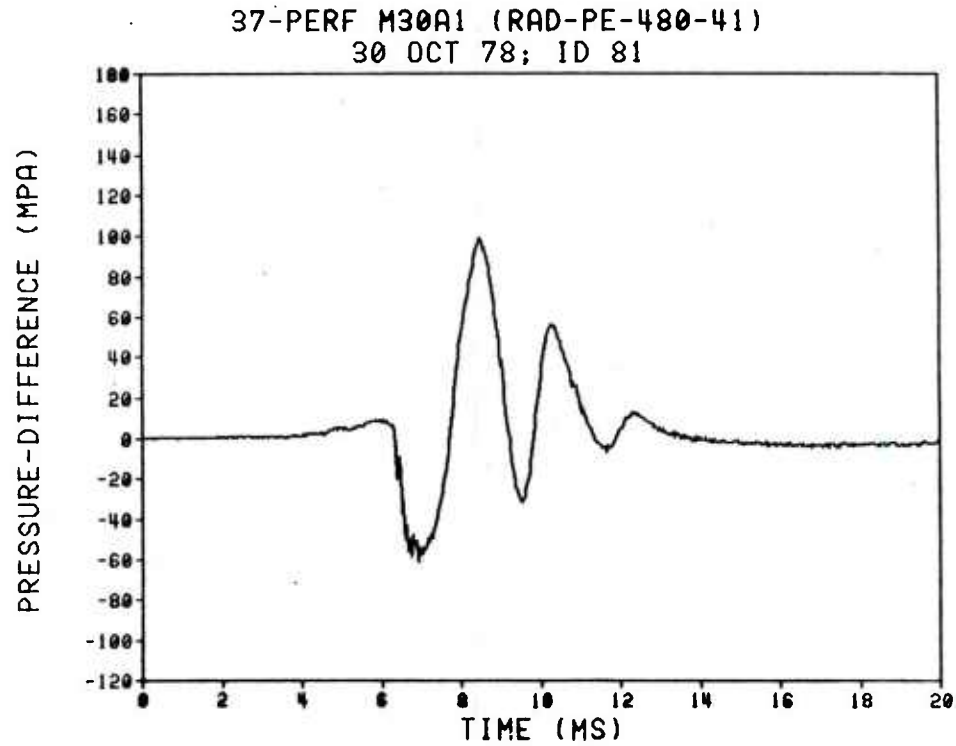
37-PERF M30A1 (RAD-PE-480-41)
30 OCT 78; ID 81
PRESSURE-DIFFERENCE (MPA)
180
160
140
120
100
80
60
40
20
0
-20
-40
-60
-80
-100
-120
0
2
4
6
8
10
12
14
16
18
20
TIME (MS)

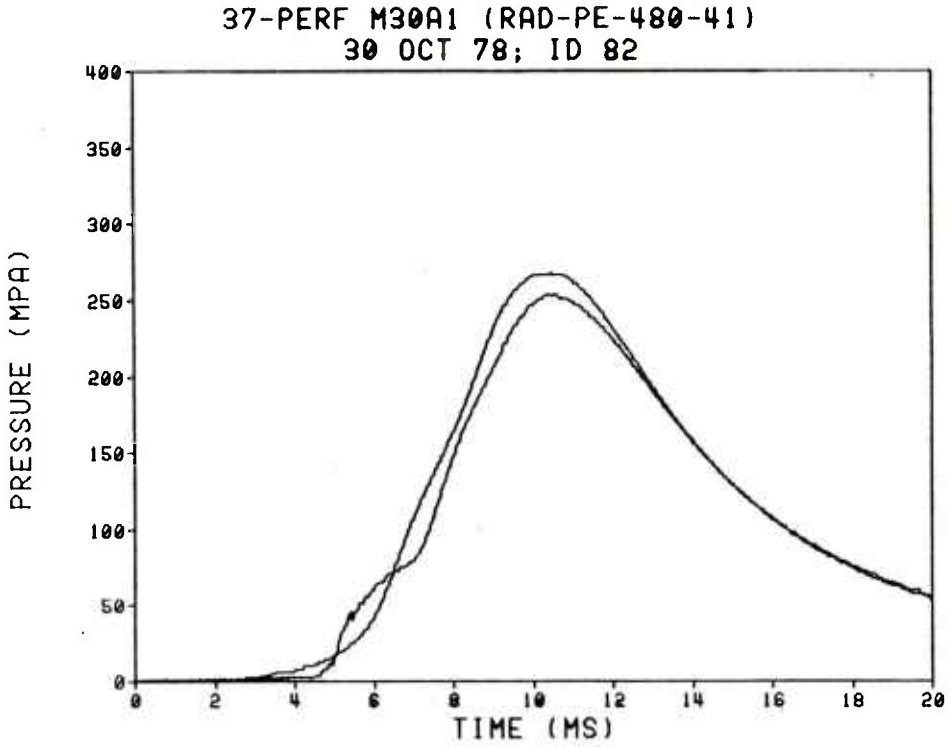
37-PERF M30A1 (RAD-PE-480-41)
30 OCT 78; ID 82
PRESSURE (MPA)
400
350
300
250
200
150
100
50
0
0
2
4
6
8
10
12
14
16
18
20
TIME (MS)

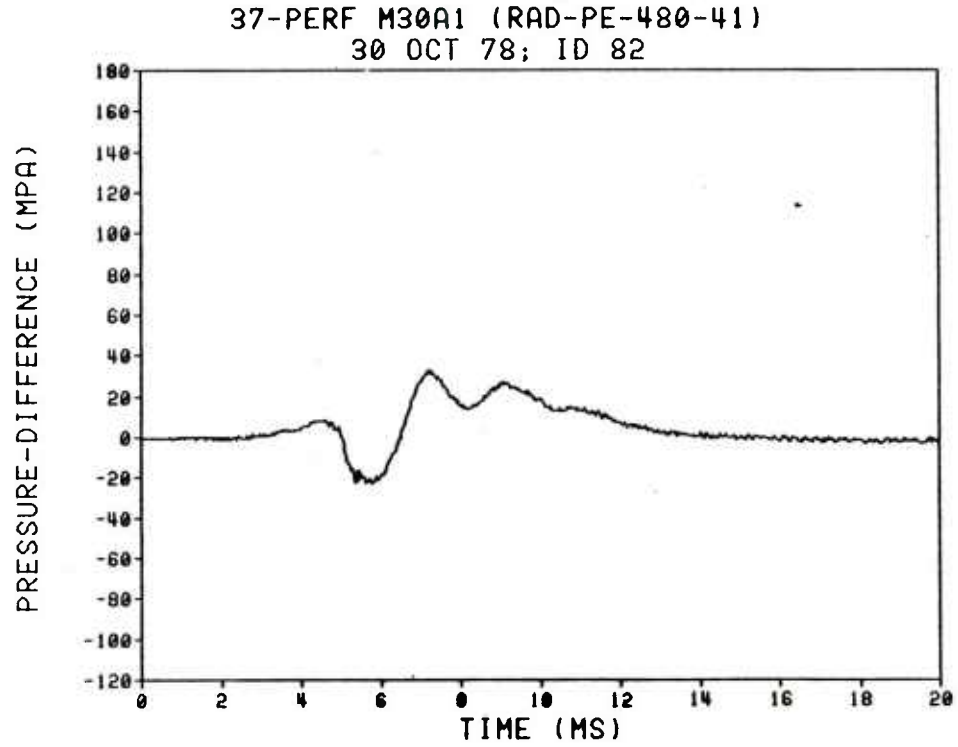
37-PERF M30A1 (RAD-PE-480-41)
30 OCT 78; ID 82
PRESSURE-DIFFERENCE (MPA)
180
160
140
120
100
80
60
40
20
0
-20
-40
-60
-80
-100
-120
0
2
4
6
8
10
12
14
16
18
20
TIME (MS)

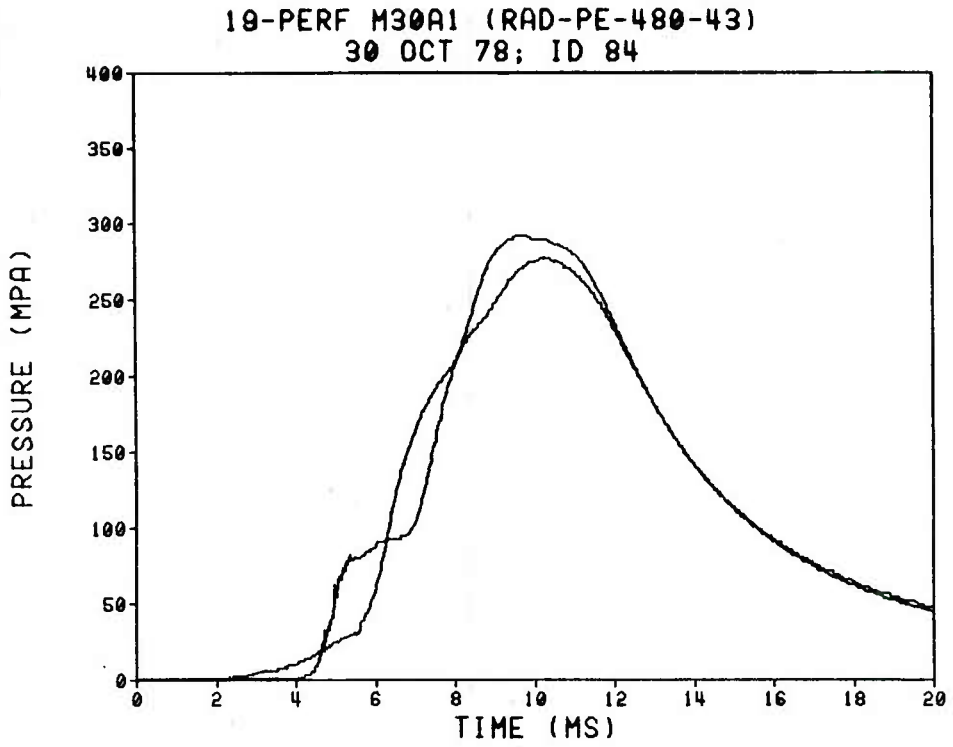
19-PERF M30A1 (RAD-PE-480-43)
30 OCT 78; ID 84
PRESSURE (MPA)
400
350
300
250
200
150
100
50
0
0
2
4
6
8
10
12
14
16
18
20
TIME (MS)

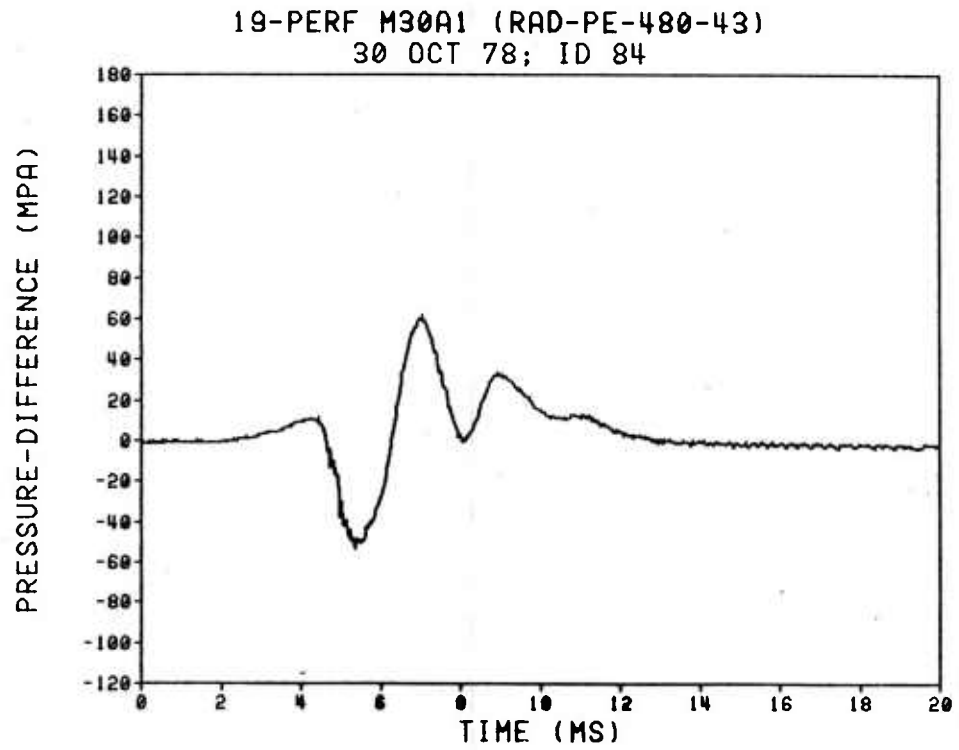
19-PERF M30A1 (RAD-PE-480-43)
30 OCT 78; ID 84
PRESSURE-DIFFERENCE (MPA)
180
160
140
120
100
80
60
40
20
0
-20
-40
-60
-80
-100
-120
0
2
4
6
8
10
12
14
16
18
20
TIME (MS)

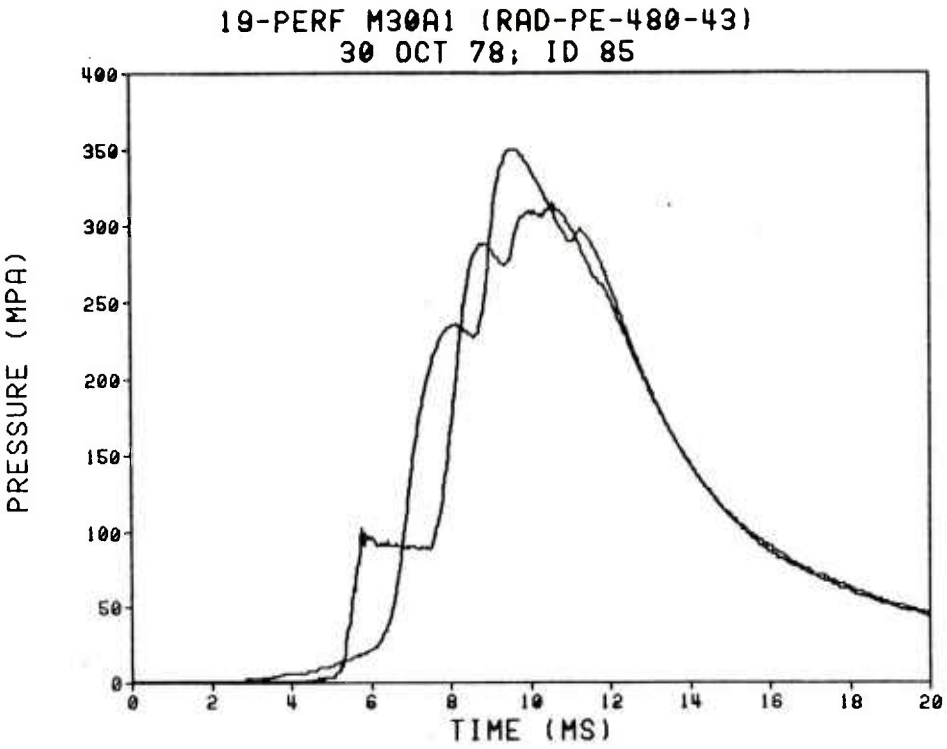
19-PERF M30A1 (RAD-PE-480-43)
30 OCT 78; ID 85
PRESSURE (MPA)
400
350
300
250
200
150
100
50
0
0
2
4
6
8
10
12
14
16
18
20
TIME (MS)

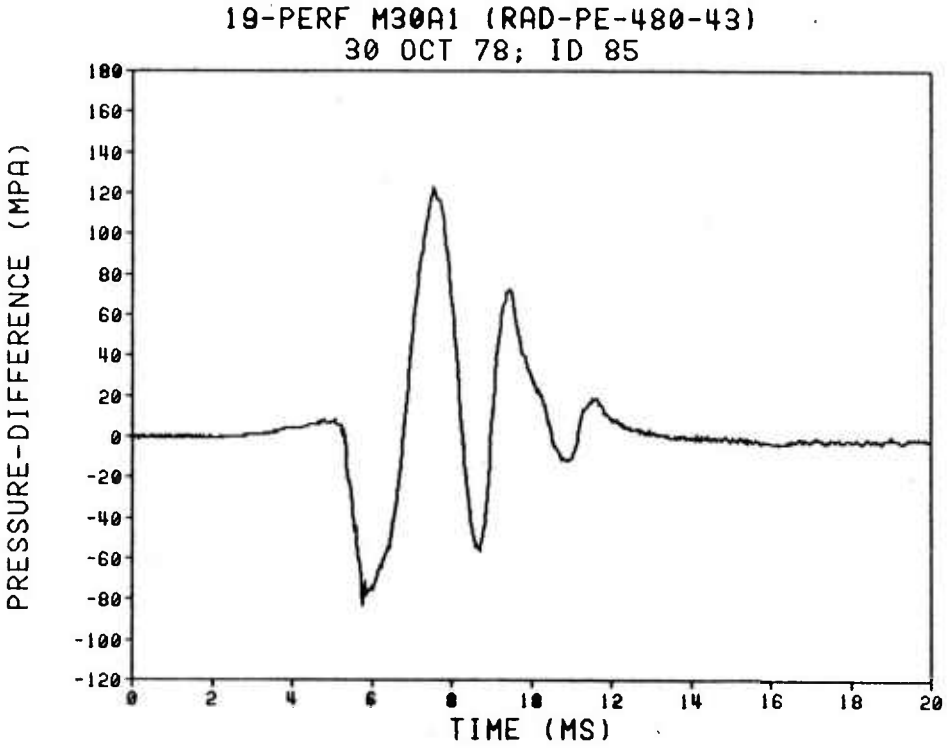
19-PERF M30A1 (RAD-PE-480-43)
30 OCT 78; ID 85
PRESSURE-DIFFERENCE (MPA)
180
160
140
120
100
80
60
40
20
0
-20
-40
-60
-80
-100
-120
0
2
4
6
8
10
12
14
16
18
20
TIME (MS)

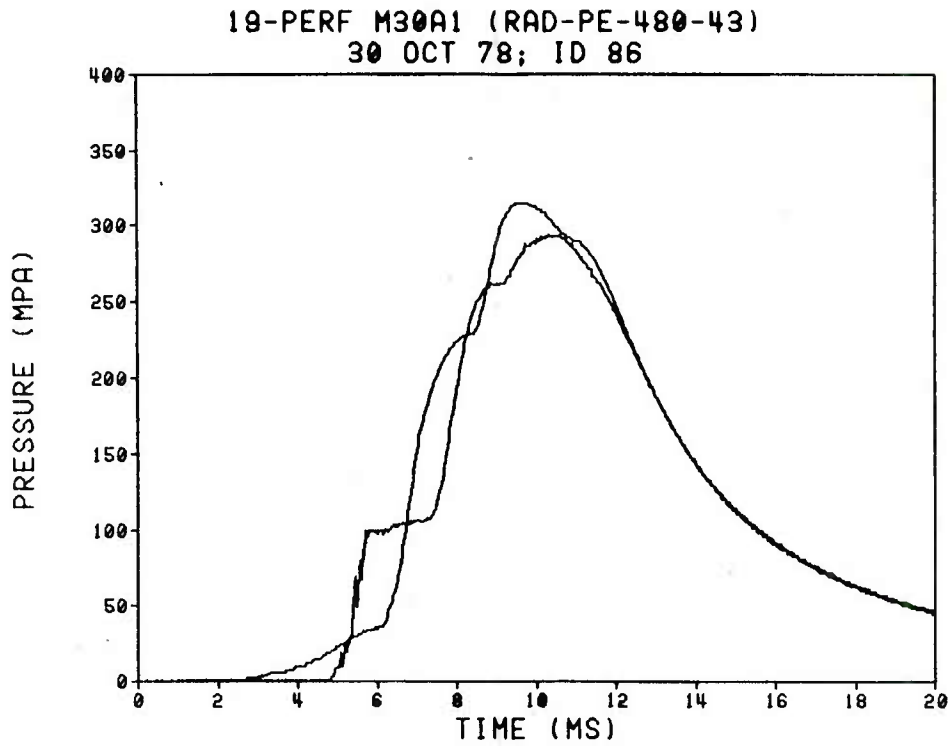
19-PERF M30A1 (RAD-PE-480-43)
30 OCT 78; ID 86
PRESSURE (MPA)
400
350
300
250
200
150
100
50
0
0
2
4
6
8
10
12
14
16
18
20
TIME (MS)

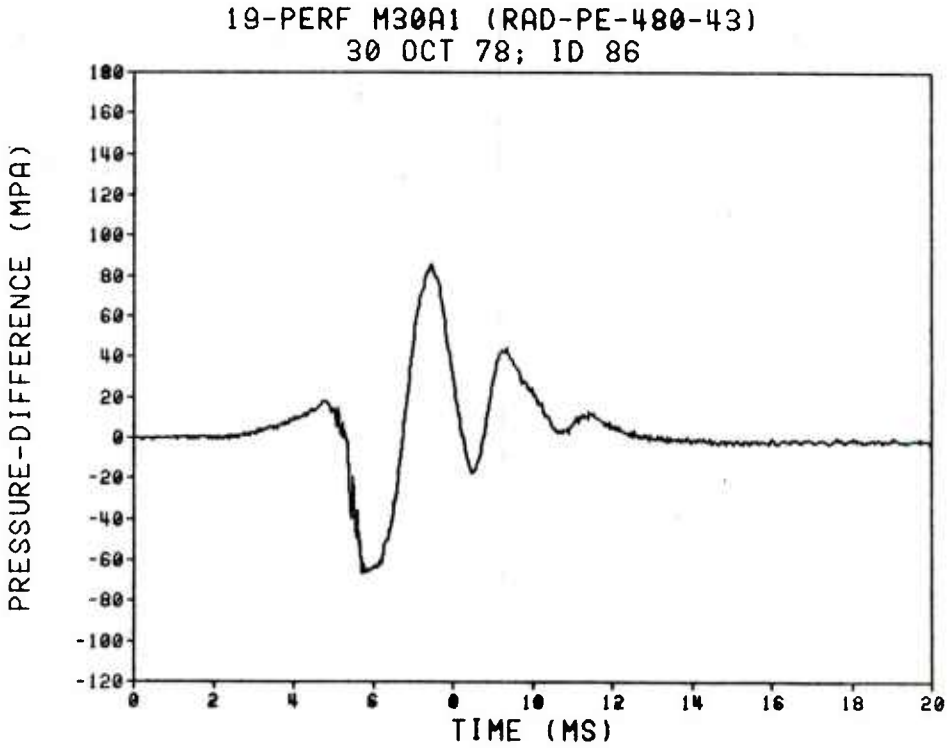
19-PERF M30A1 (RAD-PE-480-43)
30 OCT 78; ID 86
PRESSURE-DIFFERENCE (MPA)
180
160
140
120
100
80
60
40
20
0
-20
-40
-60
-80
-100
-120
0
2
4
6
8
10
12
14
16
18
20
TIME (MS)

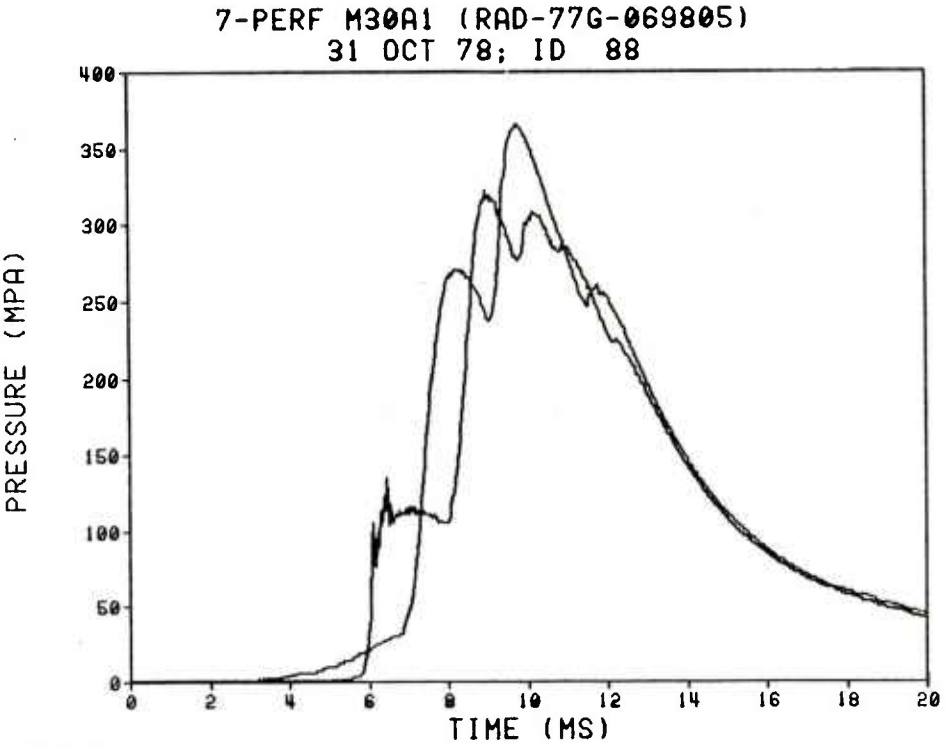
7-PERF M30A1 (RAD-77G-069805)
31 OCT 78; ID 88
PRESSURE (MPA)
400
350
300
250
200
150
100
50
0
0
2
4
6
8
10
12
14
16
18
20
TIME (MS)

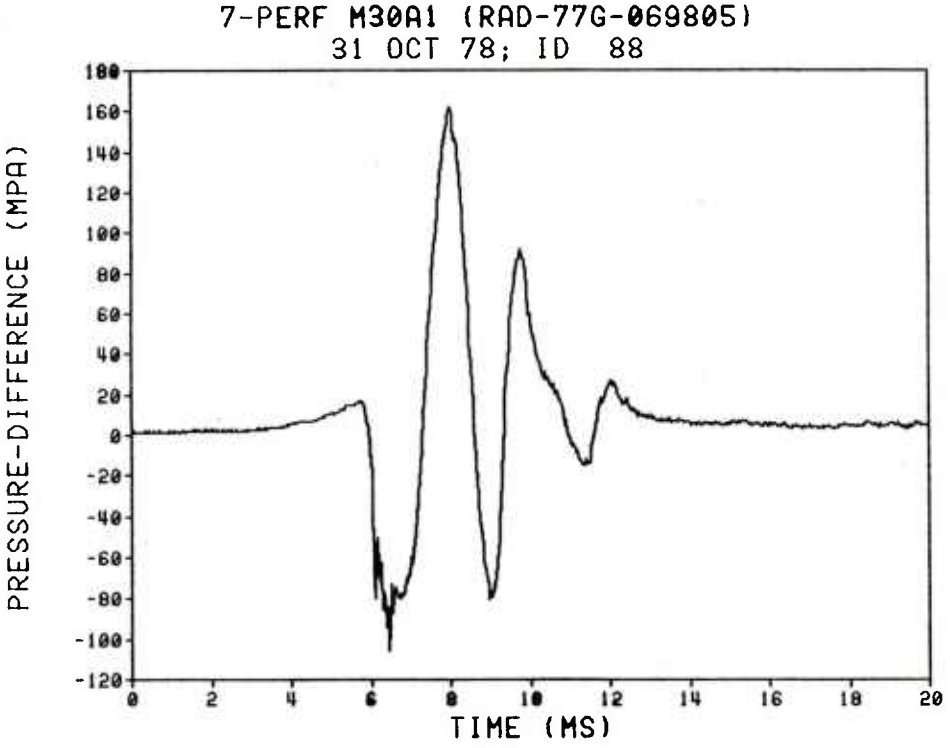
7-PERF M30A1 (RAD-77G-069805)
31 OCT 78; ID 88
PRESSURE-DIFFERENCE (MPA)
180
160
140
120
100
80
60
40
20
0
-20
-40
-60
-80
-100
-120
0
2
4
6
8
10
12
14
16
18
20
TIME (MS)

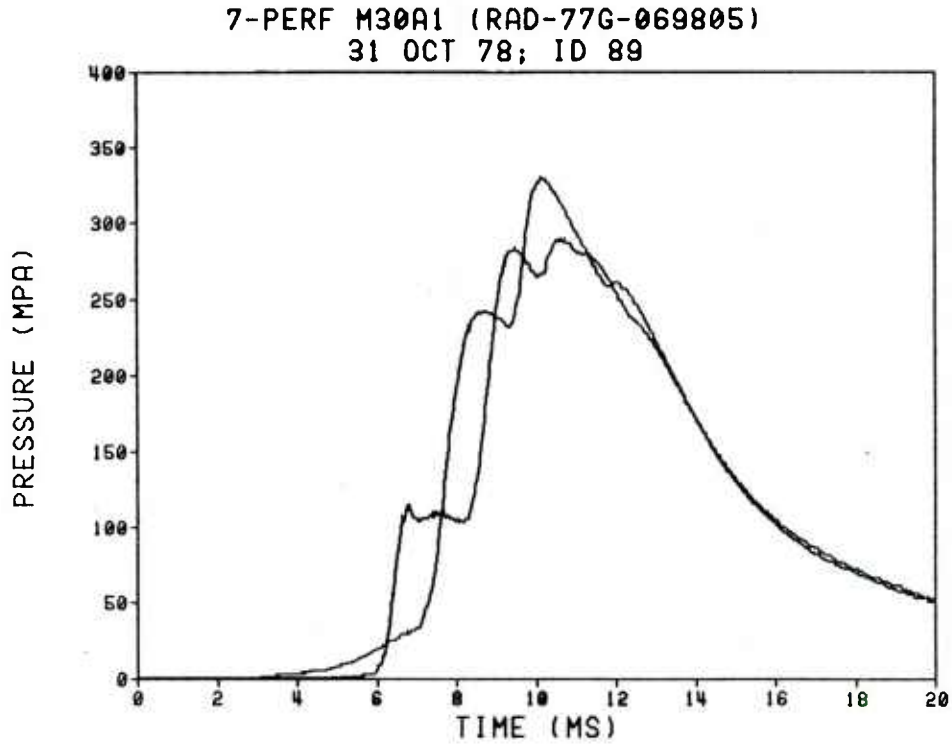
7-PERF M30A1 (RAD-77G-069805)
31 OCT 78; ID 89
PRESSURE (MPA)
400
350
300
250
200
150
100
50
0
0
2
4
6
8
10
12
14
16
18
20
TIME (MS)

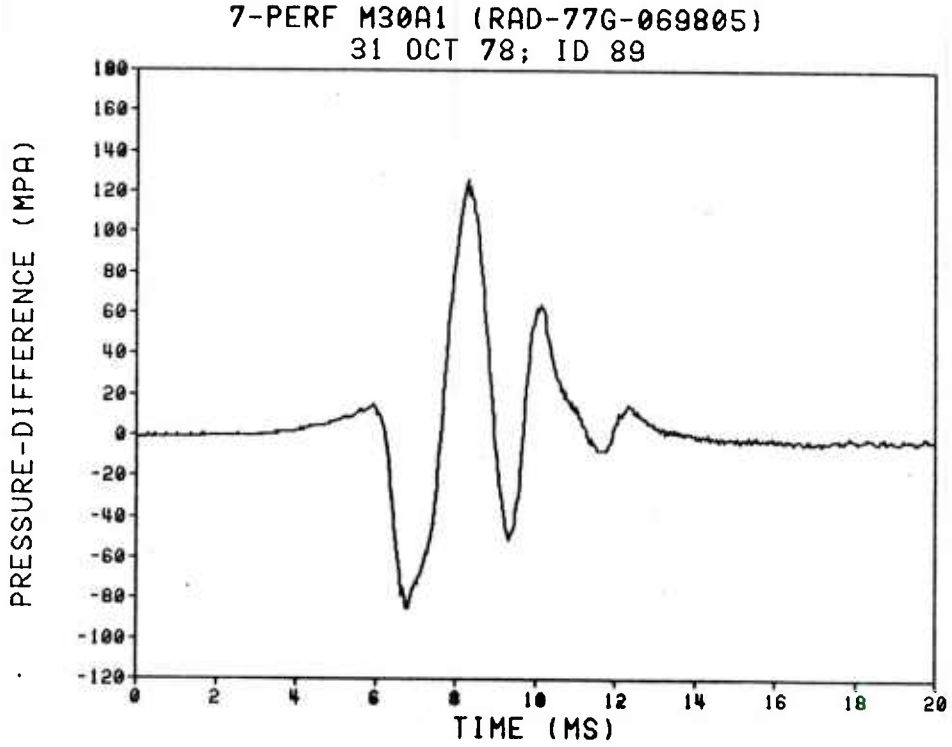
7-PERF M30A1 (RAD-77G-069805)
31 OCT 78; ID 89
PRESSURE-DIFFERENCE (MPA)
180
160
140
120
100
80
60
40
20
0
-20
-40
-60
-80
-100
-120
0
2
4
6
8
10
12
14
16
18
20
TIME (MS)

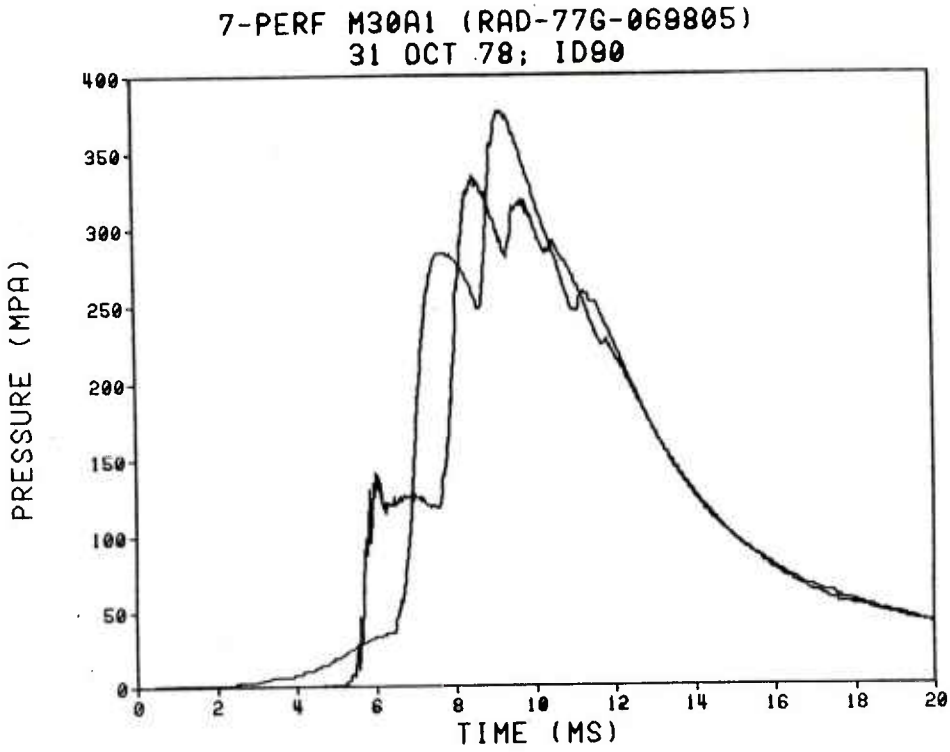
7-PERF M30A1 (RAD-77G-069805)
31 OCT 78; ID90
PRESSURE (MPA)
400
350
300
250
200
150
100
50
0
0
2
4
6
8
10
12
14
16
18
20
TIME (MS)

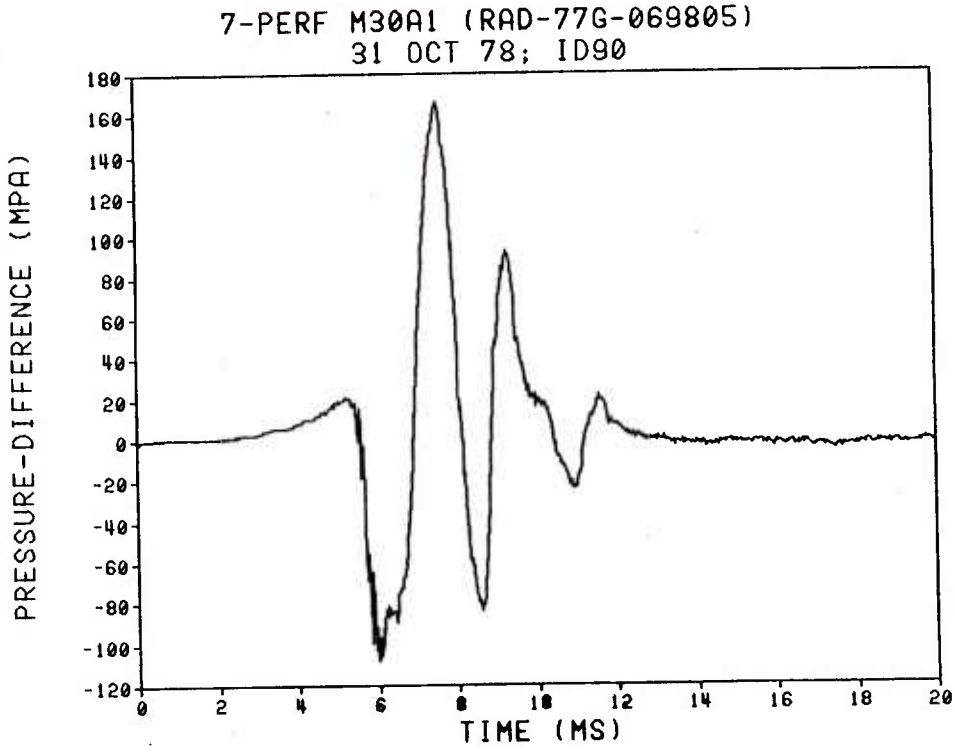
7-PERF M30A1 (RAD-77G-069805)
31 OCT 78; ID90
PRESSURE-DIFFERENCE (MPA)
180
160
140
120
100
80
60
40
20
0
-20
-40
-60
-80
-100
-120
0
2
4
6
8
10
12
14
16
18
20
TIME (MS)

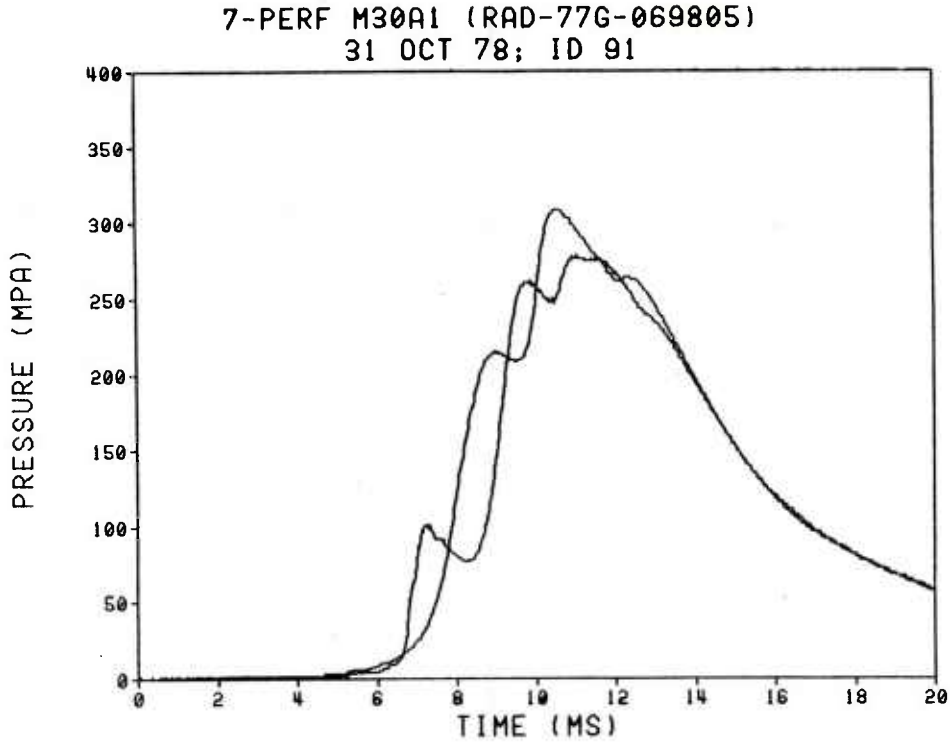
7-PERF M30A1 (RAD-77G-069805)
31 OCT 78; ID 91
PRESSURE (MPA)
400
350
300
250
200
150
100
50
0
0
2
4
6
8
10
12
14
16
18
20
TIME (MS)

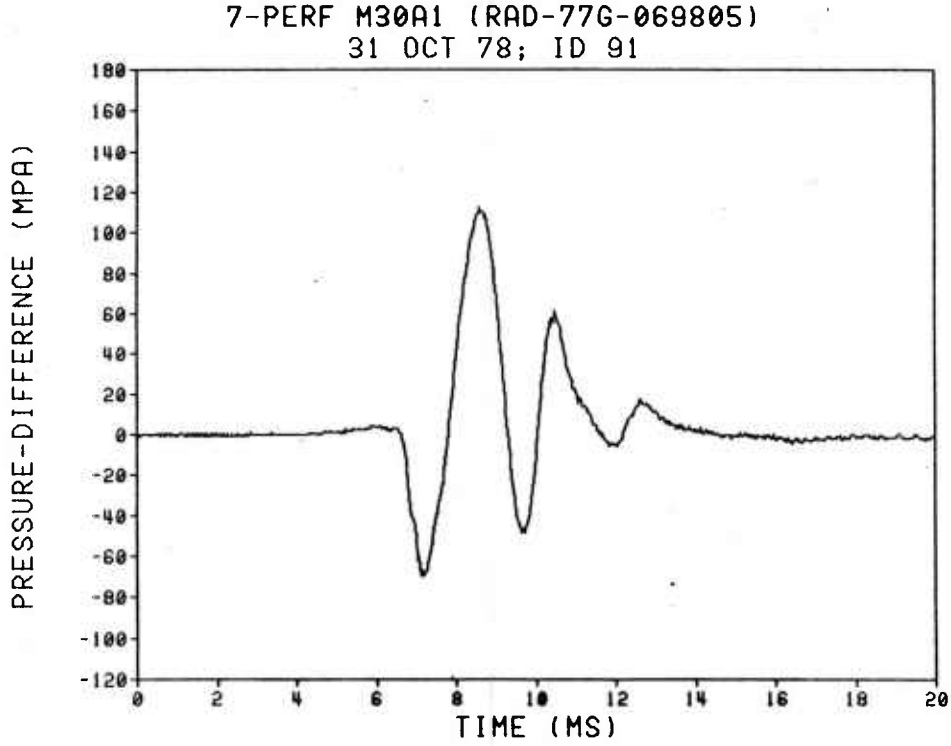
7-PERF M30A1 (RAD-77G-069805)
31 OCT 78; ID 91
PRESSURE-DIFFERENCE (MPA)
180
160
140
120
100
80
60
40
20
0
-20
-40
-60
-80
-100
-120
0
2
4
6
8
10
12
14
16
18
20
TIME (MS)

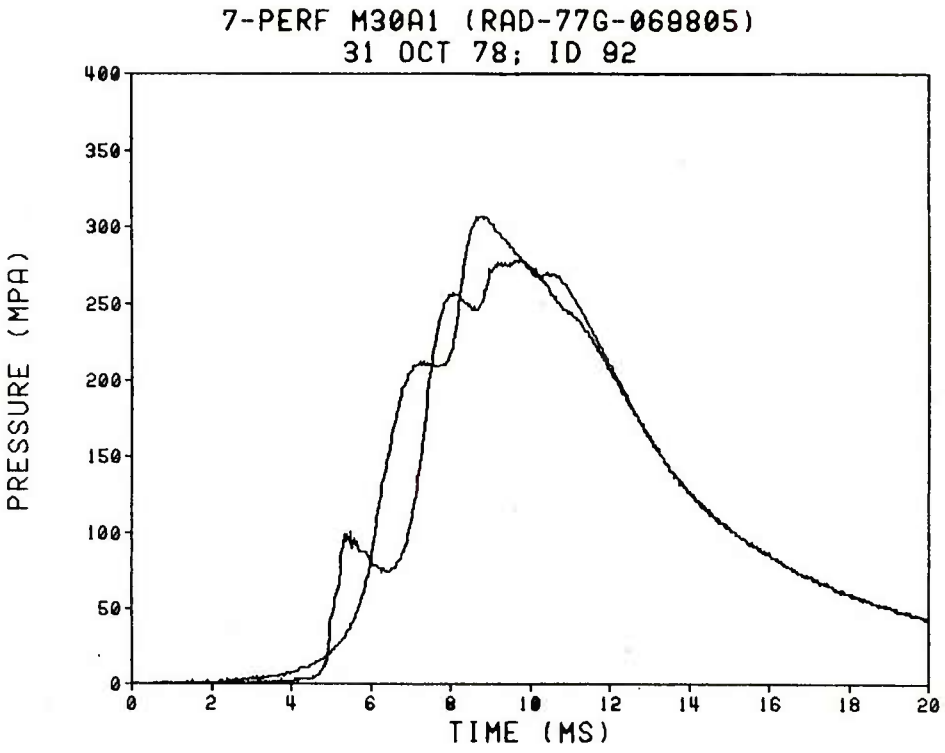
7-PERF M30A1 (RAD-77G-069805)
31 OCT 78; ID 92
PRESSURE (MPA)
400
350
300
250
200
150
100
50
0
0
2
4
6
8
10
12
14
16
18
20
TIME (MS)

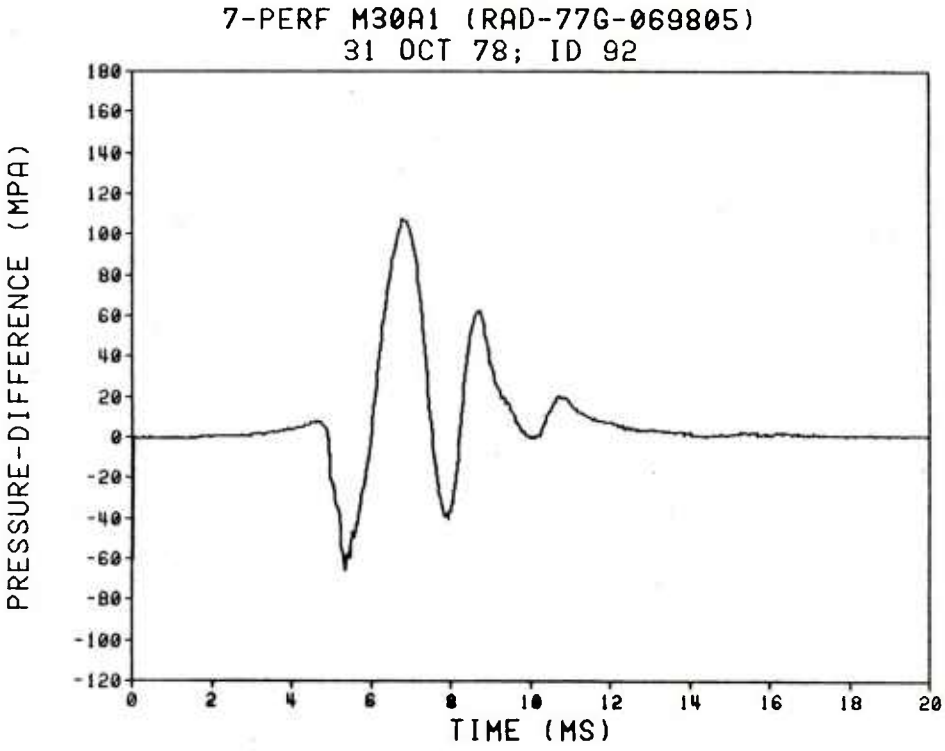
7-PERF M30A1 (RAD-77G-069805)
31 OCT 78; ID 92
PRESSURE-DIFFERENCE (MPA)
180
160
140
120
100
80
60
40
20
0
-20
-40
-60
-80
-100
-120
0
2
4
6
8
10
12
14
16
18
20
TIME (MS)

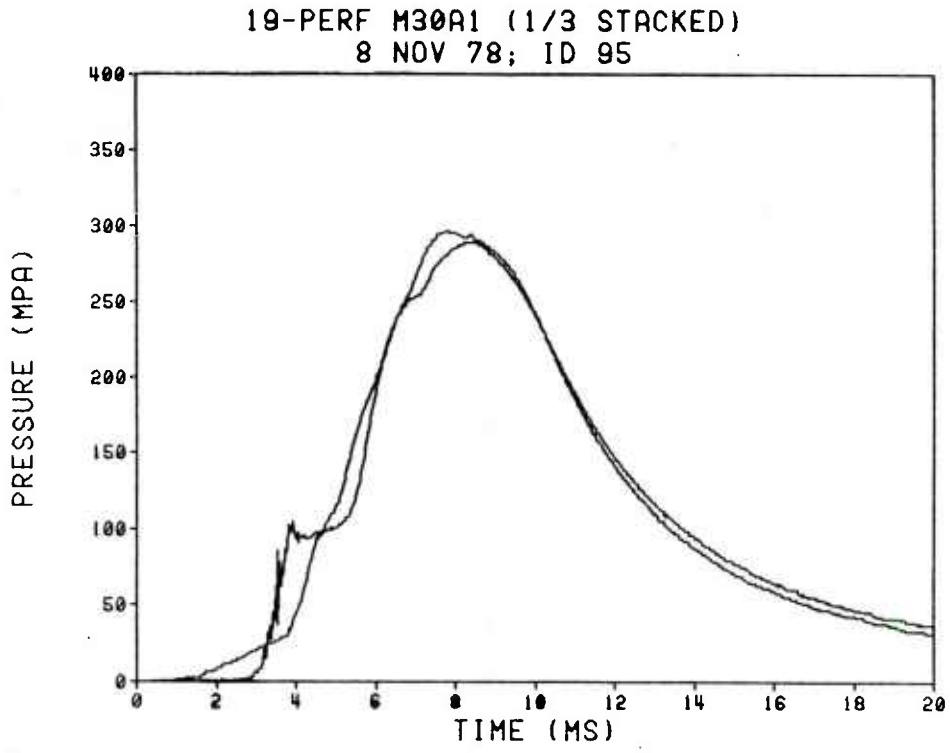
19-PERF M30A1 (1/3 STACKED)
8 NOV 78; ID 95
PRESSURE (MPA)
400
350
300
250
200
150
100
50
0
0
2
4
6
8
10
12
14
16
18
20
TIME (MS)

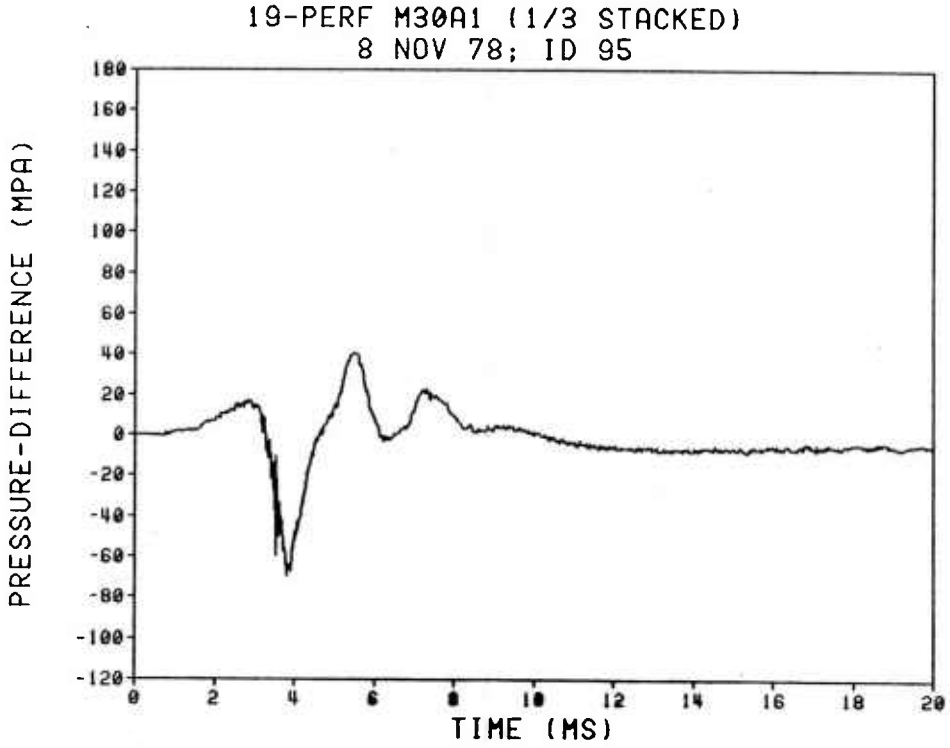
19-PERF M30A1 (1/3 STACKED)
8 NOV 78; ID 95
PRESSURE-DIFFERENCE (MPA)
180
160
140
120
100
80
60
40
20
0
-20
-40
-60
-80
-100
-120
0
2
4
6
8
10
12
14
16
18
20
TIME (MS)

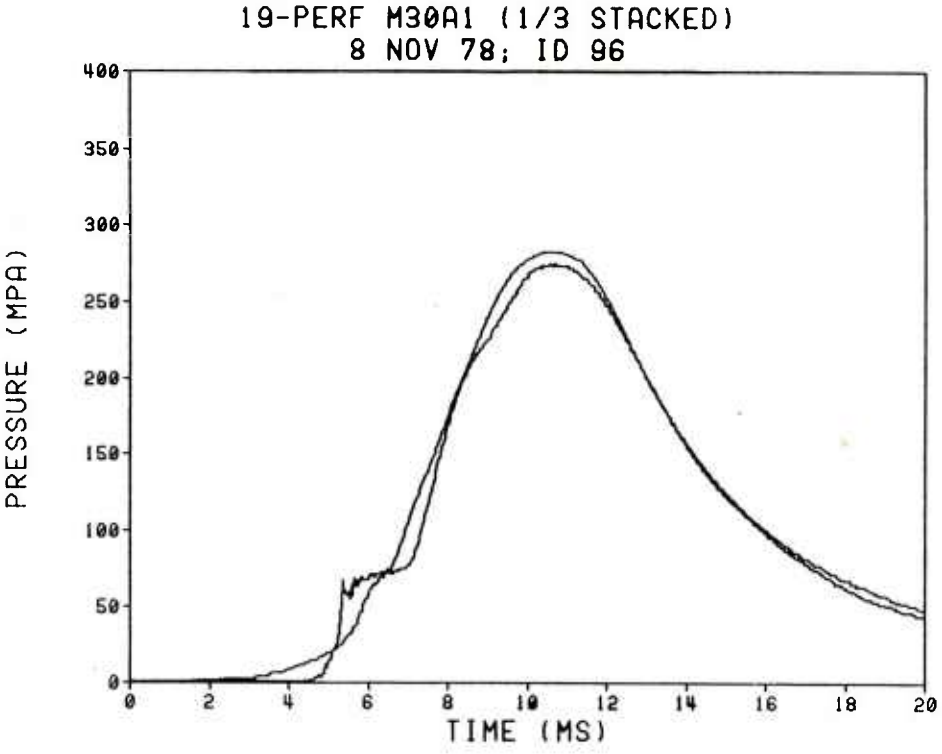
19-PERF M30A1 (1/3 STACKED)
8 NOV 78; ID 96
PRESSURE (MPA)
400
350
300
250
200
150
100
50
0
0
2
4
6
8
10
12
14
16
18
20
TIME (MS)

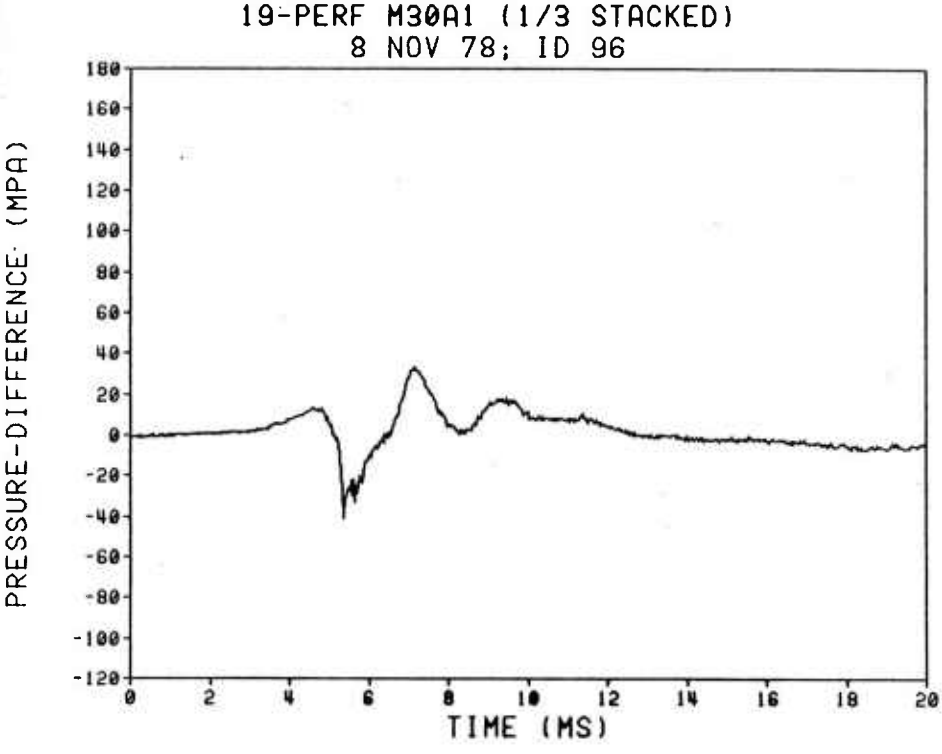
19-PERF M30A1 (1/3 STACKED)
8 NOV 78; ID 96
PRESSURE-DIFFERENCE (MPA)
180
160
140
120
100
80
60
40
20
0
-20
-40
-60
-80
-100
-120
0
2
4
6
8
10
12
14
16
18
20
TIME (MS)

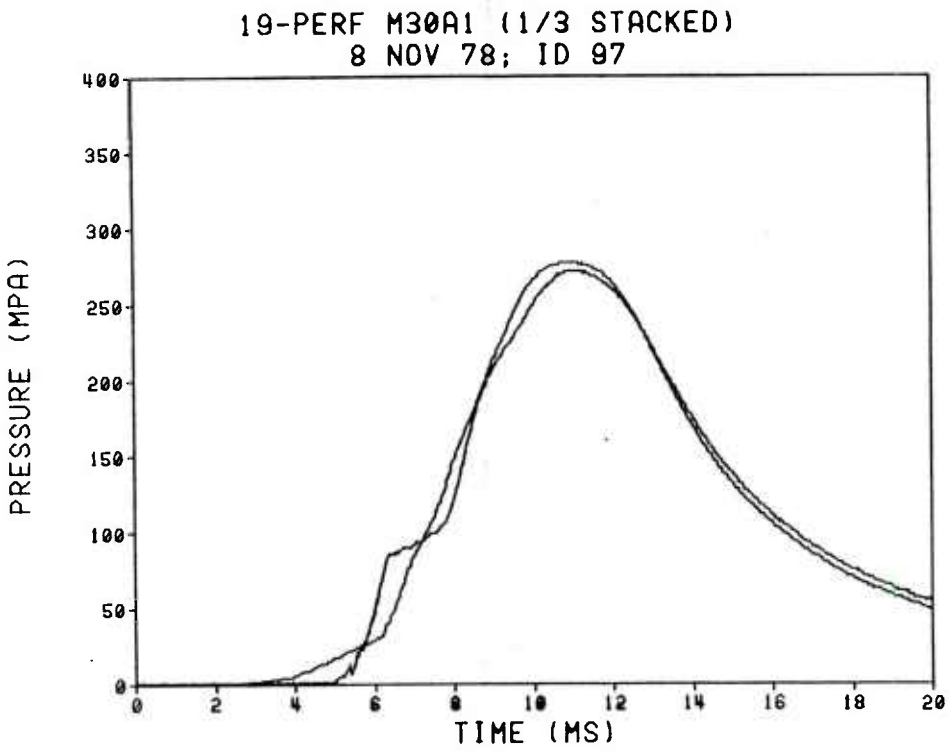
19-PERF M30A1 (1/3 STACKED)
8 NOV 78; ID 97
PRESSURE (MPA)
400
350
300
250
200
150
100
50
0
0
2
4
6
8
10
12
14
16
18
20
TIME (MS)

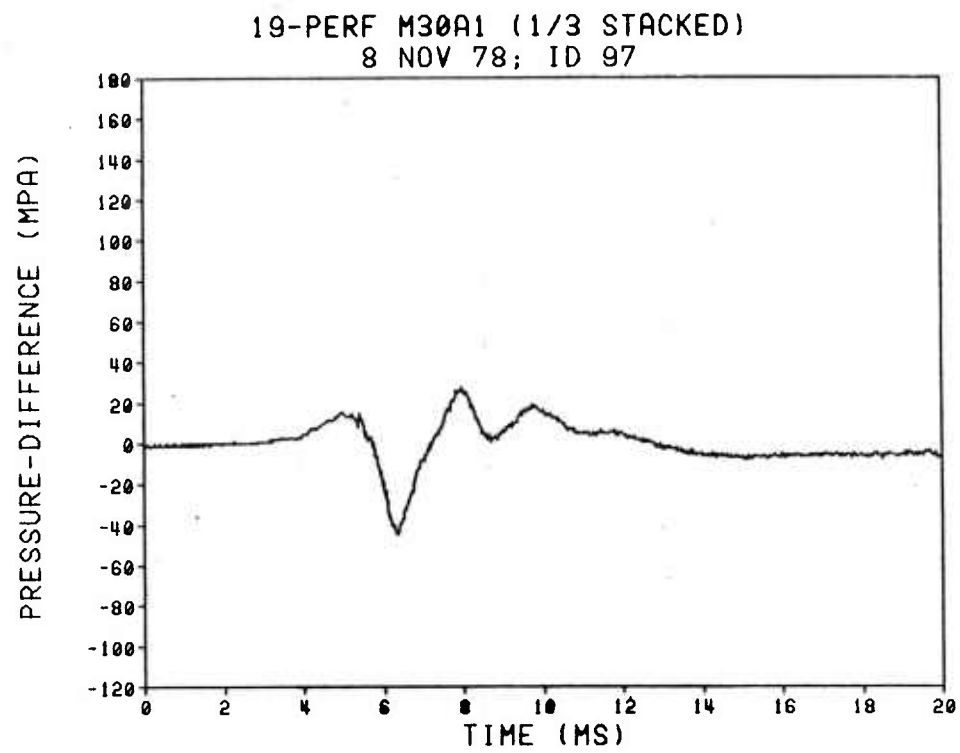
19-PERF M30A1 (1/3 STACKED)
8 NOV 78; ID 97
PRESSURE-DIFFERENCE (MPA)
180
160
140
120
100
80
60
40
20
0
-20
-40
-60
-80
-100
-120
0
2
4
6
8
10
12
14
16
18
20
TIME (MS)

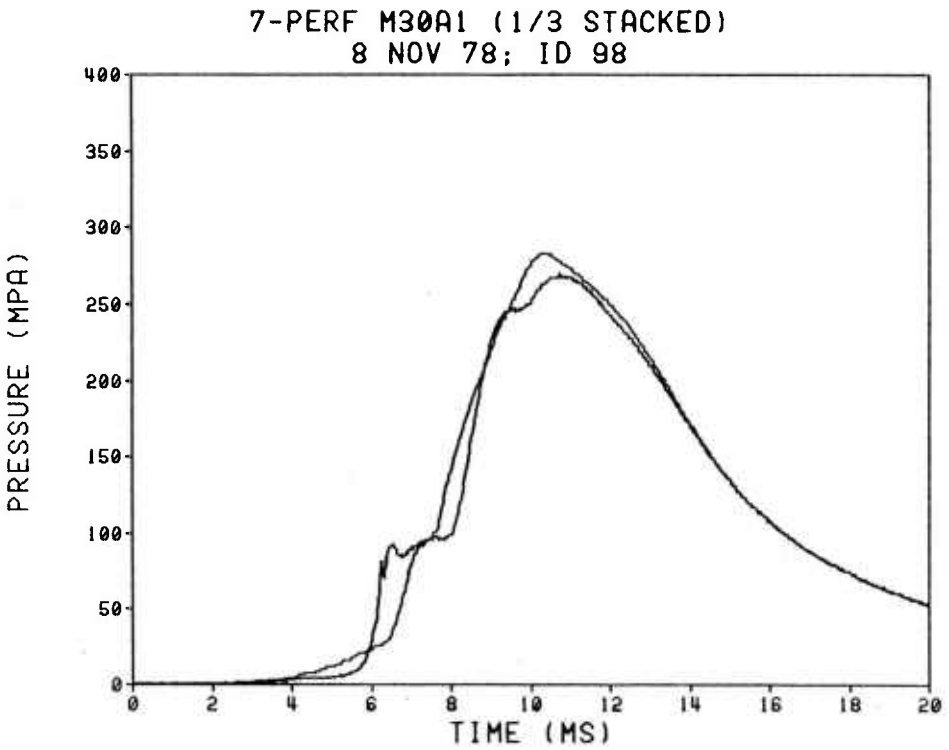
7-PERF M30A1 (1/3 STACKED)
8 NOV 78; ID 98
PRESSURE (MPA)
400
350
300
250
200
150
100
50
0
0
2
4
6
8
10
12
14
16
18
20
TIME (MS)

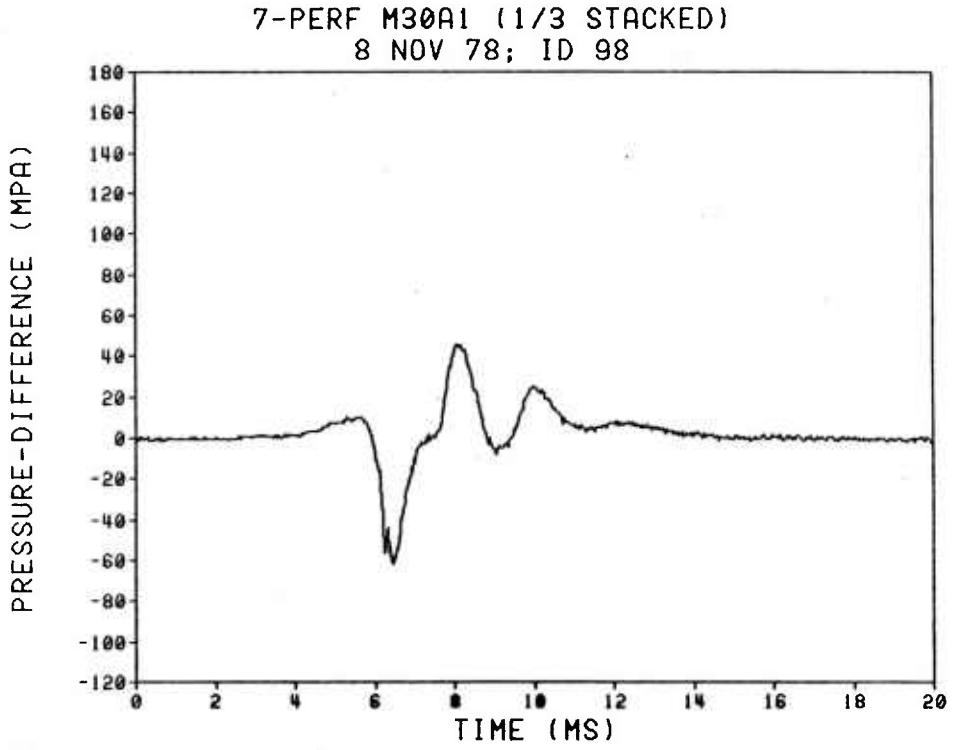
7-PERF M30A1 (1/3 STACKED)
8 NOV 78; ID 98
PRESSURE-DIFFERENCE (MPA)
180
160
140
120
100
80
60
40
20
0
-20
-40
-60
-80
-100
-120
0
2
4
6
8
10
12
14
16
18
20
TIME (MS)

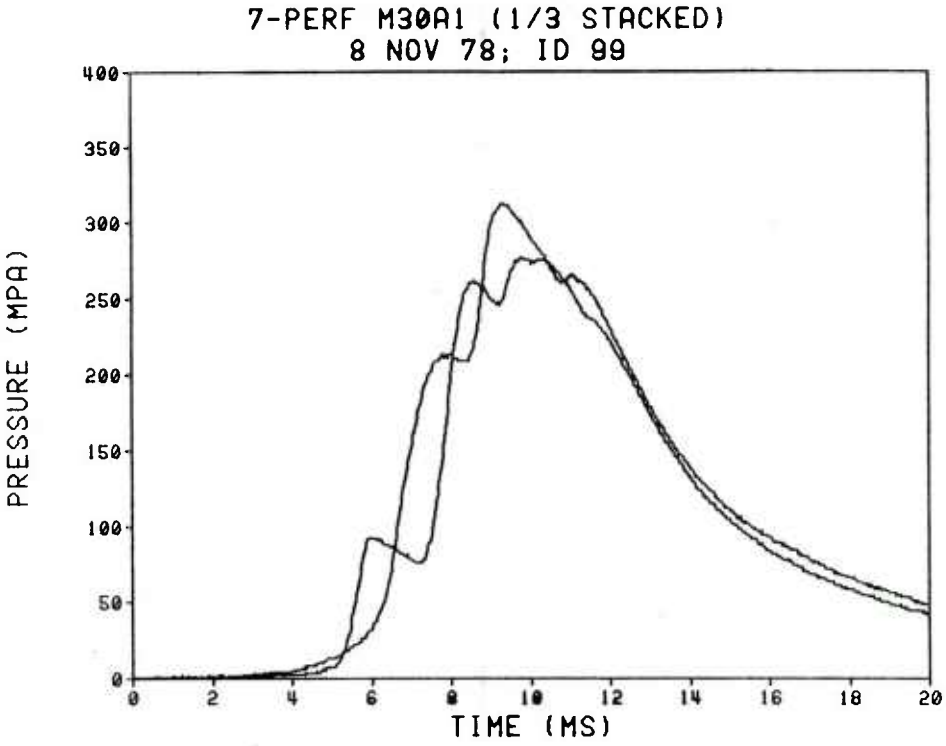
7-PERF M30A1 (1/3 STACKED)
8 NOV 78; ID 99
PRESSURE (MPA)
400
350
300
250
200
150
100
50
0
0
2
4
6
8
10
12
14
16
18
20
TIME (MS)

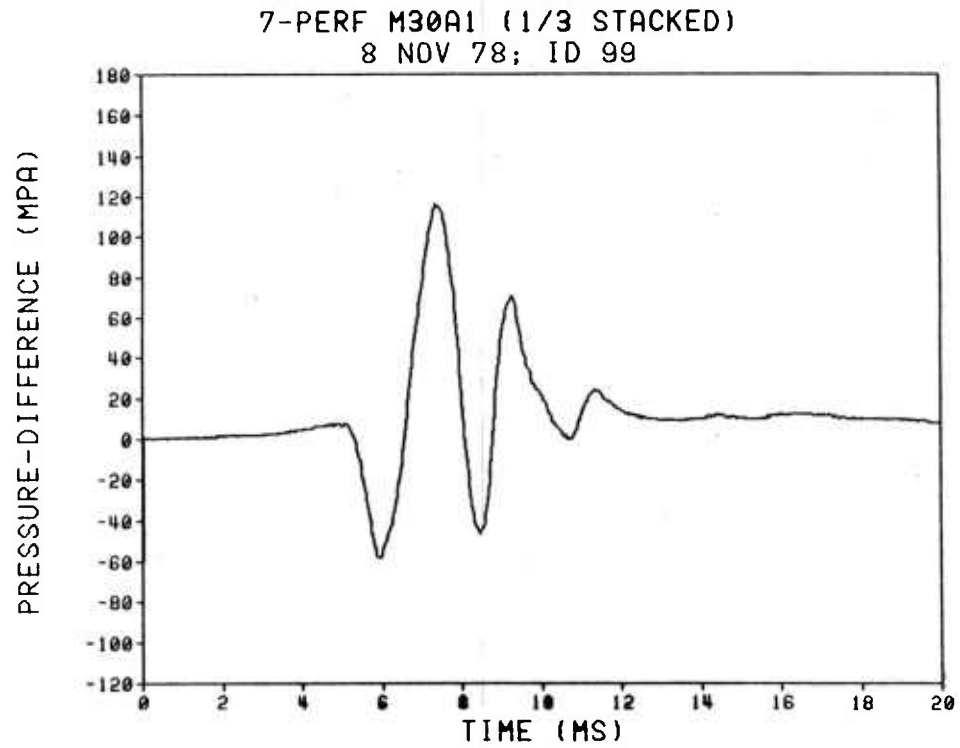
7-PERF M30A1 (1/3 STACKED)
8 NOV 78; ID 99
PRESSURE-DIFFERENCE (MPA)
180
160
140
120
100
80
60
40
20
0
-20
-40
-60
-80
-100
-120
0
2
4
6
8
10
12
14
16
18
20
TIME (MS)

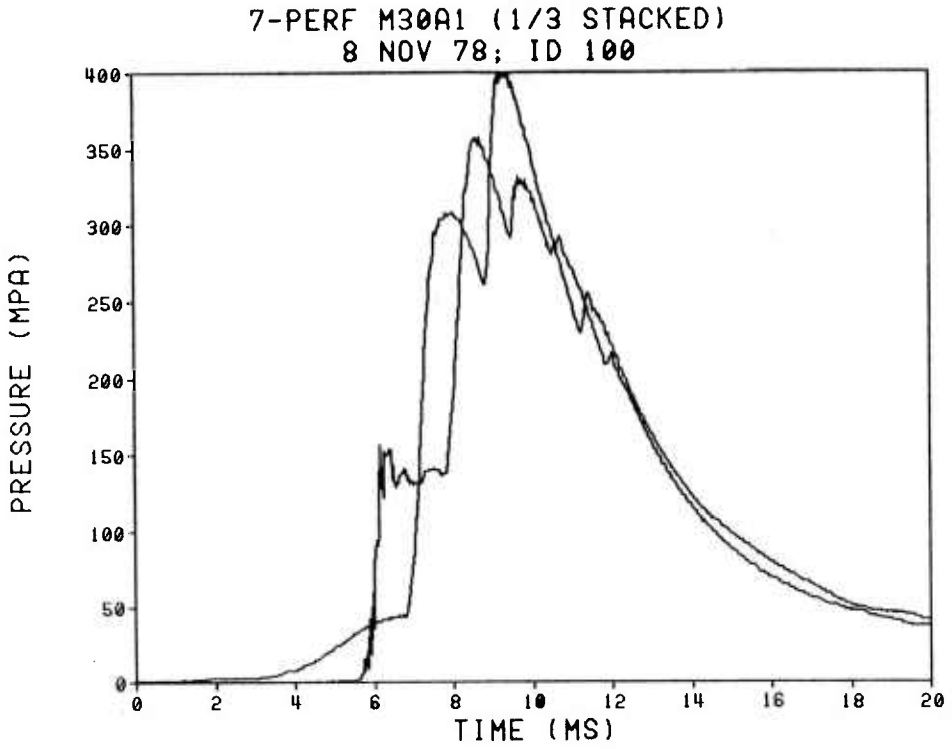
7-PERF M30A1 (1/3 STACKED)
8 NOV 78; ID 100
PRESSURE (MPA)
400
350
300
250
200
150
100
50
0
0
2
4
6
8
10
12
14
16
18
20
TIME (MS)

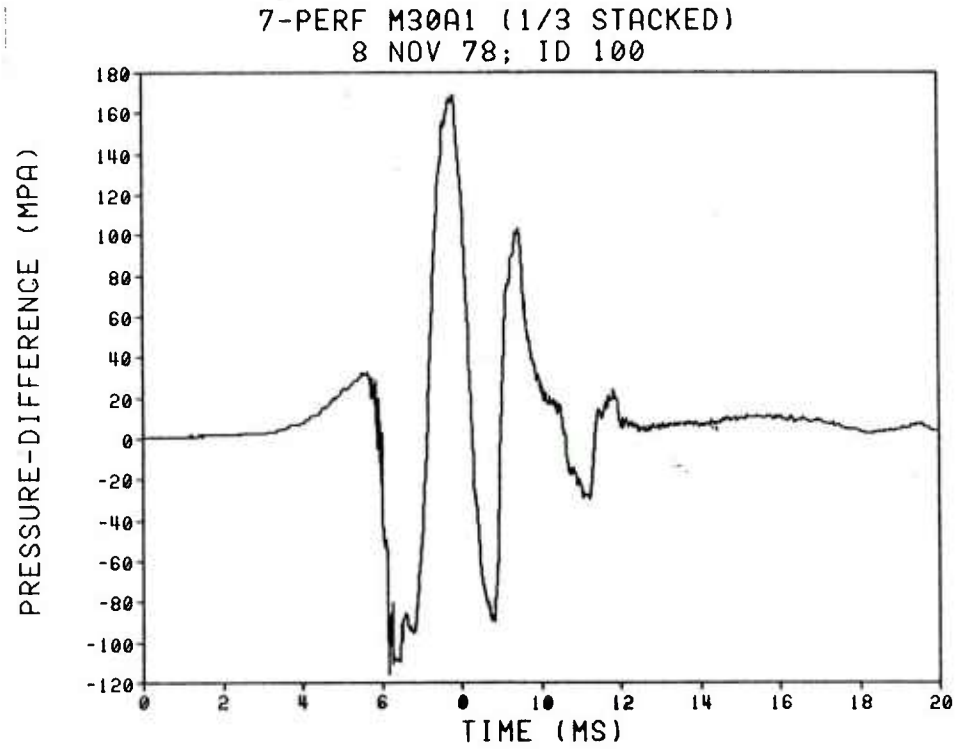
7-PERF M30A1 (1/3 STACKED)
8 NOV 78; ID 100
PRESSURE-DIFFERENCE (MPA)
180
160
140
120
100
80
60
40
20
0
-20
-40
-60
-80
-100
-120
0
2
4
6
8
10
12
14
16
18
20
TIME (MS)

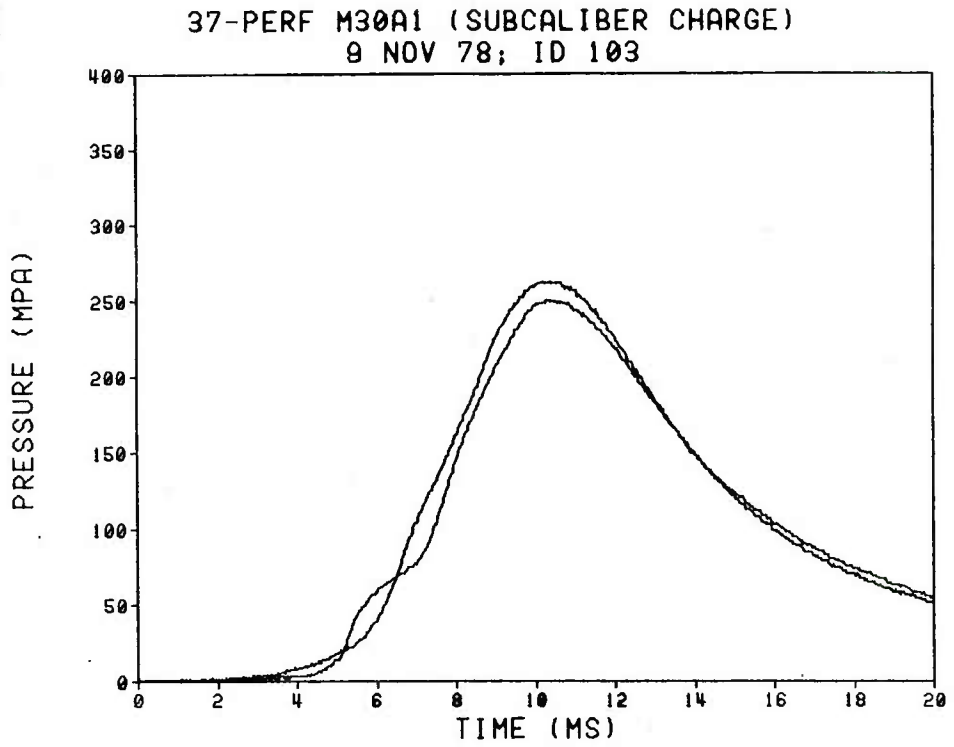
37-PERF M30A1 (SUBCALIBER CHARGE)
9 NOV 78; ID 103
PRESSURE (MPA)
400
350
300
250
200
150
100
50
0
0
2
4
6
8
10
12
14
16
18
20
TIME (MS)

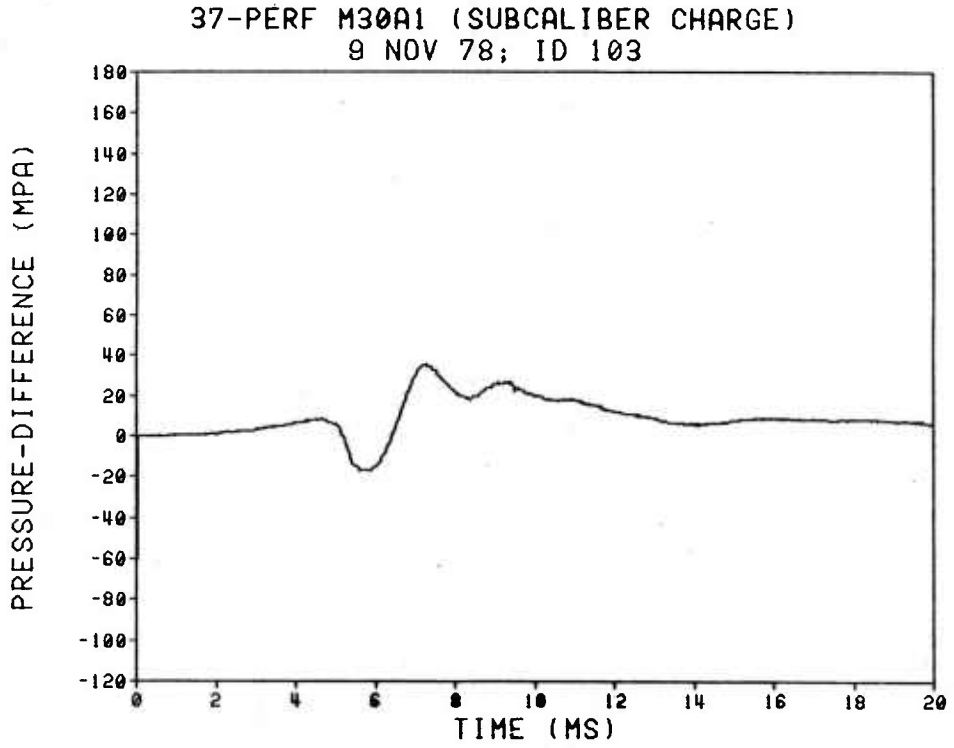
37-PERF M30A1 (SUBCALIBER CHARGE)
9 NOV 78; ID 103
PRESSURE-DIFFERENCE (MPA)
180
160
140
120
100
80
60
40
20
0
-20
-40
-60
-80
-100
-120
0
2
4
6
8
10
12
14
16
18
20
TIME (MS)

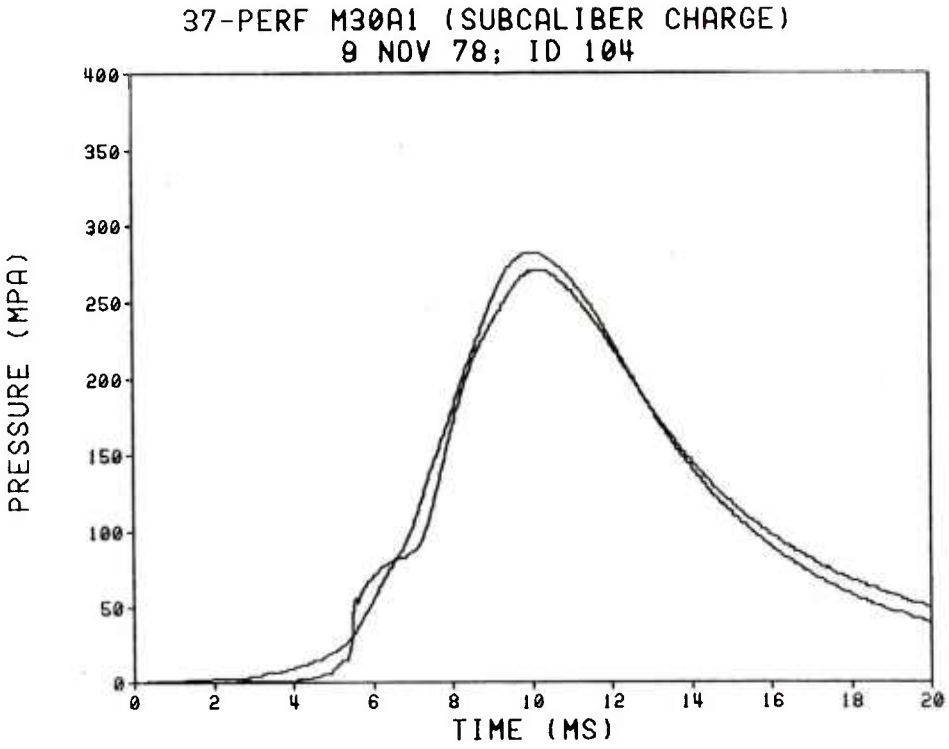
37-PERF M30A1 (SUBCALIBER CHARGE)
9 NOV 78; ID 104
PRESSURE (MPA)
400
350
300
250
200
150
100
50
0
0
2
4
6
8
10
12
14
16
18
20
TIME (MS)

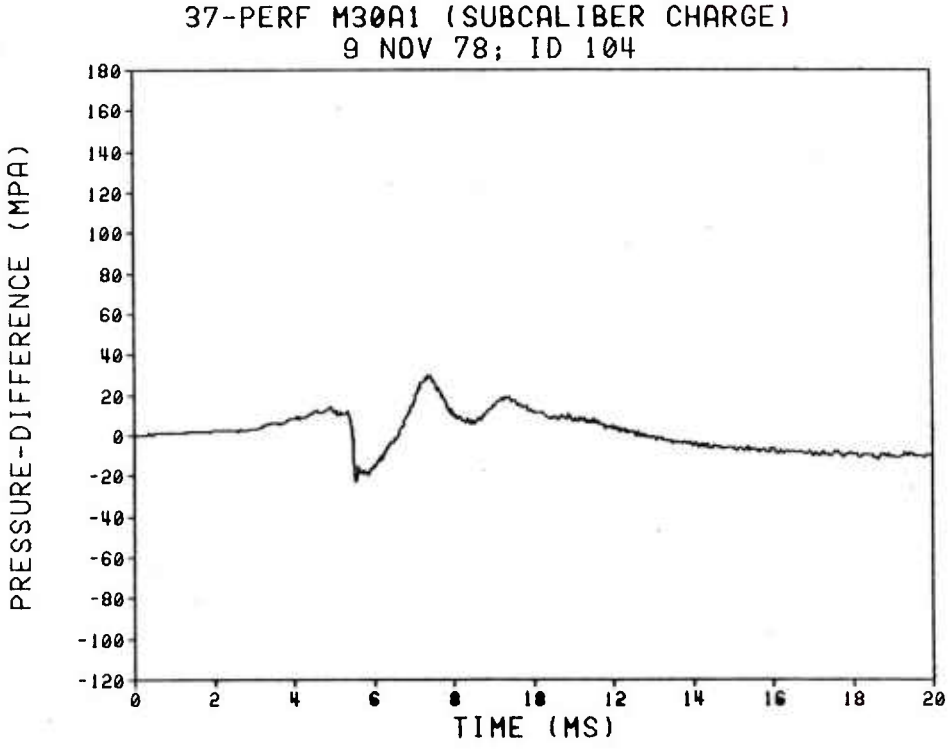
37-PERF M30A1 (SUBCALIBER CHARGE)
9 NOV 78; ID 104
PRESSURE-DIFFERENCE (MPA)
180
160
140
120
100
80
60
40
20
0
-20
-40
-60
-80
-100
-120
0
2
4
6
8
10
12
14
16
18
20
TIME (MS)

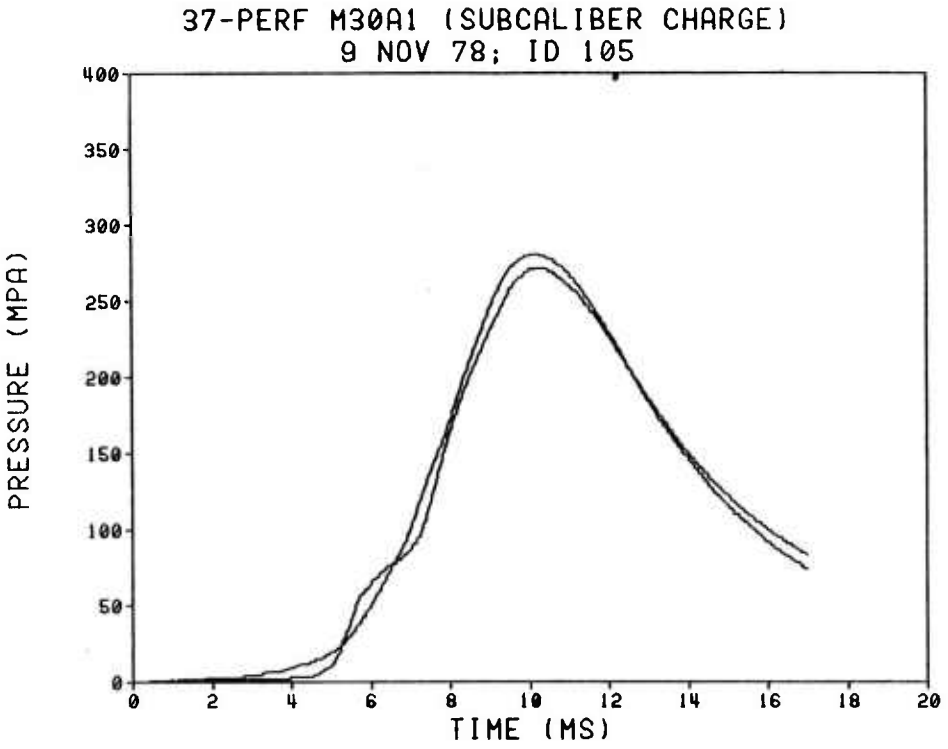
37-PERF M30A1 (SUBCALIBER CHARGE)
9 NOV 78; ID 105
PRESSURE (MPA)
400
350
300
250
200
150
100
50
0
0
2
4
6
8
10
12
14
16
18
20
TIME (MS)

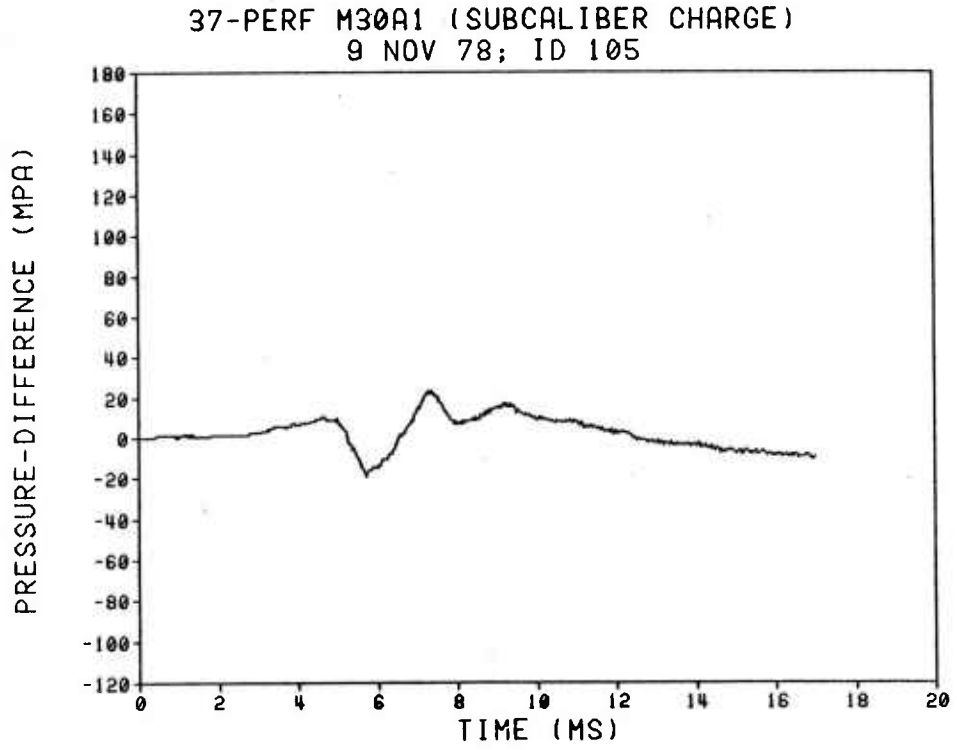
37-PERF M30A1 (SUBCALIBER CHARGE)
9 NOV 78; ID 105
PRESSURE-DIFFERENCE (MPA)
180
160
140
120
100
80
60
40
20
0
-20
-40
-60
-80
-100
-120
0
2
4
6
8
10
12
14
16
18
20
TIME (MS)

DISTRIBUTION LIST

No. of Copies	Organization
12	Commander Defense Technical Info Center ATTN: DDC-DDA Alexandria, VA 22314
2	HQDA (DAMA-CSM-CS, LTC M. Townsend; COL J. Zimmerman) Washington, DC 20310
1	Commander US Army Materiel Development and Readiness Command ATTN: DRCDMD-ST 5001 Eisenhower Avenue Alexandria, VA 22333
2	Commander US Army Armament Research & Development Command ATTN: DRDAR-CG, MG Allen H. Light,Jr. Dover, NJ 07801
6	Commander US Army Armament Research & Development Command ATTN: DRDAR-TSS(2 cys) DRDAR-LCA, H. Fair E. Wurzel K. Russell S. Westley Dover, NJ 07801
1	Director US Army ARRADCOM Benet Weapons Laboratory ATTN: DRDAR-LCB-TL Watervliet, NY 12189
1	Commander US Army Armament Materiel Readiness Command ATTN: DRSAR-LEP-L, Tech Lib Rock Island, IL 61299
1	Commander US Army Aviation Research & Development Command ATTN: DRSAV-E 12th and Spruce Streets St. Louis, MO 63166
1	Director US Army Air Mobility Research & Development Command Ames Research Center Moffett Field, CA 94035
1	Commander US Army Communications Research & Development Command ATTN: DRDCO-PPA-SA Fort Monmouth, NJ 07703
1	Commander US Army Electronics Research & Development Command Technical Support Activity ATTN: DELSD-L Fort Monmouth, NJ 07703
2	Commander US Army Missile Command ATTN: DRSMI-R DRDMI-YDL Redstone Arsenal, AL 35809
1	Commander US Army Tank Automotive Research & Development Cmd ATTN: DRDTA-UL Warren, MI 48090

DISTRIBUTION LIST

No. of Copies	Organization
5	Project Manager, Cannon Artillery Weapons System ATTN: DRCPM-CAWS COL R.E. Philip DRCPM-CAWS-AM, F. Menke DRCPM-CAWS-GP, B.Garcia DRCPM-CAWS-WP, H.Noble DRCPM-SA, J.Brooks Dover, NJ 07801
3	Product Manager M110E2 Weapons System ATTN: DRCPM-M110E2-TM S. Smith B. Walters Rock Island, IL 61299
1	Director US Army TRADOC Systems Analysis Activity ATTN: ATAA-SL, Tech Lib White Sands Missile Range NM 88002
1	Commander US Army Field Artillery School ATTN: APSF-CD-W, LT. Monigal Fort Sill, OK 73503
2	Commander Naval Surface Weapons Center ATTN: J. East Tech Library Dahlgren, VA 22448
1	Commander Naval Weapons Center ATTN: Tech Lib China Lake, CA 93555
3	Commander Naval Ordnance Station ATTN: F.W. Robbins S.E. Mitchell Tech Lib Indian Head, MD 20640
1	Calspan Corporation ATTN: E.B. Fisher P.O. Box 235 Buffalo, NY 14221
1	Paul Gough Associates, Inc. ATTN: P.S. Gough P.O. Box 1614 Portsmouth, NH 03801
1	Pennsylvania State University Dept of Mechanical Engineering ATTN: K.K. Kuo University Park, PA 16801
1	Princeton University Guggenheim Laboratories Dept of Aerospace & Mechanical Science ATTN: L.H. Caveny P.O. Box 710 Princeton, NJ 08540

Aberdeen Proving Ground

Dir, USAMSAA
ATTN: DRXSY-D
DRXSY-MP, H.Cohen
Cdr, USA TECOM
ATTN: DRSTE-TO-F
Dir, Wpns Sys Concepts Team
Bldg E3516, EA
ATTN: DRDAR-ACW

USER EVALUATION OF REPORT

Please take a few minutes to answer the questions below; tear out this sheet and return it to Director, US Army Ballistic Research Laboratory, ARRADCOM, ATTN: DRDAR-TSB, Aberdeen Proving Ground, Maryland 21005. Your comments will provide us with information for improving future reports.

1. BRL Report Number _____

2. Does this report satisfy a need? (Comment on purpose, related project, or other area of interest for which report will be used.)

_____

_____

_____

3. How, specifically, is the report being used? (Information source, design data or procedure, management procedure, source of ideas, etc.) _____

_____

_____

4. Has the information in this report led to any quantitative savings as far as man-hours/contract dollars saved, operating costs avoided, efficiencies achieved, etc.? If so, please elaborate.

_____

_____

5. General Comments (Indicate what you think should be changed to make this report and future reports of this type more responsive to your needs, more usable, improve readability, etc.) _____

_____

_____

_____

6. If you would like to be contacted by the personnel who prepared this report to raise specific questions or discuss the topic, please fill in the following information.

Name: _____

Telephone Number: _____

Organization Address: _____

_____

_____